Master's thesis

NTNU
Norwegian University of Science and Technology
Faculty of Natural Sciences
Department of Physics

Maria Stadheim

Development of macrophage characterization assays

Master's thesis in Nanotechnology

Supervisor: Torkild Visnes

August 2020

NTNU
Norwegian University of Science and Technology

SINTEF

Maria Stadheim

Development of macrophage characterization assays

Master's thesis in Nanotechnology
Supervisor: Torkild Visnes
August 2020

Norwegian University of Science and Technology
Faculty of Natural Sciences
Department of Physics

NTNU
Norwegian University of
Science and Technology

Abstract

Despite the promising advancements of immunotherapy, notifying a new pillar of cancer treatment, a limited portion of patients respond successfully to specific treatments. The development of simplified assays to investigate complex and specific cellular responses to particular treatments would aid in patient selection and advance the research on cancer immunotherapy. Macrophages play a prominent role in cancer-related inflammation, and the prevalence of tumor-associated macrophages (TAMs) within tumors often correlates with a reduced overall prognosis. Importantly, most TAMs have been found to resemble an M2-like phenotype, promoting tumor progression and suppression of an effective adaptive immune response. Several strategies of macrophage manipulation have been suggested as potential anti-cancer immunotherapeutic treatments.

In this thesis, a simplified macrophage polarization model was developed to investigate the characteristics of macrophages stimulated towards either an M1- or M2-like phenotype. Monocytes of the THP-1 cell line were exposed to phorbol 12-myristate 13-acetate (PMA) to induce differentiation into macrophages, followed by incubation with LPS and IFN-γ to develop M1-like macrophages or IL-4 and IL-13 to develop M2-like macrophages. Evaluation of the resulting THP-1 macrophage phenotypes was performed after various exposure times by flow cytometry and ELISA to investigate putative M1 and M2 specific cell surface markers and secreted cytokines, respectively.

Flow cytometry and ELISA measurements indicated a successful polarization of THP-1 macrophages towards an M1-like phenotype. The M1 polarized THP-1 macrophages were characterized by a significantly increased amount of cells expressing the surface markers MHCII and CD80, and a significantly increased secretion of TNF-α and CXCL10. In contrast, exposure to M2 polarizing stimuli did not induce the hypothesized surface expression of CD163 and CD206 or the secretion of IL-10 and IL-1Ra. Therefore, the data suggest a potential of THP-1 macrophages to develop into an M1 macrophage phenotype, whereas the activation and characterization of an M2 phenotype in THP-1 macrophages require further investigations.

With the achieved activation and characterization of M1 polarized THP-1 macrophages, the simplified macrophage model was utilized to investigate the impact of specific pathways on M1 macrophage polarization. The effect of exposing the THP-1 cells to TH5487, BMS-345541, or Rapamycin during M1 polarization was investigated by detecting the consequent secretion of TNF-α. Both TH5487 and BMS-345541 are known to prevent inflammatory gene expression by perturbing NF-κB, whereas Rapamycin is a recognized inhibitor of the mTOR pathway.

Unexpectedly, neither TH5487 nor BMS-345541 altered the secretion of TNF-α. Hence, the results suggest an NF-κB-independent mechanism of TNF-α secretion in THP-1 macrophages under the investigated experimental conditions. Similarly, exposure to Rapamycin during LPS- and IFN-γ-stimulation of THP-1 macrophages did not alter the secretion of TNF-α, showing no apparent sign to control the M1 polarization. However, the effect of TH5487, BMS-345541, and Rapamycin on their target pathways and the resulting M1 polarization profile should be further investigated by studying an assortment of cytokines, both at the mRNA and protein levels.

Sammendrag

På tross av lovende fremskritt innen immunterapi, som anses som en ny pilar i kreftbehandling, responderer kun en liten andel pasienter som ønsket på spesifikke behandlinger. Utviklingen av forenklede metoder for studie av komplekse og spesifikke cellulære responser på bestemte behandlinger, vil kunne fungere veiledende i pasientutvalg og muliggjøre økt fremdrift innen forskning på immunterapi. Makrofager har en viktig rolle i kreft-relatert inflammasjon, og en økt andel tumor-assosierte makrofager (TAMs) i tumorer korrelerer ofte med en redusert total prognose. I hovedsak er det funnet at TAMs uttrykker en M2-liknende fenotype, som fremmer tumorprogresjon og undertrykker en effektiv adaptiv immunrespons. Flere strategier for manipulering av makrofager har blitt foreslått som potensielle immunterapeutiske behandlinger mot kreft.

I dette studiet ble det utviklet en forenklet makrofag polariseringsmodell for å undersøke kjennetegn ved makrofager stimulert mot en M1- eller M2-liknende fenotype. Monocytter av THP-1 cellelinjen ble behandlet med phorbol 12-myristate 13-acetate (PMA) for å indusere differensieringen til makrofager. THP-1 makrofagene ble deretter enten eksponert for LPS og IFN-γ for å utvikle M1-liknende makrofager, eller IL-4 og IL-13 for å utvikle M2-liknende makrofager. Evaluering av THP-1 makrofagenes resulterende fenotype ble utført etter ulike eksponeringstider. Flowcytometri og ELISA ble brukt for å undersøke antatte M1 og M2 spesifikke markører på celleoverflaten og utskillelsen av karakteristiske cytokiner.

Både flowcytometri- og ELISA-målingene indikerte en vellykket polarisering av THP-1 makrofager mot en M1-liknende fenotype. De M1 polariserte THP-1 makrofagene ble karakterisert ved en signifikant økning i antall celler med overflatemarkørene MHCII og CD80, og en signifikant økning i utskillelsen av TNF-α og CXCL10. I motsetning førte M2 polariseringen verken til den forventede uttrykkelsen av CD163 og CD206, eller til den antatte utskillelsen av IL-10 og IL-1Ra. Dataene indikerer et potensiale ved THP-1 monocytter til å utvikle en M1-liknende fenotype, mens aktiveringen og karakteriseringen av en M2-liknende fenotype i THP-1 makrofager krever videre undersøkelse.

Med den oppnådde aktiveringen og karakteriseringen av M1 polariserte THP-1 makrofager, ble den forenklede makrofagmodellen brukt til å undersøke viktigheten av spesifikke aktiveringsspor for M1 polarisering. Effekten av å eksponere THP-1 celler for TH5487, BMS-345541 eller Rapamycin under M1 polarisering ble undersøkt ved å detektere følgende utskillelse av TNF-α. Både TH5487 og BMS-345541 er kjent for å hindre inflammatorisk genuttrykkelse ved å forstyrre NF-κB, mens Rapamycin er en anerkjent inhibitor av mTOR sporet.

Verken TH5487 eller BMS-345541 endret utskillelsen av TNF-α. Resultatene antyder derfor at utskillelsen av TNF-α fra THP-1 makrofager under disse eksperimentelle betingelsene er uavhengig av NF-κB sporet. Likedan førte ikke tilstedeværelsen av Rapamycin under LPS- og IFN-γ-stimulering av THP-1 makrofagene til en endring i utskillelsen av TNF-α. Dermed viste forsøkene ingen tydelig kontroll over M1 polariseringen ved å inhibere mTOR sporet. Effekten av TH5487, BMS-345541 og Rapamycin, aktiveringssporene disse angriper, og den resulterende M1 polariseringsprofilen bør undersøkes nærmere ved å studere et utvalg av cytokiner, både på mRNA- og proteinnivå.

Preface

This master's thesis concludes Maria Stadheim's M.Sc. degree within the Nanotechnology program at the Norwegian University of Science and Technology. The work presented in this master's thesis was performed during the spring semester of 2020 in collaboration with SINTEF Industry. This thesis builds on the specialization project carried out by Maria Stadheim during the fall semester of 2019 titled "Development of protocols for macrophage polarization and characterization of resulting phenotypic morphological signatures" [1]. Therefore, some sections presented herein might appear similar.

I was lucky to join the Immuno project at SINTEF, aiming to develop new methods for cancer immunotherapy. First, I would like to thank SINTEF Industry for giving me the opportunity to work on this specific project. I am thankful to my supervisor, Torkild Visnes, for the great support, assistance, and discussions of my questions during this project. I would also like to thank all the employees at the laboratory, especially Andrea Draget Hoel, for guidance and answers to my questions. Furthermore, I am grateful to Kristin Grendstad at NTNU, the Department of Physics, for her outstanding help and support during the development of the flow cytometry protocol and performance of the flow cytometry experiments. Also, I am thankful to Catharina de Lange Davies for providing feedback on this thesis.

Abbreviations

ATP	=	Adenosine TriPhosphate
APC	=	Antigen-Presenting Cell
BSA	=	Bovine Serum Albumin
CCL	=	Chemokine [C-C motif] Ligand
CD	=	Cluster of Differentiation
CTG	=	CellTiter-Glo
CXCL	=	Chemokine [C-X-C motif] Ligand
DC	=	Dendritic Cell
DMSO	=	Dimethyl Sulfoxide
ECM	=	ExtraCellular Matrix
ELISA	=	Enzyme-Linked Immunosorbent Assay
FBS	=	Fetal Bovine Serum
HEPES	=	(4-(2-hydroxyethyl)-1-piperazine-ethanesulfonic acid)
IFN	=	Interferon
IKK	=	IκB kinase
IL	=	InterLeukin
IRF	=	Interferon Regulatory Factor
JAK	=	Janus Kinase
LPS	=	LipoPolySaccharide
M-CSF	=	Macrophage Colony-Stimulating Factor
MHC	=	Major Histocompatibility Complex
mTOR	=	Mammalian Target Of Rapamycin
NF-κB	=	Nuclear Factor-Kappa B
NK cell	=	Natural Killer cell
NOS	=	Nitric Oxide Synthase
PBMC	=	Peripheral Blood Mononuclear Cell
PBS	=	Phosphate-Buffered Saline
PMA	=	Phorbol 12-Myristate 13-Acetate
PRR	=	Pattern recognition receptor
ROS	=	Reactive Oxygen Species
STAT	=	Signal Transducer and Activator of Transcription
TAM	=	Tumor-Associated Macrophage
TLR	=	Toll-Like Receptor
TME	=	Tumor MicroEnvironment
TNF	=	Tumor Necrosis Factor

Table of Contents

CHAPTER 1

Introduction

The comprehensive term of cancer includes more than 100 distinct types of diseases with the fundamental characteristic of defects in the regulatory processes controlling healthy cell proliferation and homeostasis [2, 3]. Globally, cancer is the second leading cause of deaths, emphasizing the critical need for increased effectiveness and affordability in programs of early diagnosis, screening, treatment, and palliative care [2]. The treatment methods of today mostly rely on combinations of chemotherapy, radiation therapy, and surgery, all of which are associated with damage of healthy tissues or adverse toxicities and side effects [4, 5]. Importantly, the immune system and its relation to cancer have received increased attention during the latest decades, highlighting a great therapeutic potential and promise of cancer immunotherapy [4]. Cancers hold the capacity to evade immune destruction. Besides, chronic inflammation has proved the potential to promote cancer development and progression, and inflammatory cells and mediators are considered essential constituents in most, if not all, tumor micro-environments [5, 6, 7].

Immunotherapy involves several treatment strategies based on active or passive re-engagement of a patient's immune system to induce a potent anti-tumor response, accompanied by reduced side effects [8, 9]. As only a fraction of immunotherapy treated patients respond to specific treatments, patient selection stands out as an important challenge [10]. It is essential to develop robust and reliable methods for the prediction of responsive patients to avoid treatment-related toxicities and costs.

Conventional cancer therapy and immunotherapy work differently to eradicate tumors. Immunotherapy targets immune cells rather than cancer cells and might provoke a cellular immune response before the tumor burden is affected [11]. It is necessary to reveal underlying mechanisms that contribute to regulating the interplay between cancer and the immune system [10]. Also, increased knowledge of cancer immune evasion would assist the development of new drug targets [4]. A methodological framework for early identification and investigation of immune responses would guide the therapeutic development

and assist in the selection of promising candidates for specific treatments [11, 12].

Macrophages are cells of the innate immune system that exhibit essential functions in tissue homeostasis and immunity. However, these cells have also been associated with several pathological processes, and they are essential contributors to the regulation of chronic inflammation [13]. In solid tumors, the prevalence of tumor-associated macrophages (TAMs) is often related to a reduced overall prognosis [14]. Macrophages express a high degree of plasticity and diversity. Their acquired properties depend on multiple sources of stimuli, including the microenvironmental cytokine balance and their tissue of residence [14, 15, 16]. The polarization of macrophages involves genetic reprogramming and change of phenotype and function in response to the surrounding environment [15, 17]. The polarization of macrophages is highly advanced, but an M1 versus M2 paradigm has been extensively used to simplify the classification. Generally, the M1 macrophages are considered pro-inflammatory, and they contribute to initiating adaptive immune responses, whereas M2 macrophages are considered anti-inflammatory mediators suppressing effective adaptive immune responses [14, 15, 18]. In the case of cancer, macrophages attaining M1-like phenotypes are thought to induce anti-tumor responses and cytotoxicity, desired in tumor regression. Contrary, M2-like macrophages have in common the effects of tumor promotion [14]. Although TAMs do not precisely fit into the M1 or the M2 phenotype, most TAMs resemble an M2-like phenotype. Consequently, several strategies of macrophage manipulation have been suggested as potential anti-cancer immunotherapeutic treatments [19]. An efficient method for distinguishing the pro-tumoral macrophages from their desired anti-tumoral counterparts would enable early identification of potentially useful treatment modalities [20].

This master's thesis builds upon a simplified macrophage polarization model developed in the specialization project performed by the author during the autumn 2019 [1]. The shared hypothesis of these two works is that the THP-1 monocyte cell line can be controlled to work as a simplified and robust model for macrophage polarization. In the polarization model, phorbol-12-myristate-13-acetate (PMA)-differentiated THP-1 macrophages are polarized towards different macrophage phenotypes by exposure to various polarizing stimuli. Herein, we aimed to quantitatively assess whether THP-1 macrophages could be polarized to present M1- and M2-like phenotypes. Successful polarization was evaluated by the presence or absence of phenotypic markers that have been extensively used to classify macrophages in previous literature [21, 22, 23, 24, 19, 25]. The polarized THP-1 macrophages were investigated for cell surface marker expression by flow cytometry, and secretion of putative M1 and M2 phenotype cytokines by ELISA.

Next, the aim was to investigate the effect of chemical substances targeting essential pathways of M1 macrophage polarization. Here, the priority was to investigate the potential of TH5487, BMS-345541, or Rapamycin to alter the secretion of TNF-α in THP-1 macrophages induced by LPS and IFN-γ. NF-κB is a central regulator of several genes in immune responses, and TH5487 and BMS-345541 are known to inhibit inflammatory gene expression by perturbing NF-κB [26, 27]. The mTOR pathway has presented a discordant effect on macrophage polarization, and Rapamycin is a recognized inhibitor of this pathway [28, 29, 30]. We hypothesized that incubating THP-1 macrophages in the presence of TH5487, BMS-345541, or Rapamycin during exposure to M1 polarizing agents would alter the secretion of TNF-α by affecting the NF-κB or mTOR pathway, respectively.

CHAPTER 2

Theory

2.1 Cancer

The complexity of cancer includes more than 100 distinct types of diseases characterized by defects in the cellular regulatory circuits [3]. In healthy tissues, the promotion and restraining of growth signals are carefully controlled, ensuring maintenance of normal cell proliferation and tissue homeostasis. As a result, cellular proliferation is restricted to occur only when required, such as during normal tissue turnover and wound healing. When required, the balance of growth-promoting signals is tilted to generate a temporarily local increase in cellular proliferation and differentiation. This provoked growth process ceases when a sufficient amount of cells is produced, and the homeostatic balance is restored. Contrary, the balance is not reestablished in the case of cancers, resulting in an uncontrollable chronic proliferation where the loss of differentiation might be observed [31, 32]. To create a logical framework for understanding the complexity of neoplastic diseases, Hanahan and Weinberg [32] propose an organizing principle based on various acquired biological capabilities. These hallmark capabilities collectively contribute to the transformations of healthy cells into cancerous cells, and their timing and mechanisms of development vary between tissues and tumor types. Two specified characteristics principally enable acquisition of the multiple hallmarks [32]:

1. *Genome instability and mutation:* generation of genetic diversity is seen as the most protruding characteristic that accelerates hallmark capabilities.

2. *Tumor-promoting inflammation:* immune cells and inflammation importantly contributes to foster several hallmark functions and is seen as the second most prominent characteristic.

The proposed hallmarks of cancer include evasion of growth suppressors, continu-

ous proliferative signaling, resistance against cell death, enabling replicative immortality, stimulating angiogenesis, activating invasion, and metastasis, reprogramming of energy metabolism, and evading immune destruction [32].

2.2 Immunology

Immunology is the study of the immune system, comprising a sophisticated assortment of cells, tissues, and molecules. The definition of immunity includes resistance to disease. The immune system's strategies to maintain immunity can broadly be divided into two categories: innate and adaptive immunity. While the innate immunity includes the initial defense mechanisms immediately working to protect against microbial invasion, the adaptive immunity requires expansion and differentiation of lymphocytes to defend the body effectively [33]. Different immune cells are classified into these two categories, with the principal classification illustrated in Figure 2.1.

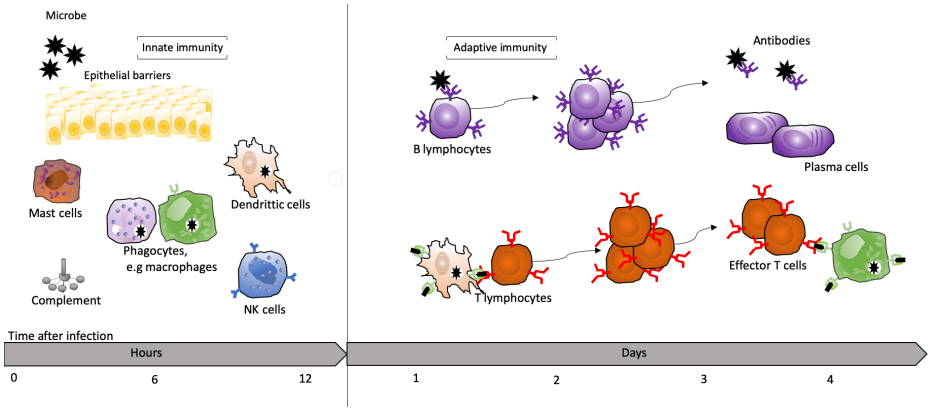

Figure 2.1: *Overview of the principal classification of cells that belong to the innate and adaptive immunity. The innate immunity provides immediate defense against threats, while the adaptive immune responses require time for expansion and differentiation of lymphocytes and their products. Illustration by the author with the idea adapted fromAbbas, Lichtman, and Pillai [33].*

The innate immune system is comprised of epithelial cells; sentinel cells in tissues, such as macrophages, dendritic cells (DCs), and mast cells; innate lymphoid cells, such as natural killer (NK) cells; and plasma proteins [34]. The adaptive immune system includes B lymphocytes, T lymphocytes, and lymphocyte products, and is further subdivided into humoral and cell-mediated immunity. In humoral immunity, B lymphocytes produce antibodies to neutralize or eliminate extracellular microbes and microbial toxins. The cell-mediated immunity includes different T lymphocyte types, mainly divided into helper T lymphocytes and cytotoxic T lymphocytes. While T lymphocytes primarily work to recruit and activate phagocytes to eliminate microbes, cytotoxic T lymphocytes aim to kill and eliminate infected host cells [33].

2.3 Inflammation

Inflammation can be described as an adaptive response triggered by harmful stimuli or conditions, including infection, tissue injury, and tissue stress or malfunction. The inflammatory response process depends upon the trigger, but the purpose of all inflammation is to remove any source of disturbance to tissue homeostasis. When working to restore tissue injury and eliminate pathogenic agents, an inflammatory response is highly beneficial. An acute inflammatory response primarily involves a systemic delivery of blood components to the organ of interest [35]. Cytokines and other mediators are secreted by the tissue-resident innate immunity cells, including macrophages, DCs, and mast cells to facilitate increased blood vessel permeability, ease the entry of plasma proteins, and recruit circulating leukocytes to the site of infection or tissue damage. The attracted leukocytes become activated to destroy microbes, eliminate damaged cells, promote amplified inflammation, or coordinate repair mechanisms [34]. A successful acute inflammatory response is transient and restores the functionality and homeostasis of the exposed tissue. Contrary, if the inflammatory response yields an insufficient effect, the abnormal condition sustains, and a chronic inflammatory state might evolve. A persistent inflammatory reaction generally continues at the expense of other physiological processes and therefore holds the potential for adverse effects [35, 36].

2.3.1 Cancer-related inflammation

About 90% of all cancers result from a combination of somatic mutations and environmental factors. Importantly, several environmental risk factors and causes of cancer are associated with chronic inflammation. Various types of inflammation have proved the potential to promote cancer development and progression [7, 6]. An inflammatory condition can both be present before and participate in the induction of an oncogenic change, or it can evolve as a result of the change. Regardless of the inflammatory origin, inflammatory cells, and mediators, such as chemokines, cytokines, and prostaglandins, are essential constituents and present in most, if not all, tumor microenvironments (TMEs) [6]. In contrast to the transient appearance of immune responses seen in normal fighting off threats and wound healing, cancer-related inflammation is considered non-resolving [32]. Importantly, inflammation can supply bioactive molecules to the TME that contributes to multiple hallmark capabilities, including sustained proliferation, survival, and angiogenesis [32, 20, 14].

2.4 The tumor microenvironment

The TME is complex and dynamic and emerges during the multistep course of tumorigenesis. The tumor itself orchestrates molecular and cellular events that shape the TME into an actively contributing environment that enables tumor growth and progression [32, 37]. The complexity of the TME involves an assemblage of different cell types, including genetically heterogeneous cancer cells, immune cells of both the innate and the adaptive immune system, and the surrounding tumor stroma. The tumor stroma consists of cancer-associated fibroblasts, endothelial cells, pericytes, and mesenchymal cells, as illustrated in

Figure 2.2 [38, 32, 6, 7]. Other important contributors to tumor progression are the extracellular matrix (ECM), and the blood and lymphatic vasculature networks [38]. The non-cellular and three-dimensional ECM surrounds and is directly linked to the cells through ECM receptors. This network is present within all tissues and organs and works as a mechanical supporting scaffold, and as a reservoir for growth factors and bioactive molecules [37, 39, 40]. Another critical component of the TME involves the leukocyte infiltrate [6]. Analogous to the inflammatory conditions seen in non-neoplastic tissues, inflammatory immune cells densely infiltrate the TME. This infiltration of innate and adaptive immune cells is present in nearly every neoplastic lesion and varies in size, composition, and distribution [6, 32]. However, tumor-associated macrophages (TAMs) are the most abundant immune cells of the TME leukocyte infiltrate [15, 14].

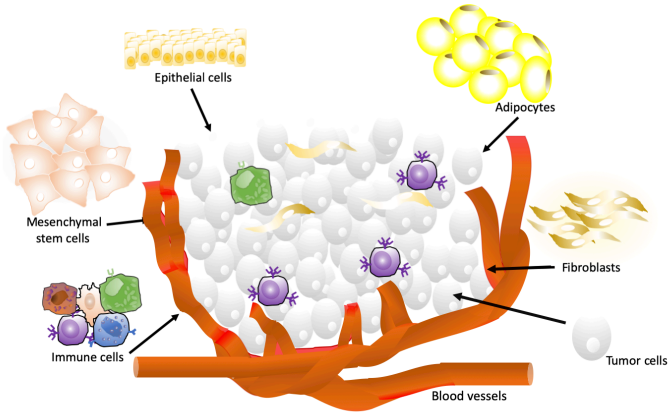

Figure 2.2: *The complexity of the TME, containing heterogeneous cancer cells in addition to a range of distinct cell types, including cancer-associated fibroblasts, adipocytes, epithelial cells, mesenchymal stem cells, and immune cells. Illustration by the author.*

2.5 Cancer Immunotherapy

The standard treatment methods of cancer currently rely on patient-specific monotherapy or combination therapy, involving chemotherapy, radiation therapy, and surgery. These treatment methods are associated with impending side effects due to damage to healthy tissues and severe toxicities [4, 5]. The promising advances in immunotherapeutic research notify a new pillar of cancer treatment, yielding decreased side effects and enabling controlled tumor growth for sustained periods. Today, there is a limited portion of immunotherapy treated patients who respond successfully. A significant area of research involves finding ways to predict the patient outcome to specific treatments. Also, a more in-depth understanding of cancers' immune evading mechanisms would facilitate the development of drugs [4].

The idea of cancer immunotherapy initially arose based on the hypothesis of cancer immune surveillance; an ability of the immune system to correctly identify and eliminate nascent tumors [41, 42]. For example, leukocytes found in connection with emerging tumors were previously thought to reflect an immunological attempt to eradicate the tumor [32, 25]. However, the paradoxical effect of tumor-promoting inflammation has become evident through increased knowledge of the intersection between inflammation and cancer pathogenesis [32, 25, 6]. The broader term of cancer immunoediting includes both the tumor protecting and the tumor developing actions of the immune system, and encompasses three phases [42, 43]:

1. *Elimination phase:* The immune system detects and eliminates developing tumor cells. If the tumor removal is insufficient, the immune system and the developing tumor might enter a temporary equilibrium state.

2. *Equilibrium phase:* The immune system contributes to an iterative selection and generation of tumor cells with an increasing ability to survive. If the immune response still fails to achieve complete elimination, the tumor is likely to enter the escape phase.

3. *Escape phase:* The immune system is no longer able to control the tumor progression.

The immunotherapeutic strategy is based on harnessing the body's immune system to induce a potent antitumor response [8, 9]. A variety of strategies attempts to re-engage the immune system to fight cancer, including stimulation of innate and adaptive immune effector mechanisms and counteraction of inhibitory and suppressive immune mechanisms [10, 41]. Immunotherapy can generally be classified as either "active" or "passive" based on their influence on the host immune system. While active immunotherapy involves engaging the patients' immune system to fight cancer, passive immunotherapy provides immune effectors that do not require an active immune response of the host. However, this classification does not adequately describe the action of most passive immunotherapeutic treatment strategies, as they often employ the host immune system to some extent. Strategies for active immunotherapy include anticancer vaccination with tumor antigens, direct administration of immune cells or oncolytic viruses to patients, increasing the cellular presentation of antigens, and using antibodies to enhance T cell activity.

Furthermore, the checkpoint blockade presents a promising approach based on blocking the inhibitory signals of lymphocytes with antibodies. While tumors can actively regulate immune-suppressing mechanisms, blocking these checkpoints might boost the host's immune response. Passive antibody strategies include treatment with monoclonal antibodies designed to target specific cancer cells, blocking growth factor signaling, and inhibiting angiogenesis. Other immunotherapeutic strategies include adoptive cellular therapy where patient-specific T lymphocytes are isolated, expanded, and improved, and genetic introduction of tumor-specific chimeric antigen receptors (CARs) that are linked to intracellular signaling domains [5, 10, 41, 10, 41].

2.6 Macrophages

Monocytes and macrophages are mononuclear phagocytes and subsets of leukocytes. These cells belong to the innate immune system, where they exhibit a broad spectrum of functions [20]. Alongside their contribution to tissue homeostasis and immunity, they are extensively involved in various pathological processes [13, 15]. During the last decade, macrophages have proved a prominent role in chronic inflammation, increasing the interest in exploiting them as therapeutic targets [20].

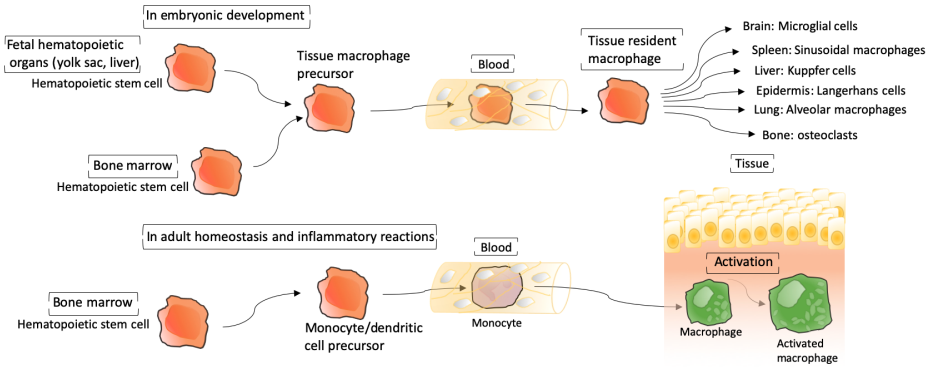

Figure 2.3: *Macrophages can mature both during embryonic development and adulthood. During embryonic development, specialized tissue-resident macrophages are seeded from precursors in the yolk sac or fetal liver. In adulthood, circulating monocytes derived from the bone marrow can enter tissues and contribute to inflammatory reactions. In peripheral tissues, these monocytes differentiate into macrophages and are further activated to specific phenotypes. Illustration by the author with the idea adapted from Abbas, Lichtman, and Pillai [33].*

Previously, homeostasis of tissue-resident macrophages was thought to depend on the constant recruitment of blood monocytes. However, recent evidence shows that monocytes and macrophages do not develop from a continuum of differentiation [13, 44, 15]. Generally, macrophages are tissue-resident cells important in homeostasis, development, and resolution of inflammation, whereas monocytes are circulating cells that are essential during inflammation and pathogen challenge [15, 44]. Macrophages can develop both dependent and independent of hematopoietic stem cells (HSCs), either during embryonic development or adulthood [45, 15]. Today, most macrophages are thought to originate from embryonic precursors that take residence in the tissues before birth [15]. The seeding of these macrophages is suggested to happen during several waves of embryonic hematopoiesis, originating from either yolk sac-derived macrophages or fetal liver-derived monocytes, as illustrated in Figure 2.3 [13, 45, 44, 15]. According to their residence tissue, macrophages take different names, such as osteoclasts in the bone, alveolar macrophages in the lung, microglial cells in the central nervous system, Langerhans cells in the skin, and Kupffer cells in the liver [46]. In an adult steady-state organism, tissue-resident macrophages proliferate to a varying extent depending on their residence tissue. In most tissues, a monocyte-derived supply is not needed to maintain a continuous population of macrophages [15,

13]. However, circulating monocytes produced by HSCs in the bone marrow might be recruited to infiltrate tissues and differentiate into macrophages [15, 44]. When normal tissue is facing a pathogenic challenge or going through a wounding process, a local increase of several chemokines, growth factors, and products of tissue breakdown arises. Successively, monocytes are attracted to the tissue of interest, where they differentiate into macrophages to mediate re-establishing responses for tissue homeostasis [47].

2.6.1 Macrophage polarization

Diversity and plasticity are hallmarks of the monocyte-macrophage lineage [6, 14, 16]. Macrophage plasticity involves genetic reprogramming, and change in phenotype and function of a mononuclear phagocyte in response to the surrounding environment [15, 17]. Macrophages present a high degree of adaptability; they acquire morphological and functional properties that are dependent upon their residence tissue and immunological microenvironment [14, 15, 16]. In the TME, macrophages can express both pro- and anti-tumor functions, as illustrated in Figure 2.4 [16].

Initially, the polarization of macrophages was separated into two distinct phenotypes. Analogous to the existing immunological nomenclatures, such as type 1 T-helper (T_H1) cells and type 2 T-helper (T_H2) cells, these separate forms of macrophage activation was denoted as M1 for classically activated macrophages and M2 for alternatively activated macrophages [14, 25, 15]. However, this dissection does not sufficiently present the extensive diversity of macrophage polarization [14, 15]. Instead, the M1 versus M2 paradigm denotes the extremes of a continuum of activation states that exists in an *in vivo* setting [14, 48]. For instance, TAMs do not fit well into the criteria for either M1 or M2 macrophages [19]. Moreover, classifying macrophage polarization states in a spectrum might appear as more informative compared to a linear scheme where M1 and M2 are placed at either end of a bipolar axis, as illustrated in Figure 2.4. A spectrum of macrophage populations illustrates that macrophages might evolve to share characteristics of several subpopulations [49].

In the growing field of macrophage research, a diversity of terminologies and inconsistent use of markers have been used to describe macrophage activation. Also, there has been a delay in comparing studies due to the lack of experimental standards. In their work, Murray et al. [50] recommend an initial set of nomenclature based on labeling the macrophage subtypes by defining the applied activation stimuli [23, 50]. In the case of M2 phenotype macrophages, several subcategories have been observed, often denoted as M2a, M2b, M2c, and M2d, induced by different stimuli and exerting different functions. M2a refers to macrophages activated by IL-4 and IL-13, M2b is is activated by immune complexes (Ic) combined with TLR ligands, and M2c is activated by glucocorticoid (GC) hormones and immunosuppressive cytokines, including IL-10. Using the tagging suggested by Murray et al. [50], the M2a group should be described as M(IL-4) or M(IL-4+IL-13), M2b as M(Ic), and M2c as M(IL-10) or M(GC), depending on the stimuli [51]. The most common method to study M2 polarization is by stimulating cells with IL-4 and IL-13, also described as M2a stimulation. However, according to previous literature, some TAMs appear similar to the M2b phenotype, while others have presented an M2c similar phenotype. Furthermore, TAMs have also been classified as another M2-like subtype, described as M2d, which is stimulated by IL-6, leukemia inhibitory factor (LIF), and adenosine [25,

19, 52]. Evidently, the nomenclature still fails to arrange the diversity of signals and activation states of macrophages. It is crucial to keep in mind that variations in the sources, receptors, combinations, and signaling pathways of the different stimuli induce diverse ranges of M1 and M2 activation states [21]. However, although the imperfect nomenclature of M1 and M2 phenotype macrophages show limited utility, it temporarily serves well to communicate the opposing phenotypes and their functions [14, 17].

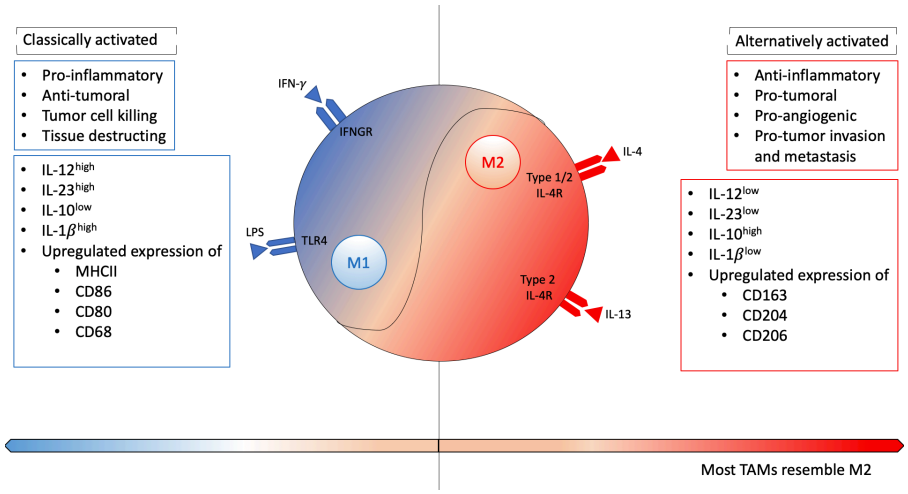

Figure 2.4: *Macrophages exert a dual yin and yang behavior in tumors. The bottom line presents the previous comprehension of macrophage classification as a linear scheme with M1 and M2 phenotypes placed at either end of a bipolar axis. A spectrum, illustrated in the middle, works better to classify the macrophage activation states, as some macrophages do not fit well into the criteria for either an M1 or an M2 phenotype. In this study, the focus is on IFN-γ and LPS activation for the M1 phenotype, and IL-4 and IL-13 activation for the M2 phenotype. In general, the M1-like macrophages share an IL-12^{high}, IL-23^{high}, IL-10^{low}, IL-1β^{high} phenotype, and it is typically identified an up-regulated expression of Major Histocompatibility Complex II (MHCII), CD68, and co-stimulatory molecules CD80 and CD86 [19, 24]. M1-like macrophages induce Th1 and Th17 cell pro-inflammatory responses, mediate resistance against tumors, directly induce tumor cell killing, and contribute to the destruction of tissue [16, 53, 19, 24]. Contrary, the M2-like phenotypes generally share an IL-12^{low}, IL-23^{low}, IL-10^{high}, and IL-1β^{low} profile [53, 19]. The M2 phenotype is associated with up-regulation of several scavenger mannose and galactose receptors, including CD163, CD204, and CD206 [14]. M2-like macrophages are known to participate in anti-inflammatory responses to promote tumor growth, angiogenesis, tumor invasion, and metastasis [19, 46]. Illustration by the author.*

Both the innate and the acquired immune responses are heavily dependent on macrophage coordination. Depending on their phenotype, macrophages play vital roles in either

triggering, instructing, or terminating an adaptive immune response. Macrophages utilize both cell-to-cell interactions and secretory mechanisms, including the release of cytokines, chemokines, enzymes, arachidonic acid metabolites, and reactive radicals to cooperate with T and B cells [22].

2.6.2 The M1 macrophage phenotype

Generally, M1 macrophages stimulate the adaptive immune responses and defend the body against bacterial infections [17]. The M1 phenotype is considered pro-inflammatory and is associated with the presentation of antigens, production of pro-inflammatory cytokines, generation of reactive oxygen species, and the ability to eliminate pathogens and cells [18, 15]. This macrophage phenotype is known to induce Th1 and Th17 cell inflammatory responses and to mediate resistance against tumors [16, 53, 19, 24]. M1 macrophage phenotypes are known to be induced by IFN-γ and bacterial products, such as lipopolysaccharide (LPS). However, several other stimulating agents have recently been linked to the M1 phenotype. Therefore, frequently, "M1" refers to macrophages activated by IFN-γ and bacterial products solely. In contrast, an "M1-like" denotation has been used to describe all polarization states leading to anti-tumor responses and cytotoxicity [14, 15]. Phenotypically, the M1 classified macrophages express high levels of MHCII, the cluster of differentiation 68 (CD68) marker, and the co-stimulatory molecules CD80 and CD86 [19, 24]. In general, the M1-like phenotype share an IL-12^{high}, IL-23^{high}, IL-18^{high}, IL-10^{low} profile, they are efficient producers of effector molecules, including inflammatory cytokines, such as interleukin 1 beta (IL-1β), tumor necrosis factor-alpha (TNF-α), and IL-6. Also, it is often identified an up-regulated expression of the intracellular protein suppressor of cytokine signaling 3 (SOCS3), and activation of inducible nitric oxide synthase (NOS2 or iNOS) to produce toxic effector molecules, including NO from L-arginine [16, 53, 19, 24].

2.6.3 The M2 macrophage phenotype

The M2 macrophage phenotype, commonly known to respond to IL-4 and IL-13, is essential in the healing of damaged tissue, and fighting off parasitic infections [17]. Generally, the M2 phenotype macrophages are considered anti-inflammatory, and they are known to participate in Th2 responses, allergy, helminth infections, tissue remodeling, and tumor promotion [46]. Like the simplification of the M1 nomenclature, "M2" might refer to macrophage phenotypes driven by IL-4 and IL-13 solely. In contrast, "M2-like" can include all the diverse phenotypes that share the effect of tumor promotion and suppression of effective adaptive immunity [14]. However, the subtypes classified as M2-like macrophages display a high degree of diversity, and they are, in several studies, assumed to cover all "non-M1" macrophages. The diverse phenotypes of M2 macrophages have in common the effects of tumor promotion and suppressing an effective adaptive immune response [15]. In general, the M2-like phenotype share an IL-10^{high}, IL-12^{low}, IL-23^{low}, and IL-$1\beta^{\text{low}}$ profile [53, 19]. The M2 phenotype is associated with the production of anti-inflammatory cytokines, and the up-regulation of several scavenger mannose and galactose receptors, including CD163, CD204, and CD206 [14, 18, 15]. Furthermore, M2 macrophages generally drive the arginine metabolism to produce ornithine and polyamine, promoting growth [19].

2.6.4 Tumor associated macrophages

As an essential component of the leukocyte infiltrate, TAMs are critical regulators of the cancer-related inflammation. Importantly, the prevalence of TAMs is often associated with a reduced overall prognosis in most solid tumors, including breast cancer, ovarian cancer, and melanoma. There are only a few exceptions that have been reported to associate a high density of macrophages with improved overall survival. These exceptions include colorectal cancer and non-small cell lung cancer. Besides, there is an uncertain role of TAMs in gastric cancer, where both positive and negative correlations between the survival rate and the presence of TAMs have been demonstrated [32, 20, 14]. In addition to the TAM density itself, overexpression of macrophage growth factors and chemokines is reported to correlate with poor prognosis [47].

The pool of TAMs in the TME can be composed of all types of macrophages, including local tissue-resident macrophages and tumor-infiltrating monocytes [14]. More research is needed on the ontogeny of TAMs in human malignant tumors. However, studies indicate that macrophages recruited from the blood contribute to the majority of TAMs [54]. Results based on murine tumor models have indicated a positive correlation between increased tumor size and the concentration of monocyte-derived TAMs. However, the origin of the TAMs does not seem to impact their phenotype. With the formation of an intratumoral vascular network, higher amounts of circulating monocytes infiltrate the tumor and differentiate into TAMs [55]. Collectively, established tumors often display abundant numbers of TAMs, and their presence is associated with increased tumor progression, invasion, and malignancy [54, 55, 14].

TAMs release pro-angiogenic growth factors and chemokines. In hypoxic areas of a tumor, transcription of hypoxia-inducible factors (HIFs), HIF-1 and HIF-2, are up-regulated, contributing to increased expression of growth factors, chemokines, and enzymes that trigger pro-angiogenic programs and attract more macrophages [16, 14]. TAMs and TAM products interact with neighboring cells and contribute to regulating cell senescence, remodeling the ECM, and suppressing adaptive immunity [16, 14]. The TAM production of growth factors and proteases, including matrix metalloproteinases (MMPs), degrades connective tissue and facilitates tumor growth and motility. Besides, TAM generation of reactive oxygen and nitrogen intermediates works to limit the effectiveness of chemotherapy and targeted therapies by accelerating cancer-cell genetic instability [14]. Elevated genetic instability in later stages of tumor progression might generate a vast diversity of subpopulations, further empowering therapeutic resistance [14, 3]. Macrophages that promote angiogenesis are commonly found in hypoxic areas of a tumor, whereas macrophages that drive invasion and metastasis are located at the tumor-stroma interface [20].

Expression of chemotactic factors in the TME both work to attract macrophages, and to activate transcriptional programs to skew their polarization towards specific phenotypes. In non-neoplastic tissues, there is an equilibrium between the M1 and M2 macrophage phenotypes [18]. In pathological conditions, the macrophage pool might consist of an unbalanced mix of M1 and M2 macrophage phenotypes, including macrophages that display intermediate activation statuses [20]. Importantly, environmental factors of the TME, such as hypoxia, are critical drivers of the macrophage diversity [14, 56]. Due to the complexity of cancer-related inflammation, a phenotypic diversity of TAMs develops both inter- and intratumorally [14]. Studies have indicated that, in progressive cancers, signals in

the TME skew the TAMs towards the M2 phenotype. In both mouse and human tumors, TAMs generally display an M2-like phenotype, supporting tumor growth through cancer cell proliferation, angiogenesis, invasion, and metastasis [16, 20, 14, 57].

2.7 THP-1 cell line

THP-1 is a human leukemia monocytic cell line isolated from the peripheral blood of a 1-year old male patient with acute monocytic leukemia [58]. This cell line consists of single, round suspension cells with the approximate doubling time varying between 16 and 26 hours. The THP-1 cells can be cultured *in vitro* up to passage 25 [59, 60, 58]. Using either phorbol-12-myristate-13-acetate (PMA), 1α,25-dihydroxy vitamin D3 (vD3), or macrophage-colony-stimulating factor (M-CSF), it is possible to differentiate THP-1 cells in the monocyte state into an adherent macrophage-like phenotype [58].

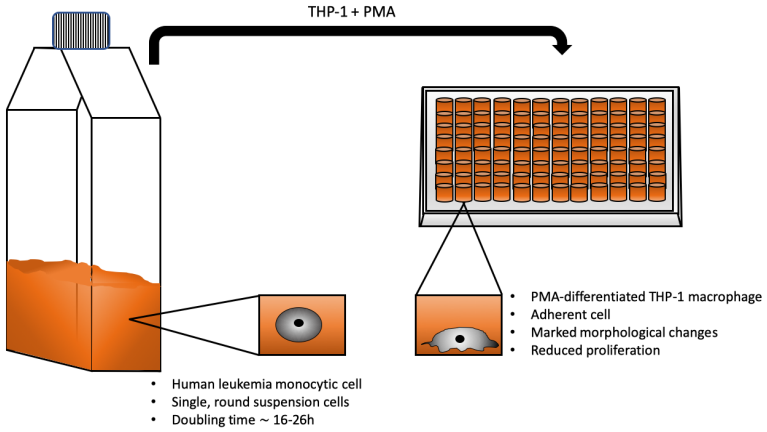

Figure 2.5: *Illustration presenting changed properties of THP-1 cells upon differentiation by PMA. The THP-1 single, round suspension cells acquire adherent properties and display marked morphological changes. In addition, the capacity to proliferate is reduced. Illustration by the author.*

Based on previous research, PMA is the most effective differentiation agent for developing mature THP-1 monocyte-derived macrophages [58, 59]. After exposure to PMA, the THP-1 cells acquire a flat and amoeboid shape, and they become strongly adherent, as illustrated in Figure 2.5 [59]. The author previously developed an optimized protocol for the PMA-differentiation of THP-1 monocytes, and this protocol is utilized and further investigated herein [1].

2.7.1 Potentials of a THP-1 macrophage model

When working to understand and investigate the polarization of macrophage phenotypes, studies on primary human macrophages hold the experimental limitations of limited life span in culture, and inability to expand *ex vivo* [61]. Additional challenges include donor variability, a heterogeneous genetic background, and possible contamination with other

blood components. Alternatively, homogeneous cell lines are widely studied to investigate a potential replacement of primary cultures. Previous literature indicates that PMA-differentiated THP-1 macrophages, exposed to the same stimuli as *in vivo*, can represent a simplified model to study macrophage polarization [58]. This macrophage-like cell line holds the potential to mimic primary human peripheral blood mononuclear cell (PBMC)-derived macrophages; hence, it is the most widely used model for primary human monocytes and macrophages [61]. The THP-1 cell line can be stored indefinitely in liquid nitrogen, and recovered without any notable reduction in cell viability or monocyte-macrophage features [58]. Besides, the homogeneous genetic background of the THP-1 cell line ensures minimal variability in the cell phenotype [59]. Although a model system based on primary human macrophages most closely represents the original situation, using a cell line simplifies the ability to develop robust and repeatable assays for the characterization of macrophage phenotypes.

Due to the large TAM population in many tumors, and their potential to support cancer development, an attractive therapeutic approach would be to deplete or re-educate them towards the M1 macrophage phenotype. Furthermore, macrophages have been found to impact the outcome of current anticancer therapy profoundly. It is essential to investigate the discovered yin-yang functions of TAMs, also combined with conventional anticancer treatment modalities, to develop more efficient therapeutic strategies [62]. Increased knowledge of macrophage diversity and related biomarkers is essential to develop improved therapeutic approaches targeting TAMs. Besides, identification of essential mechanisms determining macrophage polarization and diversity can enable the development of effective strategies for macrophage reeducation or depletion. A robust THP-1 macrophage model might contribute to the knowledge of how various pathways affects macrophage polarization [63]. Important transcription factors that contribute to the M1 polarization include nuclear factor-kappa B (NF-κB), signal transducer and activator of transcription 1 (STAT1), and interferon regulatory factor 5 (IRF5). IRF4, STAT6, and MYC, on the other hand, are related to the M2 macrophage phenotype [62]. Such a model can also be used to investigate the potential effect of specific chemical substances on macrophage polarization.

2.7.2 M1 stimuli and markers

For the polarization of macrophages into the M1 phenotype, potent stimulators include toll-like receptor (TLR) ligands, such as bacterial LPS, and cytokines, such as IFN-γ, TNF-α, and granulocyte-M-CSF (GM-CSF) [23, 24, 19]. The study presented herein focuses on stimulation by IFN-γ and LPS, also called M(IFN-γ+LPS), and detection of the putative M1 phenotype cell surface markers MHCII and CD80, and secreted cytokines TNF-α and chemokine [C-X-C motif] ligand 10 (CXCL10).

IFN-γ

IFN-γ is the principal cytokine associated with the polarization of macrophages towards the M1 phenotype. This cytokine is secreted by activated immune cells, including CD4+ T helper cell type 1 (Th1) lymphocytes, CD8+ cytotoxic T lymphocytes, NK cells, B cells, Natural killer T (NKT) cells, and professional antigen-presenting cells (APCs), including

macrophages themselves [64, 21, 22, 65]. APC secreted cytokines, particularly IL-12 and IL-18, stimulate the production of IFN-γ, whereas negative regulators include IL-4, IL-10, TGF-β and glucocorticoids [64]. IFN-γ binds to its cell surface receptors IFN-γ receptor 1 and 2 (IFNγR1 and IFNγR2), as illustrated in Figure 2.6, initiating oligomerization of the receptor subunits to activate the Janus kinases 1 and 2 (JAK1 and JAK2), facilitating trans-phosphorylation of both the JAKs and the cytoplasmic receptor domains. This phosphorylation recruits and initiates the STAT1 intracellular signal transduction pathway. After phosphorylation, STAT1 translocates to the nucleus and binds to promoter elements of DNA to stimulate transcription of STAT1 targeted genes. In addition to the JAK-STAT signaling pathway, IFN-γ also mediates gene transcription through other signaling pathways that either contributes to augmented STAT1 activity or that work independently of STAT1 [66, 64, 65].

IFN-γ control specific gene expression programs involving several cell adhesion molecules, cytokine receptors, and cell activation markers [21, 22]. Macrophages stimulated with IFN-γ express a potent ability to secrete pro-inflammatory cytokines, including IL-12, IL-15, IL-18, TNF-α, and IL-1β. Furthermore, they secrete Chemokine [C-C motif] Ligand 15 (CCL15), CCL20, CXCL9, CXCL10, CXCL11, and CXCL13, recruiting and coordinating NK and Th1 cells in type I immune responses. Besides, elevated expression of MHCII and costimulatory molecules CD80 and CD86 can be detected [22].

LPS

Pattern recognition receptors (PRRs), such as TLRs, work to detect pathogens. TLRs become activated when they recognize profiles of pathogens, known as TLR ligands, for example, bacterial LPS. LPS is a constituent on the cell wall of gram-negative bacteria [21, 22].

Through stimulation of TLR4, LPS induces the release of a potent pro-inflammatory profile of cytokines, chemokines, antigen-presenting molecules, and co-stimulatory molecules [21, 22, 67]. The LPS stimulation of TLR4 depends on interactions with several proteins, including LPS binding protein (LBP), CD14, and MD-2, illustrated in Figure 2.6. While LBP and CD14 facilitate the recognition of LPS, TLR4 and MD-2 form a receptor complex that is thought to enhance the LPS-binding [67]. Through interactions with the Toll-interleukin-1 receptor (TIR) domains, TLR4 oligomerization induces downstream signaling pathways that are either MyD88-dependent or MyD88-independent, where MyD88 works as a signaling adaptor [64, 67]. In addition to MyD88, the other TIR domain-containing adaptor proteins are TIRAP, TRIF, TRAM, and SARM. According to studies using MyD88-deficient macrophages, pro-inflammatory cytokine expression is related to the MyD88-dependent pathway, whereas induction of Type I interferons and interferon-inducible genes are linked to the MyD88-independent pathway [67]. The MyD88-dependent pathway activates the transcription factors NF-κB, activator protein-1 (AP-1), and IRF5 [21, 22, 67]. Similarly to MyD88, the MyD88-independent TRIF adaptor protein demonstrate activation of NF-κB and MAPK. Besides, this pathway activates transcription factor IRF3, which, together with NF-κB, induces transcription of Type I interferons and interferon-inducible genes [67]. The cytokine profile of LPS activation includes IL-6, IL-12, TNF-α, IFN-β, and IL-1β, and the chemokines include CCL2, CXCL10, and CXCL11. Furthermore, TLR4 activation leads to increased expression of

antigen-presenting molecules, including MHC molecules, co-stimulatory molecules, and antigen-processing peptidases [21, 22]. LPS alone is usually unable to completely develop the M1 profile due to the insufficient production of IL-12 [21].

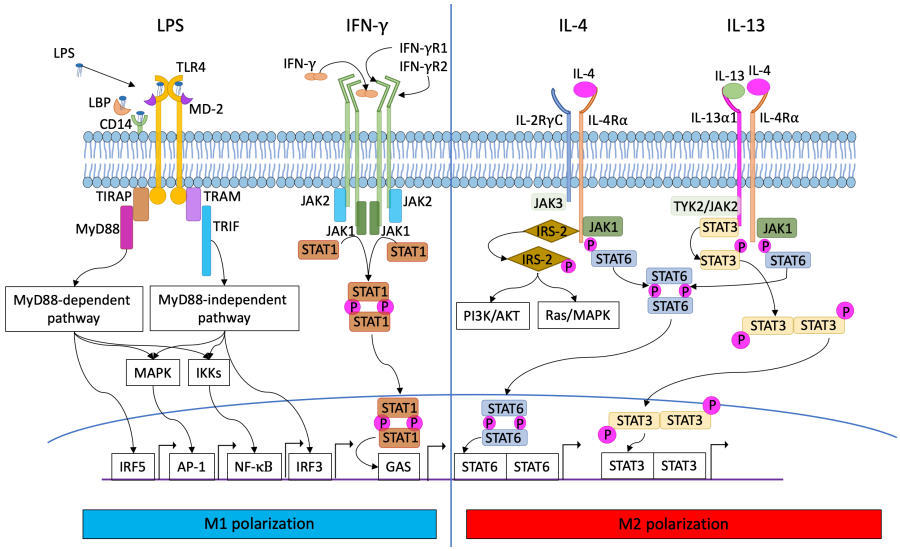

Figure 2.6: *A simplified scheme of the signaling pathways of the selected macrophage polarization agents. Illustration by the author with the idea adapted from Martinez and Gordon [21] and Lu, Yeh, and Ohashi [67].*

MHCII

MHC molecules' physiologic role is to display peptide antigens for recognition by antigen-specific T lymphocytes, thereby fundamentally regulating the immune response [26, 68]. While class I MHC molecules present intracellular antigens and are expressed on all nucleated cells, class II MHC is expressed mainly on the APCs of the immune system, including DCs, B cells, and macrophages to present internalized protein from the extracellular environment [68, 69]. The principal function of MHCII on macrophages is the presentation of antigens to CD4+ effector T-cells to induce cell-mediated immune responses. The expression of MHCII on macrophages is low or negative and markedly enhanced by IFN-γ [68].

While the antigen-specific T-cell receptors or B-cell receptors initiates the activation of T and B cells, the definitive immune response is determined by a simultaneous signal provided by co-stimulators [70, 68]. The two-signal hypothesis of T-cell activation is often used to explain T-cell interaction with APCs [71, 72];

1. Signal one: MHC molecules on the APC presents antigenic peptide to the T-cell

receptor.

2. Signal two: Co-stimulatory or co-inhibitory signals. One of the essential co-signaling pathways results from the interaction between CD80 and CD86 to their receptors CD28 and cytotoxic T lymphocyte antigen 4 (CTLA4).

CD80

CD80 (also known as B7-1) is a member of the B7 family of activating and inhibitory co-stimulatory molecules. Professional APCs and hematopoietic cells are the primary cells that present the CD80 co-signaling cell-surface glycoprotein, and it has an essential role in directing and fine-tuning T-cell responses [71, 72]. The co-signaling molecules either work as co-stimulators or co-inhibitors to promote or suppress T-cell activation, respectively. CD80 works as a co-stimulator for T-cell responses after binding to CD28, whereas it works co-inhibitory by interacting with CTLA4 [72]. The expression of co-stimulatory molecules by macrophages is low and inducible by TLR ligands, IFN-γ, and T cells [68]. Recently, an upregulated expression of specific inhibitory B7 molecules has been detected on cells of the TME, including cancer cells, stromal cells, and immune cells. Furthermore, human tumor cells and tumor-associated APCs have been found to express low levels of CD80 and CD86. Imbalance in the expression of co-stimulatory and co-inhibitory molecules might participate in tumor immune evasion, and can strongly affect the tumor-specific T-cell immunity [71].

CXCL10

CXCL10 is a pro-inflammatory chemokine that is a member of the CXC chemokine family. In response to IFN-γ, a wide range of cells, including monocytes, secret CXCL10 to preferentially attract and activate Th1 lymphocytes to the inflammatory, infectious, or neoplastic area. This chemokine participates in chemotaxis and binds to the CXCR3 receptor primarily expressed by Th1 lymphocytes, NK cells, DCs, macrophages, and B-cells. CXCL10 also attracts and activates CXCR3-positive cells, contributing to inflammation and tissue damage. Binding of CXCL10 initiates regulation of cell growth, apoptosis, and angiostatic effects. Recently, chemokines have been suggested as contributors to the initiation and progression of cancer. Importantly, based on the presence or absence of the structural domain of Glu-Leu-Arg (an ELR motif), CXC chemokines contribute to stimulation or inhibition of angiogenesis, respectively. CXCL10 does not contain the ELR motif, and at regular expression, this chemokine dampens angiogenesis and support anti-tumor functions [73].

TNF-α

TNF-α is a central pro-inflammatory cytokine and an essential regulator of macrophage function. Interestingly, while macrophages are highly responsive to TNF-α, they are also considered the primary producers of this cytokine. Other TNF-α producers include lymphoid cells, mast cells, endothelial cells, and fibroblasts [74]. TNF-α acts through two transmembrane receptors, TNF receptor 1 and 2 (TNFR1 and TNFR2), to influence essential cell functions, including survival, differentiation, and cell proliferation [75]. Potent

stimulators of TNF-α production include infection, trauma, and bacterial products such as LPS. At the transcriptional level, NF-κB is an essential factor that regulates the secretion of TNF-α and TNFα-induced reactive oxygen species (ROS) gene expression [75]. The secretion of this cytokine profoundly impacts the activation and recruitment of inflammatory cells; it is an early mediator and richly expressed in inflamed tissues. Besides, it is considered a master regulator in the pro-inflammatory cytokine network [75, 76]. However, TNF-α is a pluripotent inflammatory cytokine that can drive the generation of ROS, and contribute to the activation of both oncogenes and tumor suppressors. The role of TNF-α in cancer progression is an ongoing matter of debate, and there are questions whether it should be treated as a therapeutic or a target in malignant disease. Importantly, the chronic production of TNF-α in the TME highly contributes to the regulation of cancer-related inflammation [76, 77]. The opposing pro-tumor or anti-tumor TNF-α effect depends on an intricate balance between high and low levels of TNF-α, where a low and constitutive TNF-secretion of cancer cells has been linked to increased tumor growth [77, 76].

2.7.3 M2 stimuli and markers

For the polarization into the M2 phenotype, potent stimulators include IL-4, IL-13, and IL-10, transforming growth factor-beta 1(TGF-β1), glucocorticoids, and M-CSF [19]. The various simulators and combinations of stimulators result in several subcategories of the M2 phenotype with diverse functions [25]. The study presented herein focuses on stimulation through IL-4 and IL-13, also called M2a macrophages or M(IL-4+IL-13), and detection of the putative M2 phenotype cell surface markers CD163 and CD206, and secreted cytokines IL-1R receptor agonist (IL-1Ra) and IL-10.

IL-4 and IL-13

Th2 cells, mast cells, basophils, and macrophages themselves are the primary producers of IL-4 and IL-13 [22, 21]. The defining feature of Th1 or Th2 cells is a high secretion of either IFN-γ or IL-4, respectively, two reciprocally antagonizing cytokines [64]. As illustrated in Figure 2.6, IL-4 can bind two different receptor complexes; either the high-affinity type I IL-4 receptor, or the low-affinity type II IL-4 receptor. The type I receptor complex is formed when the IL-4/IL-4Rα binds the IL-2Rγ chain, whereas the type II IL-4 receptor complex is formed when the IL-4/IL-4Rα binds to IL-13Rα1. IL-13, on the other hand, binds to two separate chains, namely IL-13Rα1 and IL-13Rα2. If bound to IL-13Rα1, the IL-13/IL-13Rα1 complex recruits IL-R4α, forming a type II receptor. Therefore, IL-13 binding promotes signatures that resemble that of IL-4; however, they do not fully overlap [21].

IL-4 signaling through the type I receptor activates JAKs and downstream signaling to activate transcription factor STAT6 and insulin receptor substrate 2 (IRS-2), whereas type II receptor signaling predominantly activates STAT6. IRS-2 activates signaling pathways involving phosphatidylinositol 3-kinase (PI3-K) and AKT [78]. Subsequently, IL-4 and IL-13 stimulate downregulation of pro-inflammatory molecules such as IL-1, IL-6, IL-8, IL-12, TNF-α, IL-1β, IFN-γ, GM-CSF, and CCL2. These macrophages perform decreased phagocytic activity and induce macrophage fusion. Several scavenger receptors

and C-type membrane lectins are upregulated through IL-4 induction. IL-13 binding promotes signatures that resemble that of IL-4; however, they do not fully overlap [21, 22]. Moreover, IL-4/IL-13 increases the production of IL-1ra, express fibronectin 1 (FN-1), coagulation factor XIII, and insulin-like growth factor 1 (IGF-1). These signals contribute to coordinating tissue repair and proliferation [22].

CD163

CD163 is a trans-membrane scavenger receptor that binds to haptoglobin-hemoglobin complexes, thereby mediating the metabolism of hemoglobin [79, 80]. Specifically, this membrane protein is expressed at high levels by macrophages, and almost exclusively by cells of monocytic linage [81]. While M2 macrophages and TAMs have been found to express higher amounts of CD163, the expression is not restricted to the M2 phenotype [51, 79]. The upregulated expression of CD163 in macrophages is considered one of the major contributors to switching the macrophage activation towards an anti-inflammatory phenotype [82]. In addition to the trans-membrane CD163, CD163 also exists as a soluble variant (sCD163) in serum which is upregulated during severe inflammation [81, 82]. Apparently, sCD163 results from the shedding of the cell surface, and it can be mediated by activation of TLR by LPS or PMA, crosslinking of FCγR, and oxidative stress [81]. According to Møller [81], sCD163 and CD163 exists in an inverse relationship.

CD206

The macrophage mannose receptor, CD206, is a carbohydrate-binding receptor that can recognize pathogens and endogenous glycoproteins [83, 84]. Mannose bearing molecules in the extracellular environment is supposed to have a short half-life, and it signals for effective and anti-inflammatory clearance [85]. Pathogenic microbes are often covered in structures containing mannose, leading to interaction with CD206-expressing macrophages [83]. Through excellent affinity binding and scavenging of high mannose N-linked glycoproteins and hormones in the circulation, CD206 contributes to maintaining homeostasis and reduces inflammatory responses. CD206 is expressed by most tissue macrophages, DCs, and specific lymphatic or endothelial cells [85, 83]. M2-like macrophages and TAMs express high levels of CD206, and CD206 are investigated as a target for both diagnosis and therapy in cancer. Macrophages that express CD206 and CD163 are found to produce high amounts of IL-10, IL-1Ra, and CCL18 [82].

IL-10

IL-10 is one of the main anti-inflammatory associated cytokines. This cytokine works to limit the host damage by antagonizing and preventing excessive immune responses upon TLR recognition. The production of IL-10 is associated with a wide variety of immune cells, both belonging to the innate and the adaptive immune system, emphasizing an essential function in inflammatory feedback regulation [86, 87]. Upon binding to the heterodimeric IL-10 receptor (IL-10R1, IL-10R2) on macrophages and DCs, STAT3 signaling is activated and decreases the secretion of pro-inflammatory mediators. Successively, Th1-type responses, antigen presentation, and phagocytosis are prevented and scavenging,

tolerating, and inhibiting functions of the cells are increased [88, 86]. Furthermore, the IL-10R complex's activation contributes to the transition from the M1 to the M2 phenotype of macrophages and induces the expression of specific anti-inflammatory molecules, including IL-1Ra and soluble receptors of TNF-α [88, 87].

IL-1Ra

The IL-1Ra is a naturally occurring anti-inflammatory protein and an antagonist of the IL-1 receptor. Included in the IL-1Ra family of molecules are one secreted isoform (sIL-1Ra) and three intracellular isoforms (icIL-1Ra1-3). While the intracellular isoforms of IL-1Ra exhibit unclear biological roles, the secreted isoform is mainly thought to function as a regulator of the pleiotropic effects of IL-1 by preventing association between the Type I IL-1 receptor (IL-1RI) and the IL-1 receptor accessory protein (IL-1RAcP). Through competitive binding of the IL-1 cell surface receptors, IL-1 and IL-1Ra contribute to the progression or the suppression of inflammatory processes. The pro-inflammatory agonists IL-1α, and IL-1β promotes binding of IL-1RI and IL-1RAcP to initiate signal transduction leading to translocation of NF-κB to the nucleus. Successively, antagonizing effects mediated by IL-1Ra is important to prevent the development or progression of inflammatory disease. A maintained balance between IL-1 and IL-1Ra is critical in the regulation of the overall inflammatory response. [89, 90].

2.7.4 The NF-κB singling pathway

NF-κB is a crucial regulator of several genes that are important in immune responses. For example, this transcription factor is the primary driver of LPS-stimulated pro-inflammatory gene expression [26, 27]. Importantly, inflammation contributes in a complex manner in cancer, where it seems to exert both pro-tumorigenic and anti-tumorigenic functions. In particular, this dual function might also apply to the role of the NF-κB signaling pathway. Whereas a bursting activation of NF-κB is associated with an increased cytotoxic immune response against cancer cells, constitutive and moderate activation of NF-κB is often observed in several types of cancer, yielding tumor-supporting functions. Also, the fact that chronic inflammation has proved the potential to promote cancer development and progression points out the potential pro-tumorigenic effect of a constitutively increased activation of NF-κB [91].

In mammalian cells, five NF-κB proteins are known; NF-κB1/p50, NF-κB2/p52, RelA /p65, RelB, and c-Rel. These proteins share a Rel homology domain that exerts various functions, including the domain that binds to DNA, the nuclear localization sequence (NLS), and the site that binds NF-κB inhibitors (IκBs). The IκBs includes a family of proteins, where IκBα is the most extensively studied. When NF-κB is uninduced, the NLS is sterically blocked by IκBs, avoiding NF-κB nuclear translocation [26, 91, 92, 74]. Nuclear translocation of NF-κB is triggered when the NF-κB:IκB complex is disturbed. When stimulated, an IκB kinase (IKK) specifically catalyzes the phosphorylation of IκB. IKK is a protein complex consisting of two catalytic polypeptide subunits, IKKα and IKKβ, and a regulatory polypeptide subunit IKKγ [92]. Commonly, phosphorylation of IκB further initiates polyubiquitination and degradation of IκBα. Hence, NF-κB is released and able to translocate to its site of action in the nucleus [92, 74, 91].

The NF-κB transcription factor generally signals in either the canonical or the non-canonical pathway, to regulate a wide variety of genes contributing to cell stress or immunological responses. Immune responses and inflammation are associated with the canonical pathway of NF-κB activation, which is either dependent or independent of IKK [26, 91]. In the canonical NF-κB pathway, TLRs, IL-1R, TNFR, and antigen receptors can all mediate signaling upon binding to LPS, IL-1β, TNF-α or antigens, respectively [92, 74, 91]. Following an acute inflammatory response, the transcriptional activity of NF-κB is usually completely terminated to the background level. This de-activation primarily results due to an inhibitory feedback circuit, as NF-κB up-regulates its main inhibitors, namely the members of the IκB family. Inconsistently, in chronic inflammation, the transcriptional activity of NF-κB persists at an increased and constitutive level. This persistence results probably due to the disruption of the inhibitory feedback mechanism by a constant supply of activating stimuli [91].

The NF-κB transcription factor works in a highly sophisticated manner to regulate several essential effector genes, both in tumor cells and in healthy cells in the TME. Consequently, NF-κB might not be an ideal immune target itself, but investigating the pathways of NF-κB activation might work as a tool to identify the contributing genes to promotion or inhibition of tumor immunity in various cell types of the TME [26, 93]. A framework for the investigation of specific pathways contributing to immune responses would utilize in the development of targeted therapies. Herein, we investigated the role of the DNA repair enzyme 8-oxoguanine-DNA glycosylase 1 (OGG1) inactivation of THP-1 macrophages [94].

OGG1

The initiation and the progression of inflammation are associated with the generation of ROS, leading to oxidative damage of DNA [27]. The most frequent oxidative lesion in the genome is mutagenic products of oxidized guanine, mainly 7,8-dihydro-8-oxoguanine (8-oxoG), in guanine-rich promoter regions. Guanine is the nucleobase in DNA that is the most vulnerable to oxidative damage, due to its low oxidation potential. One of the main DNA repair enzymes in eukaryotic cells is OGG1. This enzyme recognizes and binds to 8-oxoG in DNA with high affinity, and catalyzes the initiating step of the DNA 8-oxoG base excision repair (BER) pathway [27, 95, 96, 94]. OGG1 is a multifunctional protein, and, in addition to repair premutagenic 8-oxoG DNA base modifications, recent literature suggests a gene regulating function of the OGG1:8-oxoG complex [95, 96]. A decreased inflammatory response is seen in the absence of functional OGG1, which might be explained by the gene regulatory functions of OGG1 [27]. Apparently, the binding of OGG1 to oxidized guanines at promoter regions facilitates the recruitment of downstream transcriptional effectors, including NF-κB [27, 94].

In their research, Seifermann et al. [96] investigated the role of OGG1 upon LPS-activation of primary mice splenocytes. Their results presented a direct role of OGG1 in signal transduction and regulation of genes. Recently, two mechanisms of the apparent OGG1 regulatory functions have been suggested [96];

1. The OGG1:8-oxoG-complex binding to and activating small guanosine triphosphate hydrolase enzymes (GTPases).

2. OGG1 working as an additional transcription factor of diverse genes that are transiently bound to 8-oxoG in the promoter region.

In case of the OGG1-dependent TNF-α secretion in mice macrophages, the results of Seifermann et al. [96] indicated a gene regulatory function of OGG1. Apparently, OGG1 contributes to a lysine-specific histone demethylase (LSD1)-dependent pathway in LPS-activated secretion of TNF-α. While LSD1 plays an epigenetic role in the local increase of 8-oxoG in regulatory regions of specific genes, subsequent recruitment and binding of OGG1 might be required to initiate an efficient transcription. Consequently, LSD1 and OGG1 might collaborate in the same mechanism of gene regulation to activate the LPS-induced expression of TNF-α in macrophages [96].

2.7.5 Targeting pathways of NF-κB activation

Visnes et al. [27] found that both TH5487 and the IκB kinase inhibitor, BMS-345541, prevent inflammatory gene expression by perturbing NF-κB. While BMS-345541 inhibits the activation of NF-κB, TH5487 prevents the recruitment of OGG1, thereby decreasing the occupancy of NF-κB to DNA that contains 8-oxoG [27].

Positive control, BMS-345541

BMS-345541 is a highly selective inhibitor of the IKK catalytic subunits, IKKα and IKKβ, which inhibit the NF-κB-dependent transcription of pro-inflammatory cytokines. BMS-345541 affects the active sites of the IKK catalytic subunits apparently by binding to the same allosteric sites on IKKα and IKKβ. This binding is thought to provide a conformational change in the IKK subunit that affects the active sites, Ser-32 and Ser-36. Hence, phosphorylation, ubiquitination, and proteolytic digestion of IκB are prevented. Successively, BMS-345541 inhibits signal-induced activation and translocation of NF-κB [97].

TH5487

In their research, Visnes et al. [27] developed TH5487, a pharmacologically useful compound that selectively engages and inhibits the active sites of OGG1 in cells. By engaging OGG1, TH5487 prevents this enzyme from recognizing and binding to its DNA substrate. When OGG1-binding to 8-oxoG at promoter regions is inhibited, the DNA occupancy of OGG1-dependent transcriptional effectors, including NF-κB, is perturbated, preventing the expression of OGG1-dependent pro-inflammatory genes. According to Visnes et al. [27], LPS-induced pro-inflammatory cytokine expression was inhibited in a dose-dependent manner in cells treated with TH5487 [27]. Therefore, inhibiting OGG1 might work as a strategy to avoid inflammation [27].

2.7.6 The mTOR signaling pathway

The mammalian target of rapamycin (mTOR) signaling pathway works as a fundamental regulator of cell growth, proliferation, metabolism, and survival [98]. The serine/threonine-protein kinase, mTOR, is present in two protein complexes, mTOR complex 1 and 2 (mTORC1 and mTORC2). The mTORC1 protein contributes as a central regulator of

cell growth and metabolism by integrating four essential signals: growth factors, energy status, oxygen, and amino acids [99, 98, 100]. However, the understanding of the mTOR signaling network is not complete, and the mTOR pathway is deregulated in several diseases, including cancer [99]. As reviewed in Weichhart, Hengstschläger, and Linke [101], the mTOR network in innate immune cells is activated via multiple signals, including growth factors and TLR ligands. Activation of the mTOR pathway plays an essential role in integrating the extracellular availability of nutrients and the intracellular metabolic processes [29]. Hence, the activation regulates the cellular metabolism to adjust the energy supply to the subsequent immune response. Besides, several transcription pathways are regulated upon mTOR activation, including NF-κB, STAT3, and HIFα [101]. In recent studies, the mTOR pathway has been suggested to play a crucial role in the survival and polarization of macrophages, although the role is complex and incompletely understood. M1 and M2 phenotypic macrophages are not only regulated by cytokines and growth factors but also environmental cues, including the presence of metabolites, suggesting a link between the metabolic pathway and the resulting phenotype [29, 16, 101]. Furthermore, results have presented a discordant effect of the mTOR pathway on macrophage viability and polarization [28, 29]. Rapamycin induced inhibition of mTORC1 has presented increased polarization towards the M1 phenotype in human macrophages, suggesting that activation of the mTOR-pathway promotes M2 macrophage polarization. However, M1 macrophage polarization has been reported upon increased mTORC1 activity and reduced mTORC2 activity. Overall, previous research indicates opposing effects on macrophage polarization following regulation of the mTOR pathway [28, 29, 101].

Rapamycin

Rapamycin was the first recognized inhibitor of the mTOR pathway. This compound is used both during organ transplants and in anti-cancer therapy, as an immunosuppressive and anti-proliferative agent. However, Rapamycin has displayed contradictory roles, and an immunostimulatory effect on blood leukocytes from patients after transplantation has also been reported [30]. Apparently, inhibition of the mTOR pathway by Rapamycin can exert multiple effects depending on the cell type and environmental stimuli. Importantly, the mTORC1 and mTORC2 protein complexes display opposing sensitivity to Rapamycin. While mTORC1 is immediately sensitive to inhibition by Rapamycin, mTORC2 is only inhibited by Rapamycin in specific tissues and cells following long-term chronic exposure [98, 100].

2.8 Experimental techniques

In this master's thesis, variously polarized THP-1 macrophages were investigated by flow cytometry for cell surface marker expression, whereas secretion of cytokines was analyzed by Sandwich ELISA. CellTiter-Glo (CTG) was used to measure the metabolic activity of the cells.

2.8.1 The fundamentals of fluorescence

In Flow cytometry, the use of fluorescence enables the identification and quantification of subpopulations of cells within a cell suspension. Fluorescence is a three-stage process based on the creation of an excited electronic singlet state, as illustrated in the Jablonski diagram in Figure 2.7. This process takes place in fluorophores, which are molecules that particularly respond to light [102, 103]. Both naturally fluorescing substances in the cells and fluorescent labeling can create fluorescent signals in flow cytometry. A fluorophore can be covalently attached to target molecules, such as a particular protein or a nucleic acid, to accomplish fluorescent labeling. Antibodies are the most commonly labeled molecules used to detect specific targets [103]. At their ground state, the electrons of the fluorophore exist in their lowest energy stable configuration (S_0), and the fluorophore does not fluoresce. Upon exposure to an external energy source, such as a laser, photons are absorbed by electrons of the fluorophore molecules. Upon absorption of this energy, the electrons will excite to a higher electronic singlet state (S_2). This process is known as excitation, and the amount of energy required for excitation varies between different fluorophores. The excited lifetime is transient and usually lasts for a short time of about 1-10 nanoseconds. When the electron is in its excited state, some energy of the S_2 state dissipates due to conformational changes in the fluorophore. This energy loss brings the excited electron to a more stable singlet excited state (S_1). From this semi-stable excited state, the electron might return to its ground state (S_0), accompanied by the emission of a photon to release the remaining excess energy. In certain instances, S_1 might also be depopulated by other processes, such as intersystem crossing, which is not included in Figure 2.7. Upon fluorescence, the emitted photon is of lower energy compared to the absorbed photon due to the energy loss. Therefore, the emitted wavelength is longer with a different color than the absorbed light. The fluorophore can absorb light again, and go through the entire process repeatedly, resulting in a cyclic fluorescence process [102, 103, 104].

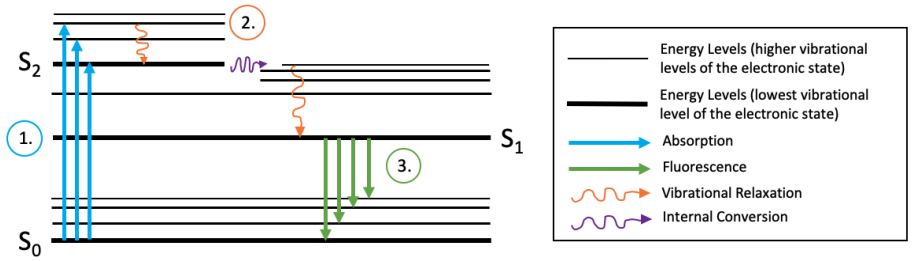

Figure 2.7: *Jablonski diagram illustrating the three-stage process of fluorescence. 1. Excitation. The energy of a photon is absorbed by the fluorophore, promoting the excitation of an electron to one of the vibrational levels of the excited electronic singlet state (S_2). 2: The time in the excited state. The fluorophore undergoes different processes that, among others, lead to dissipation of the energy of S_2 to the singlet excited state S_1. 3: Fluorescence Emission. The fluorophore has returned to its ground state S_0 when the remaining excess energy is emitted in the form of a photon. Illustration by the author, inspired by the illustration presented by Instruments [105] and Scientific [102].*

2.8.2 Flow cytometry

A flow cytometer is a sophisticated, laser-based instrument that enables detailed and rapid analysis of a heterogeneous population of particles, such as cells, in a fluid stream [106]. The approach makes it possible to measure multiple physical characteristics of single cells in suspension when they pass through a light source [106, 107]. A particular cell protein can be labeled with a specific fluorophore-conjugated antibody [108]. The main components of a flow cytometer are fluidics, optics, an electronic network, and a computer [106, 107]. A schematic of a flow cytometer is illustrated in Figure 2.8. The fluidic system transports the cells through the instrument. In the flow cytometer, a sheath fluid, commonly phosphate-buffered saline (PBS), surrounds the core sample stream, which is the cell suspension. The formation of parallel streams is accomplished through laminar flow and hydrodynamic focusing. By varying the pressure of the sample stream, relatively to the sheath stream's constant pressure, uniform illumination of single cells can be achieved [106].

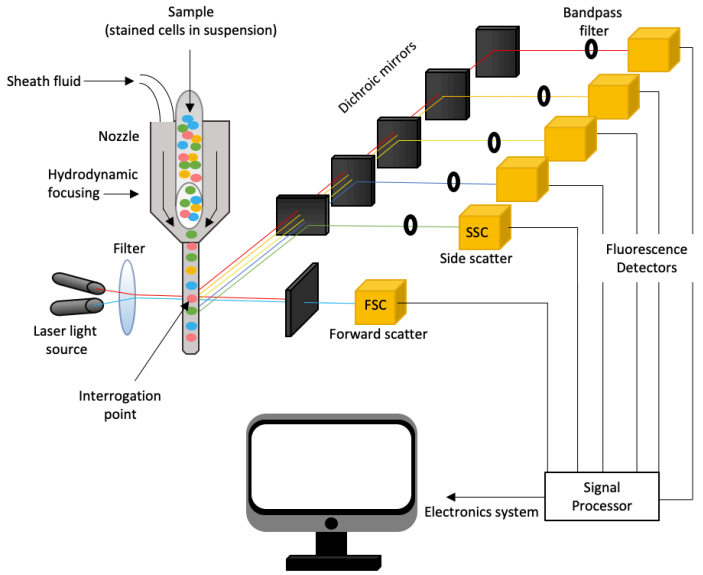

Figure 2.8: *Schematic diagram of a flow cytometry system and its critical components. Stained cells in suspension are illuminated one-by-one to induce light scattering and excitation of the cell-associated fluorophores. Various detectors detect fluorescence emission. Illustration by the author.*

At the interrogation point, a single cell interacts with the laser light to induce light scattering and excitation of the cell-associated fluorophores. Depending on how the detector is placed relative to the laser's path, forward angle scattered (FSC) and side angle scattered (SSC) light is collected and measured. The light scattering is directly related to the structural and morphological properties of the cell. Generally, FSC measurements increase proportionally to the cell surface area; hence, it provides information on the size of the cell.

On the other hand, SSC measurements are proportional to the granularity or the internal complexity of the cell and can thus be used to determine the relative cellular complexity. Furthermore, the excitation of the labeled fluorophores produces fluorescence emission that can be detected [107, 109]. The fluorescence emission gives information on the number of fluorescent probes bound to the cell or the cellular components [106]. Depending on the wavelength of the laser in the flow cytometer, specific fluorophores can be used. Several fluorochromes might exist that can absorb the laser's particular wavelength, but emit light of different wavelengths. Therefore, various fluorochrome-marker complexes can be measured simultaneously. This method is called polychromatic flow cytometry, and it is possible by the use of dichroic mirrors and several fluorescence detectors. Although band-pass filters select the ranges of excitation and emission of wavelengths, emission spectra might overlap. If these spectra overlap, a chosen detector might detect fluorescence from more than one fluorochrome, creating fluorescence spillover [110]. Fluorescence compensation through a mathematical algorithm ensures the removal of any overlap between the different emission spectra. The aim of this correction is for a particular detector to solely report the signal of one specific fluorochrome [111, 110]. The detected photocurrents are digitized and processed through an electronic network, and the results are displayed in histograms or two-dimensional dot-plot formats [107].

Compensation

Compensation is a mathematical method that is used to avoid spectral overlap and spill-over in multicolor fluorescence studies. The fluorophores used in flow cytometry emit photons of several energies, and fluorescence from various fluorochromes can be detected in a channel if there is an overlap in their emission spectra. With the use of more lasers and detectors, the importance of compensation is unavoidable. The establishment of an accurate compensation matrix is critical for the success of the experiment [112, 113]. Controls are essential in the development of the compensation file, and the following controls should minimally be included [114, 112]:

1. **Unstained samples:** The forward and side scatter detection of the cell population has to be characterized, and the unstained samples' fluorescence position has to be determined. This detection will enable separation of the results from variations due to background fluorescence and autofluorescence. Furthermore, it enables suitable settings of voltages and negative gates.

2. **Single stained samples:** Single stained samples are used to investigate the spectral overlap between different fluorophores. The spectral overlap has to be compensated between every fluorophore that is included when performing multicolor flow cytometry. The concentration and brightness of the fluorophores have to be kept constant through the experiments.

3. **Viability controls:** Because dead cells easier non-specifically bind to antibodies and present increased autofluorescence, they can disturb the quality of the fluorescent measurements and create false positives. The identification and gating on viable cells can be achieved using a live/dead dye and gating based on forward and side scatter.

2.8.3 Enzyme-linked immunosorbent assay

An enzyme-linked immunosorbent assay (ELISA) is a specific type of enzyme immunoassay (EIA) designed to detect and quantify substances of interest using antibodies. In an ELISA, one or more antigens from a variety of samples can be detected by utilizing highly specific antibody-antigen interactions [115, 116]. Immobilization of the antigen of interest is done either directly, by adsorption of the antigen to the assay plate, or indirectly, by using a capture antibody attached to the plate [115]. Subsequently, detection of the antigen is accomplished by a detection antibody. The detection antibody is either directly or indirectly linked to an enzyme or another tag. Standard enzyme labels include horseradish peroxidase (HRP) and alkaline phosphatase (AP). The conjugated enzyme activity is assessed by incubation with a substrate that fulfills the required assay sensitivity. A measurable product, such as a change in color, fluorescence, or luminescence, can then be detected and quantified by the instrument [115, 116].

Sandwich ELISA

Sandwich ELISA is a highly sensitive assay format where the antigen is bound between two primary antibodies, as illustrated in Figure 2.9. Consequently, this assay requires matched antibody pairs that detect different epitopes of the antigen. A capture antibody immobilizes the antigen, which can then be detected by a detection antibody. The detection antibody can be either enzyme-conjugated, giving direct sandwich ELISA, or dependent upon a secondary enzyme-conjugated detection antibody, giving indirect sandwich ELISA [115, 117]. Sandwich ELISAs do not require purification of the antibody before the assay and is therefore suited to the analysis of complex samples, including measuring cytokine levels of an immune response [117].

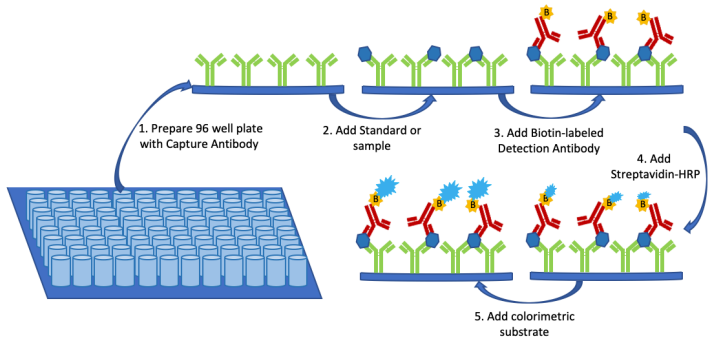

Figure 2.9: *In Sandwich ELISA, specific Capture Antibodies are coated on a 96-well plate, enabling binding of the target protein in the added standard and samples. Next, a biotin-labeled Detection Antibody is added, followed by the addition of HRP-conjugated streptavidin. In the last step, a solution containing a colorimetric substrate is pipetted into the wells, creating a color intensity that is proportional to the amount of bound target protein. Illustration by the author.*

2.8.4 CellTiter-Glo

The CellTiter-Glo Luminescent Cell Viability Assay is based on a luciferase reaction to detect the level of Adenosine triphosphate (ATP). In this method, a single CTG-reagent is added directly to the cell containing media to generate luminescence. The CTG-reagent consists of a cell lysis detergent, ATPase inhibitors to stabilize ATP released from the lysed cells, a luciferin substrate, and luciferase to catalyze a reaction to generate photons [118, 119]. When a cell dies, there is a rapid drop in the ATP level as the cell metabolism shuts down. Besides, when the cell membrane integrity is lost, remaining ATP from the cytoplasm will be removed by endogenous ATPases [118]. Upon the addition of a CTG-reagent, the detergent will lyse the viable cells. As the ATPase inhibitors are added simultaneously, the measured ATP-level will indicate the amount of metabolically active cells before the reagent addition. The luciferase enzyme will act on luciferin to produce oxyluciferin when Mg^{2+} and ATP is present. This reaction generates energy in the form of luminescence. Hence, there will be a proportional relationship between the produced luminescence and the ATP level, and the luminescent output will correlate to the amount of metabolically active cells [119].

CHAPTER 3

Material and Methods

3.1 Compounds

Phorbol 12-myristate 13-acetate (PMA) (#1652981-5MG, PeproTech) (20 mM) stock solutions were prepared in cell culture-grade dimethyl sulfoxide (DMSO). For dilution of polarizing agents, a bovine serum albumin (BSA) stock solution (0.1%) was prepared in sterilized, deionized water. Stock solutions of both Recombinant Human IL-4 (#200-04, PeproTech) and Recombinant Human IL-13 (#200-13, PeproTech) were prepared by reconstitution in sterilised deionized water to 0.1 mg/mL, followed by further dilution in the 0.1% BSA to 20 μg/mL and 50 μg/mL, respectively. The stock solution of Recombinant human IFN-γ (#300-02, PeproTech) was prepared by reconstitution in sterilized deionized water to 1.0 mg/mL, followed by further dilution in 0.1% BSA to 50 μg/mL. Stock solutions of Lipopolysaccharides (LPS) from Escherichia coli O111:B4 (#L2630-10MG, Sigma-Aldrich) were prepared by reconstitution in sterile Dulbecco's PBS (DPBS) (#D8537-500ML, Sigma-Aldrich) to 1 mg/mL and further diluted in DPBS to 100 ng/mL. All stock solutions were stored in sterile Eppendorf tubes at -20°C. Stock solutions of all polarizing agents were stored in Protein LoBind Tubes of 0.5 mL (#022431064, Eppendorf AG). For each experiment, the desired amounts of compounds were defrosted and freshly prepared in the cell culture medium. TH5487 (10 mM) was a gift from dr. Torkild Visnes, SINTEF, Trondheim. Free and poly(alkyl cyanoacrylate)(PACA)-encapsulated Rapamycin was a gift from dr. Yrr Mørch, SINTEF, Trondheim. TH5487 (10 mM), PACA-encapsulated Rapamycin (7.3 mM), free Rapamycin (10 mM), and BMS-345541 (#B9935, Sigma-Aldrich) (20 mg/mL) stock solution were all prepared in DMSO and stored at -20°C.

3.2 Cultivation of THP-1 cells

3.2.1 Thawing of THP-1 cells

Before thawing, the human THP-1 cell line (ATCC TIB-202) was stored in a liquid nitrogen vapor phase in Eppendorf tubes at $7.30 * 10^6$ cells/mL in FBS supplemented with 10% DMSO. The following procedure was used for the thawing of THP-1 cells:

1. Heat the Eppendorf tube containing THP-1 cells in a 37 °C water bath for 120 seconds.

2. Transfer the cells drop by drop to a 15 mL-tube containing 9 mL of pre-heated RPMI 1640, supplemented as detailed in Section 3.2.2.

3. Centrifuge the cell suspension at 130 x g for 5 minutes in a Heraeus Megafuge 1.0.

4. Remove the supernatant and re-suspend the remaining cell pellet in 5 mL pre-heated RPMI 1640.

5. Count the viable cells, as described in Section 3.2.3.

6. Add fresh RPMI 1640 medium to attain the approximate cell density of $2.2 * 10^5$ cells/mL.

7. Cultivate 20 mL of the cell suspension in an untreated T75 cell suspension flask (#658-195, CELLSTAR).

8. Incubate the T75 flask in the upright position at 37°C and 5% CO_2 in a HERACELL VIOS 160i CO_2 incubator (Thermo Scientific).

3.2.2 THP-1 cell cultivation

The medium used for the THP-1 cell cultivation was RPMI 1640 [318700-025, Gibco] supplemented with 10% FBS, 0.05 mM 2-mercaptoethanol, 100 U/mL penicillin-streptomycin, 2 mM L-glutamine, and 10 mM HEPES Buffer Solution (15630-056, Gibco).

The THP-1 cell suspension was stored in T75 suspension culture flasks (#658-195, CELLSTAR), incubated at 37°C and 5% CO_2 in a HERACELL VIOS 160i CO_2 incubator (Thermo Scientific). The T75 flasks were stored in the upright position, with volume kept at 20 mL. The cell suspensions were maintained by the addition of fresh medium two to three times a week to keep the approximate density of $2.2 * 10^5$ cells/mL. The cell suspensions were not allowed to exceed the density of $8 * 10^5$ cells/mL. If the cell density reached $8 * 10^5$ cells/mL, cells were split by transferring the cell suspension to a 50 mL tube. The cell suspension was centrifuged at 130 x g for 5 minutes in a Heraeus Megafuge 1.0 and resuspended in fresh RPMI 1640 to reach the desired concentration of $2.2 * 10^5$ cells/mL. Cells were cultured and used in experiments up to passage 25.

3.2.3 Counting of viable cells in culture

The *Countess II^{TM} Automated Cell Counter* (Invitrogen) was used to calculate the concentration of viable cells in suspension. In a 1:1 ratio, 10 μL Trypan blue stain 0.4% (T10282, Invitrogen) and 10 μL cell suspension were mixed, and 10 μL of this mix was transferred into a counting chamber slide. Viable cells with intact membranes are not colored by the Trypan blue stain, enabling estimation of the percentage of viable cells.

3.3 Differentiation and polarization of THP-1 cells

The protocol used for differentiation and polarization of THP-1 macrophages in this Master's thesis builds on the optimized PMA-differentiation protocol developed by the author during the specialization project [1]. The experiments conducted during the specialization project included image analysis and measurements of metabolic activity of variously differentiated and polarized THP-1 macrophages. The results indicated that in conditions of incubation with PMA-containing medium for three days, 15 nM PMA resulted in stable adhesion and differentiation of THP-1 differentiated macrophages. The exposure time to PMA was set to three days, as cells incubated for one day resulted in signs of unstable differentiation [1]. The PMA concentration was kept at 15 nM to prevent a possible up-regulated expression of specific M1 phenotype relevant genes at higher PMA concentrations, as suggested in the specialization project and previous literature [120, 121, 1]. Based on previous studies, PMA in amounts of 25-100 ng/mL has resulted in an up-regulated expression of specific M1 phenotype relevant genes [120, 121, 1].

According to Daigneault et al. [122], including days of rest in PMA-free medium after the PMA-induced macrophage differentiation results in THP-1 macrophages with retained plasticity to polarizing stimuli. The resting period also induces THP-1 macrophages that more closely resemble MDMs, and limits constitutive cytokine production [122, 121]. Results presented in the specialization project indicated a maintained and stable PMA-differentiation at 15 nM PMA following three days of rest in PMA-free medium [1].

According to studies that have observed morphology, cytokine secretion, and gene expression profiles of polarized THP-1 macrophages, the generation of the M2 THP-1 macrophage phenotype seems to acquire prolonged exposure time to polarizing agents, as compared to the M1 THP-1 macrophage phenotype [1, 63]. Therefore, in the experiments conducted herein, the time of polarization was varied between six hours, one, three, and five days.

The concentrations of all polarizing agents, except for LPS, were kept similar to those suggested in the specialization project [1]. While the LPS concentrations used in most literature varies between 1 to 100 ng/mL [123, 124, 125], Genin et al. [63] reduced their LPS concentration to 10 pg/mL. This research group found that higher concentrations of LPS were linked to a gradual loss of viability. Similar observations were noticed during the specialization project, where an increased time of exposure to LPS reduced the metabolic activity of THP-1 macrophages [1]. Furthermore, Genin et al. [63] suggested that higher concentrations of LPS might contribute to an unspecific expression of M2 macrophage markers in pro-inflammatory M1 macrophages [63]. Based on these observations, the previously used concentration of 100 ng/mL LPS was lowered to 0.1 ng/mL in the study

conducted herein.

3.3.1 Protocol for differentiation and polarization

During incubation, all well plates were stored in a humidity chamber inside a HERACELL VIOS 160i CO_2 incubator (Thermo Scientific) at 37°C and 5% CO_2.

1. Prepare the cell suspension in the desired volume and cellular concentration for the specific well plate of choice. Use RPMI 1640 [318700-025, Gibco], supplemented as detailed in 3.2.2.
    - By example, for Costar^R 6-well Clear TC-treated Multiple Well Plates, prepare THP-1 cell suspensions at the concentration of $3 * 10^5$ cells/mL.
2. Dilute the PMA stock solution in PBS and add the desired volume to achieve the total concentration of 15 nM PMA in the cell suspension. Mix thoroughly by pipetting. Add the PMA-containing cell suspension to the wells.
3. Incubate the well plates at 37°C and 5% CO_2 for three days.
4. Remove the supernatant, wash the cells once with PBS, and add fresh PMA-free RPMI 1640.
5. Incubate the well plates at 37°C and 5% CO_2 for three days.
6. Remove the supernatant, wash the cells once with PBS, and add fresh PMA-free RPMI 1640, with the specific addition of polarizing agents to achieve the desired macrophage phenotype.
    - **For M1 polarization:** add 0.1 ng/mL LPS and 20 ng/mL IFN-γ.
    - **For M2 polarization:** add 20 ng/mL IL-4 and 20 ng/mL IL-13.
7. Incubate the well plates for the desired exposure time. After six hours, one, three, or five days of exposure to the polarizing agents, investigate the cells and supernatants.

3.4 Investigation of polarized THP-1 macrophages

To assess whether the THP-1 macrophages were polarized towards the M1 and M2 phenotypes, phenotypic cell surface markers were investigated by flow cytometry, and cytokine secretions were analyzed by ELISA. Unpolarized M0 macrophages were used as biological controls, incubated in medium without any polarizing agents, for the same amount of time.

3.4.1 Flow cytometry

Flow cytometry was performed to evaluate the amount of polarized THP-1 macrophages expressing putative M1 and M2 specific cell surface markers. The flow cytometry investigations were performed using a Gallios Beckman Coulter Flow Cytometer (Calibur) with four lasers and ten colors.

Staining of macrophages

Fluorescent-conjugated antibodies were used to stain the M1 and M2 phenotype macrophage markers MHCII (M1), CD80 (M1), CD206 (M2), and CD163 (M2). In addition to these antibodies, PI was included as a dead stain to enable gating on viable cells. PI labels DNA by intercalating between the nucleic acids. Importantly, PI can only label the DNA of dead and membrane-compromised cells, as this fluorescent stain is membrane-impermeant [126]. Table 3.1 lists the fluorescent-conjugated antibodies that were used, their expected expression based on literature ([19, 24, 16, 53, 18, 14, 15]), and details on the lasers, wavelengths, and detectors of the flow cytometer that were used.

Table 3.1: *Table presenting the fluorescent-conjugated antibodies used for detection of the M1 and M2 phenotypes and their expected expression. In the table, M1 denotes M(IFN-γ + LPS), and M2 denotes M(IL-13 + IL-4). M0 denotes macrophages that are not exposed to any polarizing stimuli.*

Fluorescent-conjugated antibodies and expected expression			
Fluorescent-conjugated antibody	**Expected expression**	**Excitation laser**	**Detector**
PerCP-Cy 5.5 Mouse Anti-Human HLA-DR (#552764, BD Pharmingen^{TM})	$M1^{high}$ $M2^{low}$ $M0^{low}$	Blue laser, λ = 488 nm	FL4, λ = 695 nm, 30 nm bandpass filter
APC-H7 Mouse Anti-Human CD80 (#561134, BD Pharmingen^{TM})	$M1^{high}$ $M2^{low}$ $M0^{low}$	Red laser, λ = 633 nm	FL8, λ = 755 nm Low-pass filter
FITC Mouse Anti-Human CD206 (#551135, BD Pharmingen^{TM})	$M1^{low}$ $M2^{high}$ $M0^{low}$	Blue laser, λ = 488 nm	FL1, λ = 525 nm 40 nm bandpass filter
BV421 Mouse Anti-Human CD163 (#562643, BD Pharmingen^{TM})	$M1^{low}$ $M2^{high}$ $M0^{low}$	Violet laser, λ = 405 nm	FL9, λ = 450 nm 50 nm bandpass filter
Propidium Iodide (L7011COMPONENTB, Invitrogen)	Stains dead cells	Blue laser, λ = 488 nm	FL3, λ = 620 nm 30 nm bandpass filter

Development of the fluorescence compensation matrix

To prepare for multicolor fluorescence flow cytometry experiments, it is essential to establish an effective protocol, and an accurate compensation matrix. In the development of these necessities, following cell samples were analysed after one, three, and five days of exposure to polarizing agents:

- Separate samples of unstained M1, M2 and M0 polarized THP-1 macrophages.
- Separate samples of M1, M2 and M0 macrophages, dead stained by PI.
- Separate and single stained samples of M1, M2 and M0 macrophages with either of the fluorescent-conjugated antibodies.

- Separate samples of M1, M2 and M0 macrophages single stained with either of the fluorescent-conjugated antibody together with PI.

Compensation ensures that the fluorescence detected in each specific detector results from its target fluorochrome. The compensation matrix was developed as listed below, and the resulting compensation matrix is included in Appendix A, Table 1.

1. Unstained samples were used to set the voltages for the fluorescence channels. The cell population was defined by adjusting the forward and side scatter. These adjustments work to exclude much of the dead cells and debris.
2. Single stained samples of each cell type (M1, M2, M0) were used to analyse their expression of each fluorochrome. These measurements were used solely to observe the signal in all channels and to set the compensation.
3. The compensation were investigated in all channels, using Kaluza Analysis 1.5 a Software. The compensation began with the fluorochromes of higher wavelengths, and continued down to the lower wavelength end of the spectrum.

When the protocol and the compensation matrix were developed, the multicolor fluorescence experiments were performed. However, the combination of PerCP-Cy5.5 Mouse Anti-Human HLA-DR to the other fluorochromes had to be avoided due to the high degree of emission overlap, especially against APC-H7 Mouse Anti-Human CD80.

Flow cytometry protocol

For the whole procedure, store cells and reagents on ice, and keep out of direct exposure to light.

1. Prepare FACS buffer: 1% FBS in DPBS (#D8537-500ML, Sigma-Aldrich)
2. Collect supernatant for ELISA, as described in Section 3.4.3.
3. Wash cells with 1 mL/well PBS (if using a 6-well plate).
4. Detach cells with Accutase solution (#A6964-100ML, Sigma-Aldrich):
    - Thaw the Accutase solution overnight in the refrigerator. Do not pre-warm.
    - Add 1 mL/well of Accutase and incubate at room temperature (RT) for 30 min.
    - Inspect under a microscope for signs of cell detachment.
    - If cells do not appear significantly detached, incubate an additional 2-3 minutes.
    - If there are significant signs of detachment, add 1 mL/well of medium and triturate.
    - Transfer each cell suspension to a separate 2.0 mL microcentrifuge tube.
5. While the cells are incubated with Accutase, prepare the antibody mix. A volume of 30 μL is needed per microcentrifuge tube.

- Mix APC-H7 Mouse Anti-Human CD80, BV421 Mouse Anti-Human CD163, FITC Mouse Anti-Human CD206, and FACS buffer in ratio 1:1:2:20.
- Mix PerCP-Cy 5.5 Mouse Anti-Human HLA-DR and FACS buffer in ratio 1:10.

6. Count the cells to be able to adjust the volume for further analysis. The desired concentration is $1.0 * 10^6$ cells/mL.
7. Centrifuge at 1300 rpm for 5 minutes and remove the supernatant.
8. Add antibody mix:
   - Add 30 μL antibody mix/tube.
   - Incubate for 30 minutes at 4°C.
   - Add 100 μL FACS buffer/tube.
9. Centrifuge at 1300 rpm for 5 minutes and remove the supernatant.
10. Add 300 μL FACS buffer/tube, or adjust the volume to attain the desired concentration.
11. Add PI:
    - Gently vortex the PI to dissolve the dye prior to opening the vial.
    - Add 5 μL of room tempered PI per 1 mL solution. With 300 μL FACS buffer, add 1.5 μL PI.
    - Incubate for 15 minutes at RT while transferring the solution to FACS tubes.
12. Run the Flow cytometer.

3.4.2 Flow Cytometry Data Analysis

The results acquired during the flow cytometry measurements were analyzed using Kaluza Analysis 1.5 a software.

Development of Density plots

The stained samples investigated in the flow cytometry experiments in this thesis included a single population of cells, which were polarized towards either the M1, M2, or M0 macrophage phenotype. Successively, the generated flow data only presents a shift in fluorescence, and a density plot can not be directly created from each data set. However, density plots can be created from samples where several fluorescent-conjugated antibodies are added to a single population. Thus, analysis can reveal the percentage of cells exposed to M1 polarizing stimuli that either develop into the M1 phenotype, continue the M0 status, or develop into the M2 phenotype. Similarly, the expression of M0, M1, and M2 phenotype macrophages can be investigated in the population of cells that were unexposed to polarizing agents, or exposed to the M2 polarizing agents. The parameter histograms were utilized to generate such density plots, as illustrated in Figure 3.1. The procedure for the construction of these density plots is described next.

- Make single parameter histograms that display the relative fluorescence of a specific antibody on the x-axis and the cell count on the y-axis, gated on viable cells (Histogram 1 and 2 in Figure 3.1).

    1. Make an overlay histogram with the data sets attained from both the M1 and M2 polarized cells, and the M0 control cells. Present the data from the specific channel that is to be investigated (for example, FL9 in Histogram 1, and FL8 in Histogram 2, Figure 3.1), and gate on viable cells. An overlay of the different populations allows the identification and comparison of cells signaling positive for the specific antibody.

    2. Add a region by inserting an overlay marker to evaluate the percentage of cells that express the antibody of interest. Present the percentage of gated cells, and adjust the overlay marker so that 2.5% of the control cells (M0) are included in the gate (marked in red squares in Figure 3.1).

- Create a density plot for the specific sample that is to be investigated (in Figure 3.1, this is the M0 sample) by including the same data set of this sample that was used in the single parameter histograms. Add data from the specific channels that were investigated in both of the Histogram 1 and 2, and gate on viable cells. As illustrated in Figure 3.1, the FL8 channel of the data set (also analyzed in Histogram 2) is presented on the x-axis of the density plot, whereas the FL9 channel of the data set (also analyzed in Histogram 1) is presented on the y-axis of the density plot.

    1. Add a quadrant gate to the density plot. Investigate the overlay marker in both the single parameter histograms to find their interceptions with the x-axis (as presented in the enlarged parts of Histograms 1 and 2 in Figure 3.1).

    2. As the FL8 channel is presented along the x-axis of Density plot 3 (Figure 3.1), the interception between the vertical gate and the x-axis is set equal to the interception on the x-axis in Histogram 2 presenting the FL8 data.

    3. As the FL9 channel is presented along the y-axis of Density plot 3 (Figure 3.1), the interception between the horizontal gate and the y-axis is set equal to the interception on the x-axis in Histogram 1 presenting the FL9 data.

    4. When the quadrant gate is adjusted correctly, it can be used to investigate the percentage of macrophage phenotypes expressed within an equally exposed group of cells.

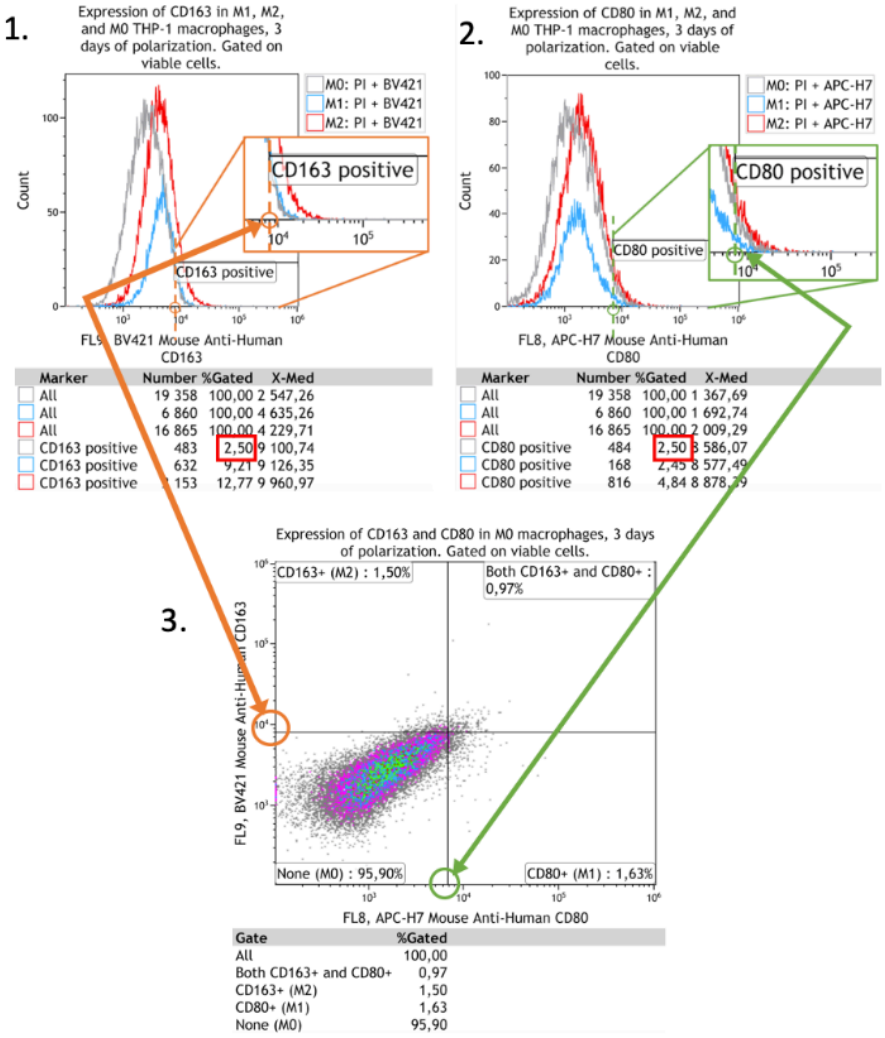

Figure 3.1: *Histogram 1 and 2 present the BV421 Mouse Anti-Human CD163 and APC-H7 Mouse Anti-Human CD80 fluorescence intensities, respectively, on the x-axis and the cell count on the y-axis, gated on viable cells. These histograms were constructed based on the same sample of cells, stained with both these fluorescent-conjugated antibodies. These two histograms was further used to develop the Density plot 3, and enable analysis of the percentage of the unpolarized control cells, in addition to possible expressions of the M1 or the M2 macrophage phenotypes.*

3.4.3 Sandwich ELISA

Sandwich ELISA was performed to evaluate the secretion of the putative M1 and M2 phenotype specific cytokines and chemokines; TNF-α (M1), CXCL10 (M1), IL-10 (M2), and IL-1Ra (M2).

The following DuoSet ELISA kits containing Capture Antibody, Detection Antibody, and Recombinant Standard were used for the analyses:

- Human CXCL10/IP-10 DuoSet ELISA (#DY266-05, R&D Systems)
- Human IL-10 DuoSet ELISA (#DY217B-05, R&D Systems)
- Human IL-1ra/IL-1F3 DuoSet ELISA (#DY280-05, R&D Systems)
- Human TNF-alpha DuoSet ELISA (#DY210-05, R&D Systems)

The contents of each kit were reconstituted, aliquoted, and stored according to the manufacturer's instructions. All the ELISA analyses were performed in Corning^{R} 96 Well Half-Area Microplates (#CLS3695, Sigma-Aldrich). An Infinite 200 PRO microplate reader (Tecan Life Sciences) was used to determine the optical density of each well.

Sample preparation

- Following exposure to polarizing agents for the desired amount of time, pipette supernatant from separate wells into 2 mL centrifuge tubes. Centrifuge at 1500 rpm for 10 minutes at 4°C.
- Immediately aliquot the supernatant and store samples at -80°C. Minimize freeze-thaw cycles.
- Before use after thawing, centrifuge samples at 10.000 rpm for 5 minutes at 4°C to remove any precipitate. Store the samples on ice during the ELISA procedure.

Sandwich ELISA protocol

Day 1, Plate preparation:

1. Prepare Capture Antibody in DPBS to the desired working concentration.
2. Coat the 96 Well Half-Area plates with 50 μL/well of the diluted Capture Antibody. Seal the plate with an adhesive strip, and incubate overnight at RT.

Day 2, Plate preparation:

1. Prepare Reagent Diluent (RD) and Washing Buffer (WB). For all DuoSet ELISA kits used herein, the following are required:
    - RD: 1% BSA in PBS 1x, pH 7.2-7.4. Dissolve BSA in powder (#A9418, Sigma-Aldrich) in DPBS by pipetting and vortexing. Vacuum filter the RD to remove unsuspended solutes.
    - WB: 0.05% Tween 20 (#P1379, Sigma-Aldrich) in PBS, pH 7.2-7.4.

2. Aspirate each well and wash the plate three times with 75 μL/well of WB. Completely remove any remaining WB by inverting the plate and blotting it against a clean paper towel.

3. Block the plates by adding 50 μL/well of RD. The BSA will bind to non-specific sites of the Capture Antibody, allowing a more specific binding to the target molecule.

4. Incubate for 1 hour at RT. In the meanwhile:

   - Thaw the samples you want to study. Follow the Sandwich ELISA sample preparation guide above. Prepare a 1:3 dilution of all samples, diluted in RD. The dilutions are tested to ensure that one of the samples falls within the linear range of the standard curve.
   - Prepare the Standard solution by dilution in RD to achieve the maximum working concentration, presented in the specific ELISA kit data sheet. Vortex the Standard, and prepare a 2-fold serial dilution of the Standard solution in RD to achieve seven dilutions. Include a blank sample composed of only the buffer.

5. Repeat the aspiration and wash as in Step 2.

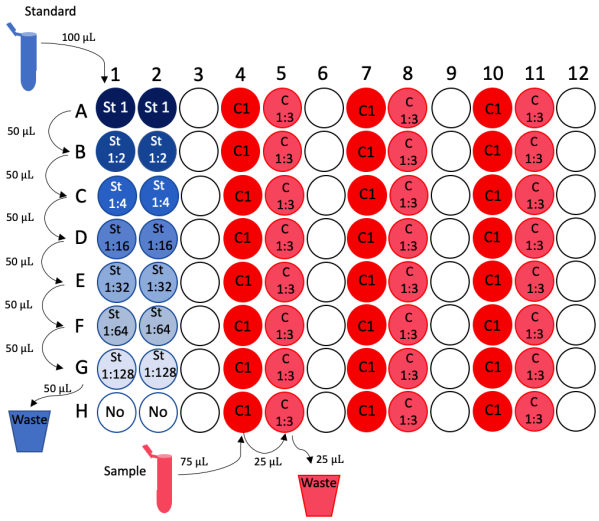

Figure 3.2: *Illustration of how the Standard solutions and samples were added in the 96-well half area plates. Rows of wells were left empty between the various samples and the Standard to minimize spillover.*

Day 2, Assay procedure:

1. Add 50 μL/well of sample or standard solutions, following the scheme in Figure 3.2. Add both standards and samples in duplicate.

2. Cover the plate with an adhesive strip and incubate for 2 hours at RT. At the end of the incubation time, prepare Detection Antibody in RD to the desired working concentration.

3. Repeat the aspiration and wash as in Step 2 of Day 2, Plate preparation.

4. Add 50 μL/well of the diluted Detection Antibody.

5. Cover the plate with a new adhesive strip and incubate for 2 hours at RT. At the end of the incubation time, prepare Streptavidin Conjugated to horseradish-peroxidase (Streptavidin-HRP) 40x (#RPN1231-2ML, R&D Systems). As Streptavidin-HRP is photosensitive, cover the Falcon tube in aluminium foil.

6. Repeat the aspiration and wash as in step 2 of Day 2, Plate preparation.

7. Add 50 μL/well of Streptadivin-HRP 40x. Streptavidin-HRP binds to the Fc segment of the Detection Antibody, allowing the binding of TMB-ELISA.

8. Incubate for 20 minutes in the dark at RT. In the meanwhile, aliquot the necessary amount of TMB ELISA (3,3',5,5'-Tetramethylbenzidine) (#T0440, Sigma-Aldrich) in a Falcon tube covered in aliuminium foil, and equilibrate to RT.

9. Repeat the aspiration and wash as in step 2 of Day 2, Plate preparation.

10. Add 50 μL/well of TMB-ELISA. TMB-ELISA reacts with Streptavidin-HRP bound to the Detection Antibody, resulting in a classical blue color.

11. Incubate for 20 minutes in the dark at RT. In the meanwhile, prepare 2.5 mL/plate of H_2SO_4 2N (1M). Do it under the hood.

12. Add 25 μL/well of H_2SO_4 2N (1M). Gently tap the plate to ensure thorough mixing. Sulfuric acid blocks the reaction between Streptavidin-HRP and TMB-ELISA, resulting in a classical yellow color.

13. Determine the optical density of each well by using a microplate reader set to 450 nm. Also determine the optical density of each well at 570 nm. A Tecan infinite 200 PRO microplate reader was used herein.

3.4.4 Sandwich ELISA Data Analysis

The data attained from the Tecan Infinite 200 PRO microplate reader was was processed using Microsoft Excel version 16.36.

1. Subtract readings at 570 nm from the readings at 450 nm to correct for optical imperfections of the plate.

2. Calculate the average absorbance for each set of duplicate standards and samples.

3. Use the blank sample to subtract the background absorbance from all the averages.

4. Generate a Standard curve for the target protein by using a 4-parameter algorithm. In the graph, the values of the mean standard absorbance (y-axis) is plotted against the associated known concentrations (x-axis).

5. Apply the dilution factors. In the 3-fold diluted samples, the absorbance is multiplied by 3.

6. The mean absorbance value of each sample is plotted in the Standard curve equation to get the final concentration of the target protein.

3.5 Utilizing the M1 polarized THP-1 macrophages

3.5.1 Titration of M1-polarizing agents

A titration study of various concentrations of LPS and IFN-γ was performed to depict the dose-response relationships and find a condition of polarization where the cells were not over-stimulated. The purpose of this concentration study was to enable investigation of a potential effect of TH5487, BMS-345541, and Rapamycin on the LPS- and IFN-γ-stimulated THP-1 macrophage secretion of TNF-α. It the THP-1 macrophages are over-stimulated, a potential inhibitory effect might not be observable. Herein, we investigated for concentrations of LPS and IFN-γ activating stimuli, the agonists, that resulted in a response somewhere between the maximum and the baseline responses. Therefore, to enable the definition of these concentrations, the baseline, and maximum response must first be defined [127].

In the titration study, 96-well culture plates (#165305, Thermo Scientific^{TM} Nunc^{TM}) were prepared with 100 μL/well of medium containing $2 * 10^5$ cells/mL and 15 nM PMA, as described in Section 3.3.1. Following PMA-exposure and rest in PMA-free medium, three-fold dilution series of LPS and IFN-γ were added, as illustrated in Figure 3.3. The starting concentration of the dilution series were the previously investigated concentrations of 100 pg/mL LPS and 20 ng/mL IFN-γ used in the polarization studies, multiplied by three.

Following exposure to the various concentrations of LPS and IFN-γ for 24 hours, the supernatant was collected and prepared as described in the ”Sample preparation guide” in Section 3.4.3. Successively, the concentrations of TNF-α were measured and analyzed by Sandwich ELISA, as described in Section 3.4.3 and 3.4.4, respectively.

GraphPad Prism version 8.4.2 for macOS was used to create semi-logarithmic XY scatter charts presenting the average measured secretion of TNF-α $\pm$ standard deviations on the y-axis, versus the increasing concentrations of either LPS or IFN-γ presented on a logarithmic x-axis. In a semi-logarithmic XY scatter chart, the dose-response curve typically has a characteristic sigmoidal shape. From this curve, a secreted concentration less than the maximal response can be chosen on the y-axis, and the agonist concentration can be estimated by calculating the anti-log value of the corresponding x-value. This method was utilized herein to estimate concentrations of LPS and IFN-γ for the subsequent experiments.

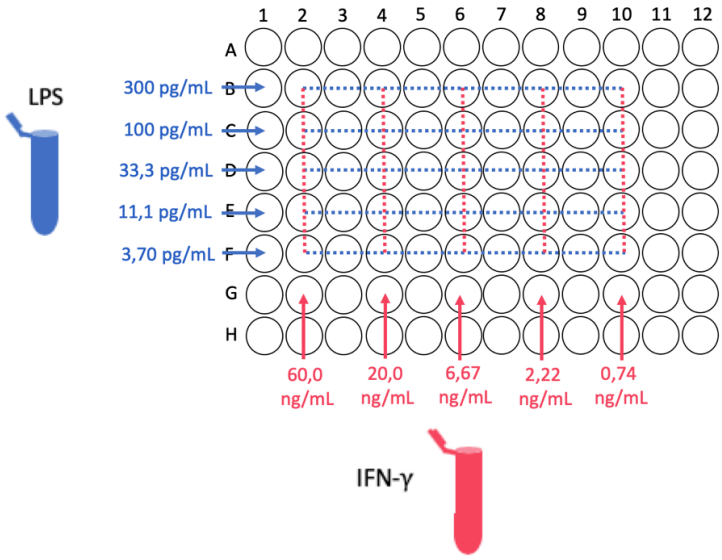

Figure 3.3: *Illustration of how the three-fold dilution series of LPS and IFN-γ were combined and added in the titration study.*

3.5.2 Investigating the effect of TH5487, BMS-345541, and Rapamycin

After estimating concentrations of IFN-γ and LPS that did not over-stimulate the cells, potential effects of TH5487, BMS-345541, and Rapamycin on the TNF-α-secretion could be investigated.

In this study, two similar 96-well culture plates (#165305, Thermo Scientific^{TM} Nunc^{TM}), one for collection of supernatans and one for CTG-measurements, were prepared with 100 μL/well of medium containing $2 * 10^5$ cells/mL and 15 nM PMA, as described in Section 3.3.1. Following PMA-exposure and rest in PMA-free medium, separate dilution series of TH5487, BMS-3455541, encapsulated Rapamycin, and dispersed Rapamycin were prepared and added, with the following concentrations:

- **TH5487:** 1:2 dilution series between 20μM to 0.16μM.
- **BMS-345541:** 1:3 dilution series between 5μM to 2.3nM.
- **Rapamycin, encapsulated:** 1:3 dilution series between 5μM to 2.3nM.
- **Rapamycin, dispersed:** 1:3 dilution series between 5μM to 2.3nM.

The starting concentration of TH5487, BMS-345541, and both forms of Rapamycin was first achieved by dilution in DMSO, followed by further dilution in RPMI 1640. For each subsequent dilution series, DMSO was added to the RPMI 1640 medium to attain the equal DMSO concentration in each dilution. In this way, a potential effect resulting

from various concentrations of DMSO was prevented. The investigated dilution series were chosen based on concentrations used in previous literature ([27, 97, 30]). Also, preliminary studies were performed as described above, by exposing THP-1 macrophages to several dilutions to enable exclusion of concentrations that resulted in an unacceptably low metabolic activity measured by CTG.

Concentrations of LPS (25 pg/mL) and IFN-γ (20 ng/mL) was estimated following the method in Section 3.5.1. These concentrations were added to the wells immediately after TH5487, encapsulated Rapamycin, dispersed Rapamycin, or BMS-345541. Also, as a negative control for the secretion of TNF-α, cells were exposed solely to the concentrations of BMS-345541, without the addition of LPS and IFN-γ, for the same amount of time. BMS-345541 was investigated as a positive control for inhibition of the NF-κB pathway.

Subsequently, the THP-1 cells were cultured in the presence of M1 polarizing agents and either of the various compounds for 24 hours. CTG measurements were performed directly in one of the plates, whereas the other and equally treated plate was used to collect supernatants for the ELISA measurements. The supernatants were prepared as described in the "Sample preparation guide" in Section 3.4.3. Successively, the concentrations of TNF-α were measured and analyzed by Sandwich ELISA, as described in Section 3.4.3 and 3.4.4, respectively.

3.5.3 CellTiter-Glo

The *CellTiter-Glo™ Luminescent Cell Viability Assay* was used to investigate the metabolic activity in each well. A multi-mode detection platform SpectraMax i3 (Molecular Devices) was used to record the luminescence. The CTG studies were performed to investigate whether increasing concentrations of the compounds in Section 3.5.2 presented increased toxicity and successively decreased metabolic activity. With unaltered cellular toxicity following exposure to increasing concentrations of a compound, cytotoxicity can be excluded as an explanation for a possible decrease in the secretion of TNF-α. The THP-1 monocytes were seeded and treated in 96-well culture plates (#165305, Thermo Scientific™ Nunc™) as described in Section 3.5.2. A row of control wells containing only medium was prepared to obtain a value for the background luminescence of only medium and CellTiter-Glo™ reagent. The following protocol was performed for all CTG measurements.

CTG Protocol

1. Equilibrate the culture plate and the CellTiter-Glo™ reagent to RT.
2. Directly add 100 μL/well of CellTiter-Glo™ reagent. Cover the plate in aluminium foil.
3. Incubate the plate for two minutes at 900 rpm on an orbital shaker (Biomek i7 Automated Workstation, Beckman Coulter) to induce cell lysis.
4. Leave the plate at the bench in RT for 10 minutes to stabilize the luminescent signal.
5. Record the luminescence by using the multi-mode detection platform SpectraMax i3 (Molecular Devices).

CTG-data analysis

The CTG-data obtained from the multi-mode detection platform SpectraMax i3 (Molecular Devices) was transferred and analyzed using Excel software, version 16.36, to subtract the background luminescence and calculate the average values of the duplicate measurements [128]. Followingly, the RLU measurements of each well were transferred to GraphPad Prism version 8.4.2 for macOS, where the results from several independent experiments were used to generate bar charts.

Statistical analysis

Statistical analysis of all measurements was performed by using GraphPad Prism 8.4.2 for macOS software. Parametric, unpaired t-tests were employed to calculate statistical significance. For all analyses, a two-tailed calculation was used, and the confidence level was set to 95%, defining possible statistical significance at $p < 0.05$. Statistical significance is indicated in the figures by asterisks as follows: * $p < 0.05$; ** $p < 0.005$; *** $p < 0.0005$.

CHAPTER 4

Results

4.1 Polarization of THP-1 macrophages

To quantitatively assess the polarization of the PMA-differentiated THP-1 macrophages, the cells and their supernatants were investigated by Flow cytometry and Sandwich ELISA. The protocol in Section 3.3.1 was used to induce M1 and M2 polarized THP-1 macrophages.

4.1.1 Surface expression of M1 and M2 macrophage markers

Flow cytometry was used to investigate if M1 and M2 polarized THP-1 macrophages could be characterized by the expression of putative M1 and M2 phenotypic cell surface markers. Classical surface markers of M1 or M2 polarized macrophages are MHCII and CD80, or CD163 and CD206, respectively. These surface markers were investigated on M0, M1, and M2 macrophages after one, three, or five days of polarization. However, five days of exposure to M2 polarizing stimuli did not evidently increase the number of cells expressing the CD163 and CD206 cell surface markers, as presented in Appendix B, Figure 1. Also, a limited amount of M1 polarized THP-1 macrophages could be detected following five days of exposure, as presented in Appendix B, Figure 2. Therefore, the subsequent analysis focused on macrophages exposed up to three days of polarization. In all Flow cytometry plots, dead cells have been excluded using propidium iodide as a viability dye.

Surface expression of M1 phenotypic markers measured by flow cytometry

In Figure 4.1 a-d, the overlay plots of histograms represent the detected cell surface expression of CD80 and MHCII after polarization for one or three days.

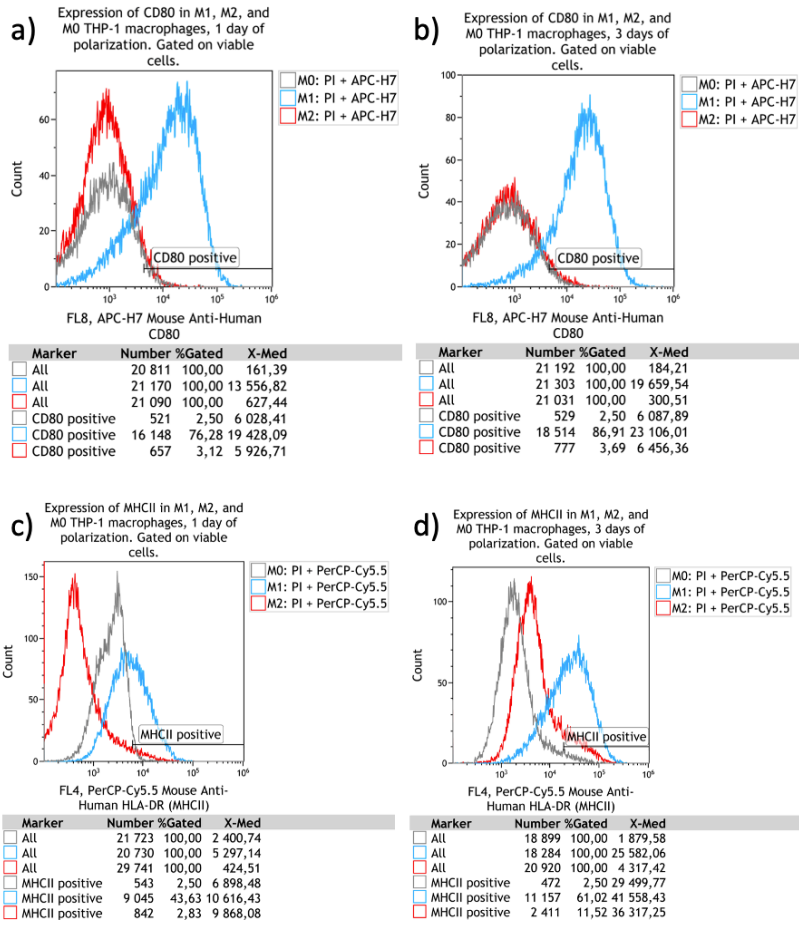

Figure 4.1: *Overlay plots of histograms presenting the expression of the classical M1 phenotypic cell surface markers, CD80 and MHCII, by M1 (blue line), M2 (red line) and M0 (grey line) polarized THP-1 macrophages. Overlay plot a) and b) present the fluorescence intensity (log) of APC-H7 Mouse Anti-Human CD80 against the number of cells after one and three days of polarization, respectively. Overlay plot c) and d) presents the fluorescence intensity (log) of PerCP-Cy5.5 Mouse Anti-Human HLA-DR (MHCII) against the number of cells after one and three days of polarization, respectively. THP-1 macrophages unexposed to polarizing stimuli, M0, works as biological controls. An overlay marker in each overlay plot is included to evaluate the percentage of cells that express the antibody of interest. 2.5% of the control group (M0) is included in the gate. The number of cells and X-median for the fluorescence intensity signal from the different samples are included. Representative overlay plots from three independent biological replicates.*

As can be seen in Figure 4.1, the M1 polarized THP-1 macrophages, represented by the blue line in all histograms, show an evident increase in the expression of CD80 (a and b) and MHCII (c and d) as compared to M0 and M2 polarized THP-1 macrophages. The tables below the histograms in Figure 4.1 includes both information on the percentage of

cells gated positive for each marker, and information on the measured median channel fluorescence intensity (X-Med). Based on three biological replicates, similar overlay plots of histogram were generated. Successively, information from all overlay markers was collected to calculate the mean percentages of CD80 and MHCII positive cells of M1 and M2 polarized THP-1 macrophages. The resulting bar charts are presented in Figure 4.2. Bar charts presenting the CD80 and MHCII median fluorescence intensities of the cells gated positive for CD80 and MHCII, respectively, are presented in Figure 4.3.

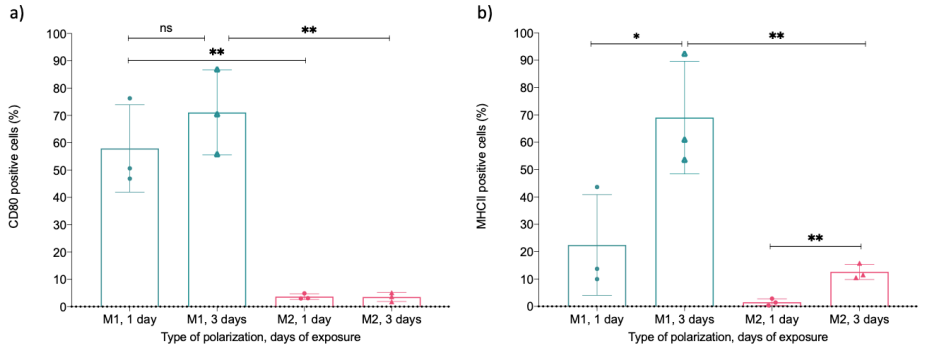

Figure 4.2: *The bar charts present the mean percentage of gated cells, measured by flow cytometry, and collected from all the generated overlay plots of histograms. Graph a) presents the percentage of CD80 positive cells after M1 and M2 polarization for one or three days, whereas graph b) presents the percentage of MHCII positive cells. 2.5% of the control group (M0) were included in the gates. Results are expressed as means ± standard deviation (n=3 independent biological replicates). Statistical analysis was carried out using unpaired t-tests by GraphPad Prism version 8.4.2 for macOS. ns: not significantly different. ∗, ∗∗ or ∗ ∗ ∗: significantly different respectively with p <0.05, 0.005 or 0.0005.*

Statistical analysis indicated a significant increase in the percentage of CD80 positive cells (p = 0.0163) and MHCII positive cells (p = 0.0093) on M1 polarized compared to M2 polarized cells following polarization for three days. 2.5% of the control group (M0) was included in the gates, further indicating that the expression of CD80 and MHCII in M1 polarized THP-1 macrophages significantly increased compared to the M0 macrophage group. The percentage of CD80 positive cells in the M1 polarized group was already significantly increased (p = 0.0042) after one day of polarization. No significant increase in the percentage of CD80 positive macrophages was measured between one to three days of M1 polarization. In contrast, although M1 polarized macrophages presented an increased percentage of MHCII positive cells after one day of polarization, this increase was calculated as non-significant. However, between one and three days of polarization, a significant increase (p = 0.043) in the percentage of MHCII positive M1 polarized cells was detected. The expression of MHCII also significantly increased on M2 macrophages following one to three days of polarization (p = 0.0033). Collectively, these data indicate that it is possible to identify a high percentage of the M1 polarized THP-1 macrophages from the M2 and M0 polarized THP-1 macrophages, based on their increased abundance of CD80 and

MHCII on the surface. Although both markers function to detect the M1 polarized cells, CD80 is earlier and more specifically expressed than MHCII.

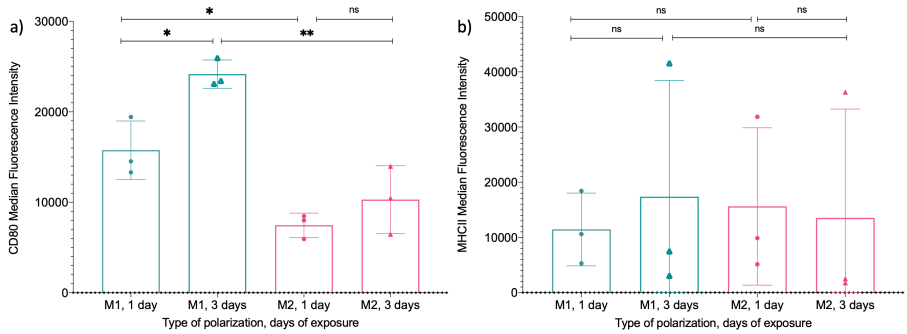

Figure 4.3: *The bar charts present the median fluorescence intensity (X-Med) of the gated cells, measured by flow cytometry and collected from all the generated overlay plots of histograms. Graph a) presents the median fluorescence intensity of CD80 on CD80 positive cells after M1 and M2 polarization for one or three days, whereas graph b) presents the median fluorescence intensity of MHCII on MHCII positive cells. Results are expressed as means ± standard deviation (n=3 independent biological replicates). Statistical analysis was carried out using unpaired t-tests by GraphPad Prism version 8.4.2 for macOS. ns: not significantly different. ∗, ∗∗ or ∗∗∗: significantly different respectively with p <0.05, 0.005 or 0.0005.*

Concerning the median fluorescence intensity of CD80 on the cells gated positive for CD80, the statistical analysis presented a significantly increased intensity of the M1 polarized cells compared to the M2 polarized cells following one (p = 0.0149) and three (p = 0.0041) days of polarization, seen in Figure 4.3a. Hence, the M1 positive cells both show a significantly higher percentage of CD80 positive cells, and the median intensity of the CD80 expression is higher in these cells compared to the CD80 positive M2 polarized cells. The intensity significantly increased (p = 0.0155) between one to three days of polarization in the CD80 positive M1 polarized cells. Consequently, although the percentage of CD80 positive cells does not increase between one to three days of polarization, the amount of CD80 molecules on the CD80 positive cells continues to increase significantly.

A similar observation was not found for the expression of MHCII, presented in Figure 4.3 b. Here, the median fluorescence intensity of MHCII indicated no significant difference between the MHCII positive M1 and M2 polarized cells. Successively, although the percentage of MHCII positive cells is significantly higher following M1 polarization for three days, the number of MHCII molecules appears similar in all MHCII positive cells, both M1 and M2 polarized.

Expression of M2 phenotypic markers measured by flow cytometry

In Figure 4.4 a-d, the overlay plots of histograms represent the cell surface expression of CD163 and CD206 after polarization for one or three days.

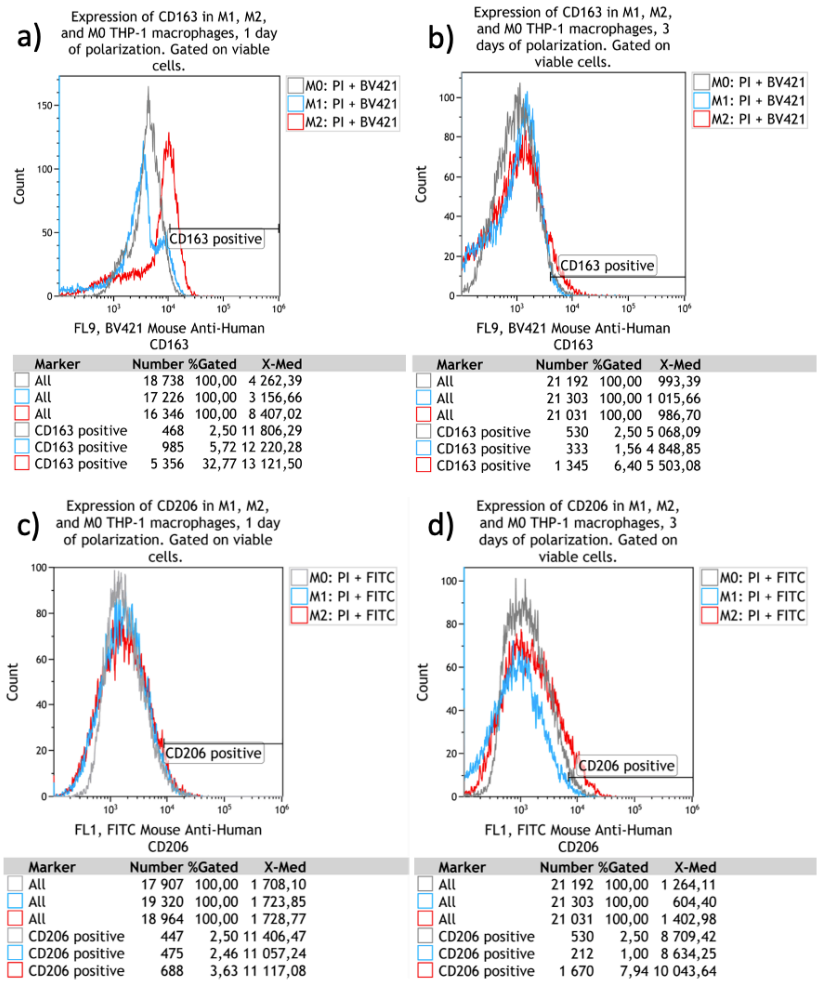

Marker	Number	%Gated	X-Med
All	18 738	100,00	4 262,39
All	17 226	100,00	3 156,66
All	16 346	100,00	8 407,02
CD163 positive	468	2,50	11 806,29
CD163 positive	985	5,72	12 220,28
CD163 positive	5 356	32,77	13 121,50

Marker	Number	%Gated	X-Med
All	21 192	100,00	993,39
All	21 303	100,00	1 015,66
All	21 031	100,00	986,70
CD163 positive	530	2,50	5 068,09
CD163 positive	333	1,56	4 848,85
CD163 positive	1 345	6,40	5 503,08

Marker	Number	%Gated	X-Med
All	17 907	100,00	1 708,10
All	19 320	100,00	1 723,85
All	18 964	100,00	1 728,77
CD206 positive	447	2,50	11 406,47
CD206 positive	475	2,46	11 057,24
CD206 positive	688	3,63	11 117,08

Marker	Number	%Gated	X-Med
All	21 192	100,00	1 264,11
All	21 303	100,00	604,40
All	21 031	100,00	1 402,98
CD206 positive	530	2,50	8 709,42
CD206 positive	212	1,00	8 634,25
CD206 positive	1 670	7,94	10 043,64

Figure 4.4: *Overlay plots of histograms presenting the expression of classical M2 phenotypic cell surface markers, CD163 and 206, by M1 (blue line), M2 (red line) and M0 (grey line) polarized THP-1 macrophages. Overlay plot a) and b) presents the fluorescence intensity (log) of BV421 Mouse Anti-Human CD163 against the number of cells following one and three days of polarization, respectively. Overlay plot c) and d) presents the fluorescence intensity (log) of FITC Mouse Anti-Human CD206 against the number of cells following one and three days of polarization, respectively. THP-1 macrophages unexposed to polarizing stimuli, M0, works as biological controls. An overlay marker in each overlay plot is included to evaluate the percentage of cells that express the antibody of interest. 2.5% of the control group (M0) are included in gate. The number of cells and X-median for the fluorescence intensity signal from the different samples are included. Representative overlay plots from three independent biological replicates.*

As shown in Figure 4.4, the M2 polarized THP-1 macrophages, represented by the red line in all histograms, presented a minimal increase in the expression of CD163 (a and b) and CD206 (c and d) compared to the M0 and M1 polarized THP-1 macrophages. Most

noticeable was the increased percentage of gated cells for CD163 detected on M2 polarized macrophages following one day of polarization, and CD206 following three days of polarization. The information in the tables under the histograms, presenting the percentage of gated cells and the measured median channel fluorescence intensity (X-med), was collected to generate bar charts. Based on three biological replicates, similar overlay plots of histograms were generated, and information from all overlay markers was collected to calculate the mean percentages of CD163 and CD206 positive cells. The resulting bar charts are presented in Figure 4.5. Bar charts presenting the CD163 and CD206 median fluorescence intensities of the cells gated positive for the respective markers are presented in Figure 4.3.

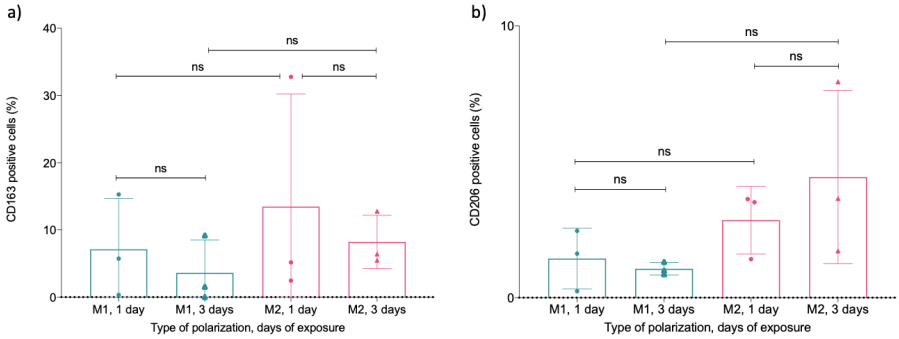

Figure 4.5: *The bar charts present the mean percentage of gated cells, measured by flow cytometry and collected from all the generated overlay plots of histograms. Graph a) presents the percentage of CD163 positive cells after M1 and M2 polarization for one or three days, whereas graph b) presents the percentage of CD206 positive cells. Results are expressed as means ± standard deviation (n=3 independent biological replicates). Statistical analysis was carried out using unpaired t-tests by GraphPad Prism version 8.4.2 for macOS. ns: not significantly different. ∗, ∗∗ or ∗∗∗: significantly different respectively with p <0.05, 0.005 or 0.0005.*

Figure 4.5 indicates that a minor increase in the percentage of CD163 and CD206 positive cells could be indicated on THP-1 macrophages exposed to M2 polarizing agents compared to cells exposed to M1 polarizing agents for one day. After three days of polarization, the mean percentage of M2 polarized cells that gated positive for CD163 decreased, whereas the mean percentage of CD206 positive cells increased. However, statistical analysis indicated no significant increase between M2 and M1 polarized macrophages and no significant increase between one to three days of exposure to M2 polarizing stimuli. Consequently, these data indicate that it is challenging to identify and characterize the M2 polarized THP-1 macrophages from the M1 and M0 polarized THP-1 macrophages, based on the surface expression of CD163 and CD206.

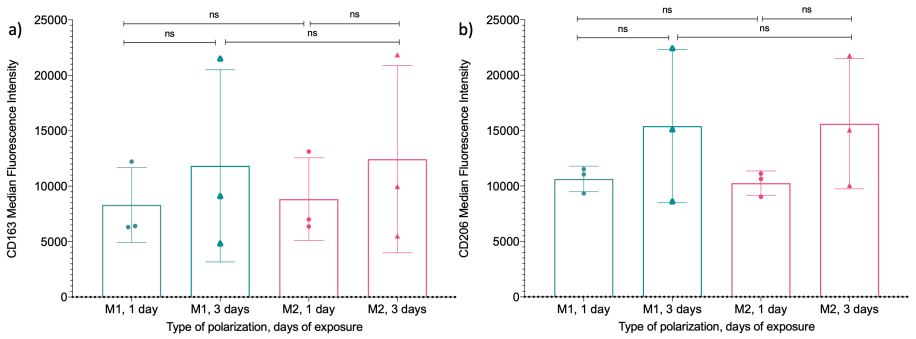

Figure 4.6: *The bar charts present the median fluorescence intensity (X-Med) of the gated cells, measured by flow cytometry and collected from all the generated overlay plots of histograms. Graph a) presents the median fluorescence intensity of CD163 on CD163 positive cells after M1 and M2 polarization for one or three days, whereas graph b) presents the median fluorescence intensity of CD206 on CD206 positive cells. Results are expressed as means ± standard deviation (n=3 independent biological replicates). Statistical analysis was carried out using unpaired t-tests by GraphPad Prism version 8.4.2 for macOS. ns: not significantly different. ∗, ∗∗ or ∗∗∗: significantly different respectively with p <0.05, 0.005 or 0.0005.*

When investigating the median fluorescence intensity of CD163 and CD206 on the cells gated positive for the respective markers, Figure 4.6 indicates a high degree of similarity between M1 and M2 polarized THP-1 macrophages. The similarity was confirmed by statistical analysis, presenting no significant difference between M1 and M2 polarized cells after one or three days of polarization in any of the investigated markers. Furthermore, although minor increases in the median fluorescence intensities of both markers could be seen between one to three days of exposure in both M1 and M2 polarized THP-1 macrophages, they were calculated non-significant. Successively, the percentage of CD163 and CD206 positive cells does not significantly increase following M2 polarization, and the number of CD163 and CD206 molecules appears similar in all CD163 and CD206 positive cells, respectively, both in M1 and M2 polarized THP-1 macrophages.

Percentual expression of surface markers on variously polarized THP-1 macrophages

Density plots were generated, as described in Section 3.4.2, to investigate the percentual expression of different surface markers on the variously polarized THP-1 macrophages. The expression of CD80, CD163, and CD206 could be compared in each cell population. However, the expression of MHCII could not be included, as PerCP-Cy5.5 Mouse Anti-Human HLA-DR (MHCII) had to be added separately from the other fluorescent stains to avoid excessive spillover. Representative density plots indicating the expression of CD80, CD163 and CD206 on THP-1 macrophages exposed to M1 polarizing agents are presented in Figures 4.7 and 4.8. Investigating these figures, the relative proportion of M1, M2, and M0 macrophages, as defined by their expression of surface markers, can be visualized. The four quadrants in each density plot enable determination of macrophages that are single positive, double negative, or double-positive for two markers.

In Figure 4.7, it is evident that most of the M1 polarized THP-1 macrophages actually develop to express the CD80 surface marker. A considerable percentage of the M1 polarized macrophages express CD80 both following one (Figure 4.7a) and three (Figure 4.7b) days of polarization. In addition, the percentage of M1 polarized THP-1 macrophages that are single positive for CD163 or double positive for CD163 and CD80 are minimal.

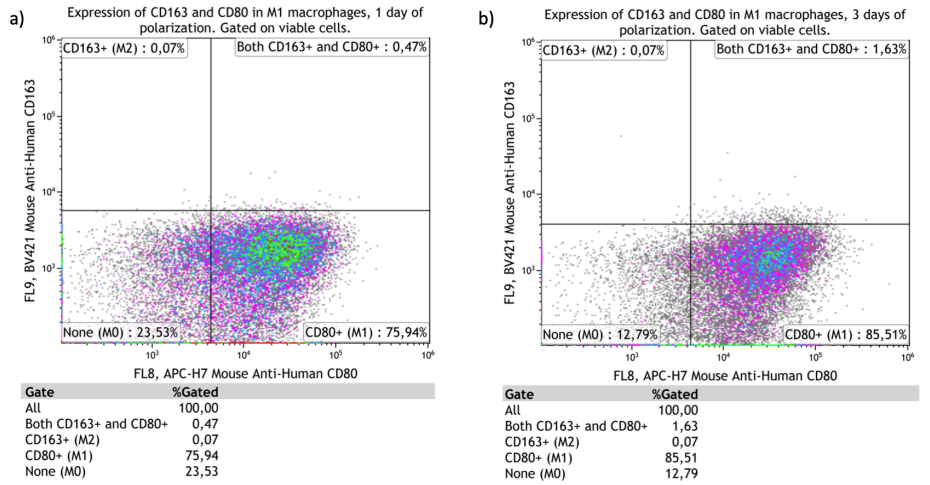

Figure 4.7: *Density plots presenting the APC-H7 Mouse Anti-Human CD80 fluorescence intensity (log) versus the BV421 Mouse Anti-Human CD163 fluorescence intensity (log) by M1 polarized THP-1 macrophages following exposure to LPS and IFN-γ for one (a) or three days (b). The density plots are generated from the overlay histograms and their associated overlay markers, as described in Section 3.4.2. 2.5% of the control group (M0) was included in each gate. The dispersion of cells in each quadrant indicates the percentage of M1 polarized macrophages that, as defined by CD80 and CD163 expression, remain unpolarized as M0 macrophages or develop into the M1 or M2 macrophage phenotype. Representative density plots from three independent biological replicates.*

Correspondingly, as seen in Figure 4.8, a noteworthy percentage of M1 polarized THP-1 macrophages are single positive for CD80 when compared to the expression of CD206, both following one (4.8a) and three (4.8b) days of polarization. The percentage of M1 polarized THP-1 macrophages that are single positive for CD206 or double positive for CD206 and CD80 are close to non-existent. Similar dot plots as presented in Figure 4.7 and 4.8 were generated for M2 polarized THP-1 macrophages and M0 unexposed THP-1 macrophages. Representative density plots presenting the percentual expression of CD80 versus CD163, CD80 versus CD206, and CD206 versus CD163 for M2 polarized macrophages are included in Appendix C, Figure 3, 4, 5.

The percentages of negative, single positive, or double-positive macrophages of each antibody, determined using this gating method, were collected for three independent biological replicates of M0, M1, and M2 polarized macrophages and summarized in bar charts.

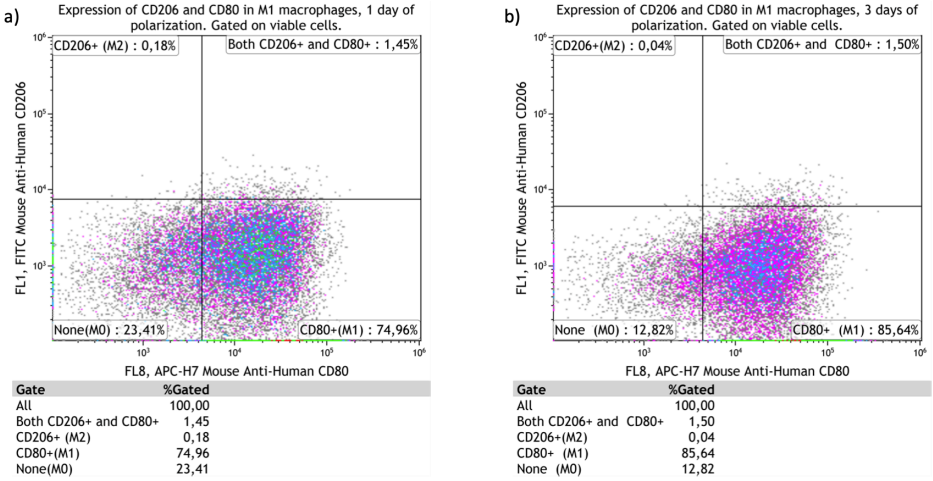

Figure 4.8: *Density plots presenting the APC-H7 Mouse Anti-Human CD80 fluorescence intensity (log) versus the FITC Mouse Anti-Human CD206 fluorescence intensity (log) by M1 polarized THP-1 macrophages following exposure to LPS and IFN-γ for one (a) or three days (b). The density plots are generated from the overlay histograms and their associated overlay markers, as described in Section 3.4.2. 2.5% of the control group (M0) was included in each gate. The dispersion of cells in each quadrant indicates the percentage of M1 polarized macrophages that, as defined by CD80 and CD206 expression, remain unpolarized as M0 macrophages or develop into the M1 or M2 macrophage phenotype. Representative density plots from three independent biological replicates.*

Figure 4.9 and Figure 4.10 present the summarized expression of CD80 and CD163, or CD80 and CD206, respectively, for M0, M1 and M2 polarized THP-1 macrophages. As can be seen in Figure 4.9 and 4.10, a high percentage of M1 polarized THP-1 macrophages develop to express the CD80 surface marker, both following one and three days of polarization. Furthermore, CD80 is detected on a minimal percentage of THP-1 macrophages exposed to M2 polarizing agents. As denoted in Figure 4.9, a significantly higher percentage of M1 polarized macrophages express CD80 compared to M0 macrophages following one ($p = 0.0124$) and three ($p = 0.0018$) days of polarization. For CD163, there is a small significant increase in the percentage of M2 polarized THP-1 macrophages that express this marker following three days of polarization ($p = 0.0382$), compared to the M1 polarized THP-1 macrophages.

As indicated in Figure 4.10, M2 polarization yield no significant increase in the percentage of cells that express CD206 on the surface, neither compared to the M0 or the M1 polarized macrophages. The percentual expression of CD80, on the other hand, clearly increased upon exposure to M1 polarizing agents and was calculated as significant after three days of polarization ($p = 0.0124$), compared to M2 polarized THP-1 macrophages. As seen in Figure 4.9 and 4.10, a minimal percentage of M2 polarized THP-1 macrophages develop to express CD163 or CD206 on the surface. The lack of M2 surface marker expression is further supported in the bar chart included in Appendix C, Figure 6, comparing the percentual expression of CD206 and CD163 on M0, M1 or M2 polarized macrophages THP-1 macrophages.

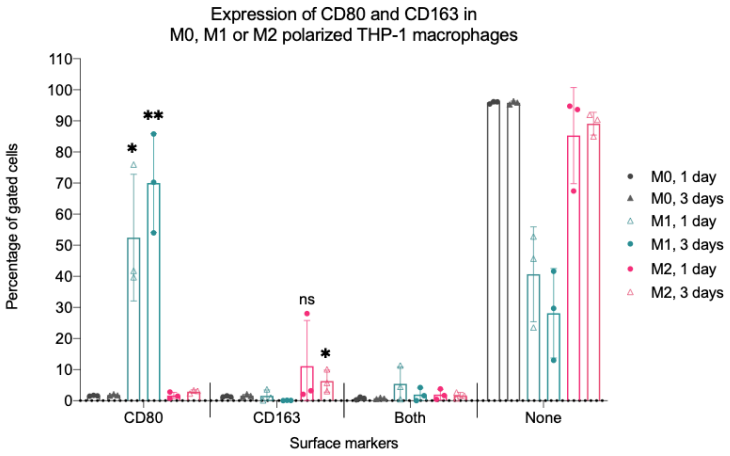

Figure 4.9: *The bar chart presents the mean percentage of M0, M1, or M2 polarized THP-1 macrophages that express either CD80, CD163, CD80 and CD163, or none of these markers. The data was measured by flow cytometry and collected from all generated density plots. The graph includes macrophages exposed to polarizing stimuli for one and three days. Results are expressed as means ± standard deviation (n=3 independent biological replicates). Statistical analysis was carried out using unpaired t-tests by GraphPad Prism version 8.4.2 for macOS. ns: not significantly different. ∗, ∗∗ or ∗ ∗ ∗: significantly different respectively with p <0.05, 0.005 or 0.0005.*

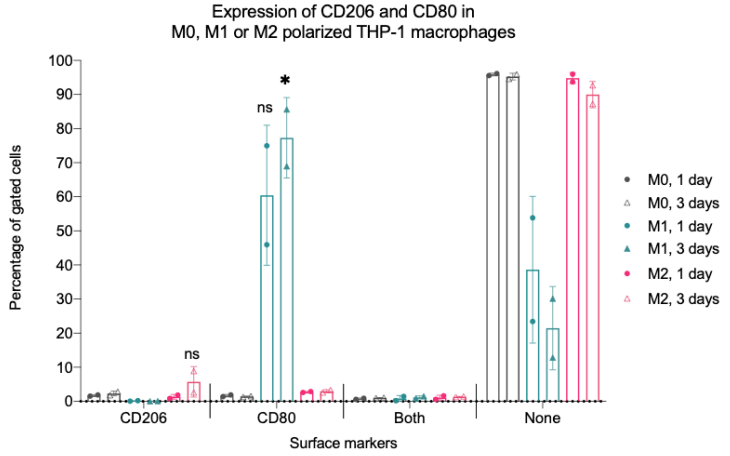

Figure 4.10: *The bar chart presents the mean percentage of M0, M1, or M2 polarized THP-1 macrophages that express either CD80, CD206, CD80 and CD206, or none of these markers. The data was measured by flow cytometry and collected from all generated density plots. The graph includes macrophages exposed to polarizing stimuli for one and three days. Results are expressed as means ± standard deviation (n=2 independent biological replicates). Statistical analysis was carried out using unpaired t-tests by GraphPad Prism version 8.4.2 for macOS. ns: not significantly different. ∗, ∗∗ or ∗ ∗ ∗: significantly different respectively with p <0.05, 0.005 or 0.0005.*

Consequently, based on all flow cytometry measurements performed herein, exposure to IL-4 and IL-13 does not satisfyingly work to generate increased amounts of M2 polarized THP-1 macrophages that express the classical CD163 and CD206 M2 surface markers.

Contrary, exposure to LPS and IFN-γ indeed works to stimulate a high number of cells to express classical M1 surface markers, CD80 and MHCII. The results indicate a specific M1 macrophage expression of these markers, as they are minimally expressed on unexposed M0 macrophages, and an insignificant percentage of cells exposed to M2 polarizing agents develop their expression.

4.1.2 Secretion of phenotypic M1 and M2 macrophage markers

Sandwich ELISA was performed to measure if the differently polarized THP-1 macrophages could be characterized and identified by their secretion of specific M1 and M2 phenotypic cytokines. The secreted concentration of CXCL10, TNF-α, IL-1Ra and IL-10 in the supernatant was analyzed following six hours, one day or three days of exposure to polarizing agents for M0, M1, and M2 polarized THP-1 macrophages.

Secretion of M1 phenotypic markers measured by Sandwich ELISA

Figure 4.11 and 4.12 present the measured secretion of M1 specific macrophage markers, CXCL10 and TNF-α, respectively, in the supernatant of variously polarized THP-1 macrophages.

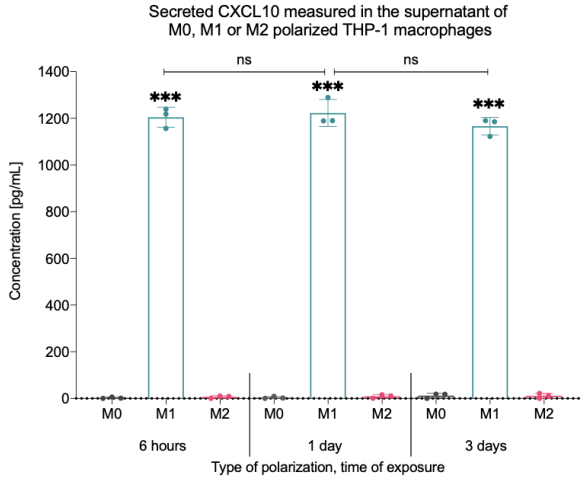

Figure 4.11: *Bar chart presenting the secretion of CXCL10 in the supernatant of M0, M1, or M2 polarized THP-1 macrophages following six hours, one day or three days of polarization. Each point represents the average of duplicate measurements. Results are expressed as means ± standard deviation (n=3 independent biological replicates). Statistical analysis was carried out using unpaired t-tests by GraphPad Prism version 8.4.2 for macOS. ns: not significantly different. ∗, ∗∗ or ∗ ∗ ∗: significantly different respectively with p <0.05, 0.005 or 0.0005.*

As seen in Figure 4.11, a significantly increased secretion of CXCL10 was measured in the supernatant of M1 polarized THP-1 macrophages compared to both M2 ($p<0.0005$) and M0 ($p<0.0005$) THP-1 macrophages. The secretion of CXCL10 in M1 polarized THP-1 macrophages does not significantly increase or decrease between six hours, one day or three days of exposure. As the medium was not changed following various exposure times, it can be hypothesized that all CXCL10 is secreted during the first six hours of exposure.

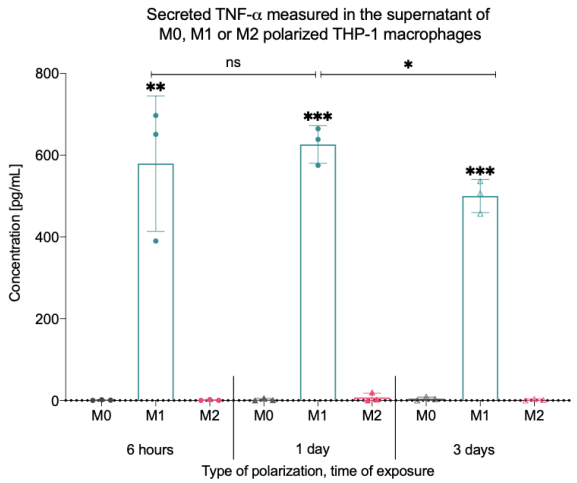

Figure 4.12: *Bar chart presenting the secretion of TNF-α in the supernatant of M0, M1, or M2 polarized THP-1 macrophages following six hours, one day or three days of polarization. Each point represents the average of duplicate measurements. Results are expressed as means $\pm$ standard deviation (n=3 independent biological replicates). Statistical analysis was carried out using unpaired t-tests by GraphPad Prism version 8.4.2 for macOS. ns: not significantly different. $*$, $**$ or $***$: significantly different respectively with $p < 0.05$, 0.005 or 0.0005.*

As seen in Figure 4.12, TNF-α also proves a specific and significant increase in the supernatant of M1 polarized THP-1 macrophages compared to M0 and M2 polarized THP-1 macrophages ($p = 0.0038$ at six hours, and $p<0.0005$ at one and three days, both compared to M2 and M0). The secretion of TNF-α in the supernatant of M1 polarized macrophages does not significantly increase between six hours and one day of exposure. However, there is a significant decrease between one to three days of exposure ($p = 0.0235$).

Evidently, as seen for both CXCL10 and TNF-α, LPS and IFN-γ work to stimulate their secretion, as neither of these cytokines are detected in the supernatant of unpolarized M0 THP-1 macrophages. Also, minimal amounts of CXCL10 and TNF-α is secreted in the supernatant of M2 polarized THP-1 macrophages.

Secretion of M2 phenotypic markers measured by Sandwich ELISA

Figure 4.13 and 4.14 present the measured secretion of M2 specific macrophage markers, IL-1Ra and IL-10, respectively, in the supernatant of variously polarized THP-1 macrophages.

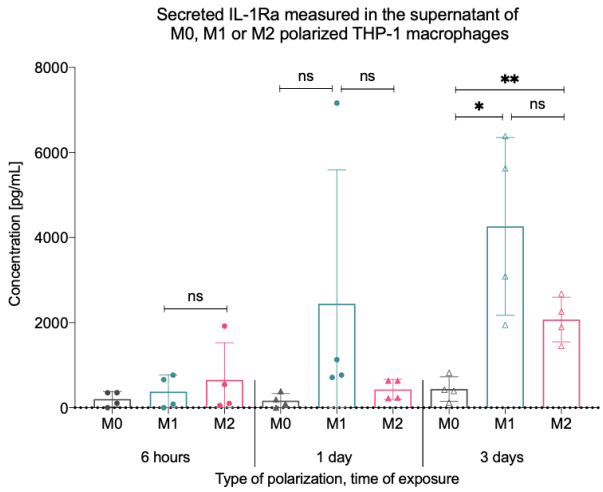

Figure 4.13: *Bar chart presenting the secretion of IL-1Ra in the supernatant of M0, M1, or M2 polarized THP-1 macrophages following six hours, one day or three days of polarization. Each point represents the average of duplicate measurements. Results are expressed as means ± standard deviation (n=4 independent biological replicates). Statistical analysis was carried out using unpaired t-tests by GraphPad Prism version 8.4.2 for macOS. ns: not significantly different. ∗, ∗∗ or ∗ ∗ ∗: significantly different respectively with p <0.05, 0.005 or 0.0005.*

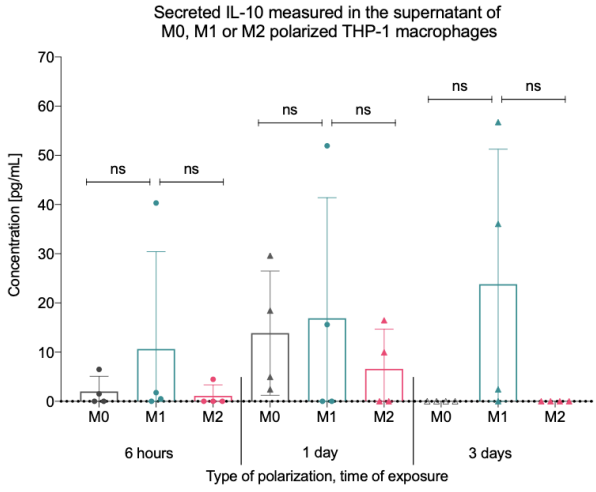

Figure 4.14: *Bar chart presenting the secretion of IL-10 in the supernatant of M0, M1, or M2 polarized THP-1 macrophages following six hours, one day or three days of polarization. Each point represents the average of duplicate measurements. Results are expressed as means ± standard deviation (n=4 independent biological replicates). Statistical analysis was carried out using unpaired t-tests by GraphPad Prism version 8.4.2 for macOS. ns: not significantly different. ∗, ∗∗ or ∗ ∗ ∗: significantly different respectively with p <0.05, 0.005 or 0.0005.*

As presented in Figure 4.13, M2 polarized THP-1 macrophages did not, at any investigated time point, significantly increase the secretion of IL-1Ra compared to M1 polarized THP-1 macrophages. No statistical significance was found between any of the macrophage phenotypes, M1, M2, or M0, after six hours or one day of polarization. Following three days of polarization, a significantly increased secretion of IL-1Ra was detected in the supernatant of both M1 ($p = 0.011$), and M2 ($p = 0.0016$) polarized THP-1 macrophages compared to unpolarized M0 THP-1 macrophages.

Figure 4.14 indicates that no significant increase in the secretion of IL-10 was measured in the supernatant between any of the variously polarized THP-1 macrophages at any of the investigated time points. Although not significant and at levels under 100 pg/mL, the secretion slightly increases in M1 polarized rather than M2 polarized THP-1 macrophages.

Collectively, IL-4 and IL-13 do not satisfyingly work to stimulate the secretion of IL-1Ra or IL-10 in THP-1 macrophages under the experimental conditions used herein. Instead, following prolonged exposure times, there is a tendency towards increased secretion of the M2 specific cytokines from M1 polarized THP-1 macrophages.

4.1.3 Summarizing results of the M1 and M2 polarization study

Table 4.1: *This table summarizes the obtained results from flow cytometry and ELISA measurements used to investigate the characterization of polarized of THP-1 macrophages.*

Marker	**M1 polarization:** LPS (0.1 ng/mL) + IFN-γ (20 ng/mL)	**M2 polarization:** IL-4 (20 ng/mL) + IL-13 (20 ng/mL)
Flow cytometry		
MHCII	Significant increase (3 days) compared to both M0 and M2	Significant increase on M2 (3 days) compared to M2 (1 day)
CD80	Significant increase (1 and 3 days) compared to both M0 and M2	Minimal expression
CD163	Minimal expression	Minor increase (1 day), not significant
CD206	Minimal expression	Minimal expression
ELISA		
CXCL10	Significant increase (6 hours, 1 day, 3 days)	Minimal secretion
TNF-α	Significant increase (6 hours, 1 day, 3 days)	Minimal secretion
IL-1Ra	Significant increase (3 days) compared to M0	Significant increase (3 days) compared to M0
IL-10	Minimal secretion	Minimal secretion

Collectively, as summarized in Table 4.1, the THP-1 macrophage polarization protocol satisfyingly work to achieve polarization towards the M1 macrophage phenotype. Contrary, the conditions for M2 polarization utilized herein do not induce M2 phenotypic macrophages that can be identified by the specific markers investigated herein.

4.2 Utilizing the M1 polarized THP-1 macrophages

As the THP-1 macrophage polarization protocol proved capable of polarizing THP-1 macrophages towards the M1 phenotype, this protocol was further utilized to investigate the effect on M1 polarization upon cultivation with specific chemical substances. Specifically, the protocol was used to investigate the NF-κB-dependent secretion of TNF-α by exposure to various concentrations of TH5487 and BMS-34554. It was also investigated for a potential effect on the secretion of TNF-α upon exposure to free Rapamycin and PACA-encapsulated Rapamycin known to inhibit the mTOR pathway.

4.2.1 Titration study of LPS and IFN-γ

A titration study was performed to investigate the dose-response relationship between exposure to various concentrations of the M1 polarizing agents, and the resulting secretion of TNF-α. This investigation aimed to decide concentrations of LPS and IFN-γ that did not overstimulate the THP-1 macrophages. In conditions where the cells are not excessively stimulated, a potential decrease in the secretion of TNF-α can be detected.

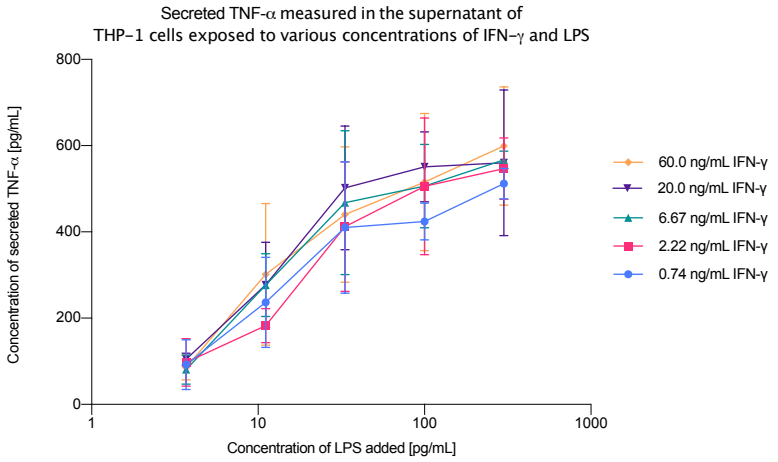

Figure 4.15: *Semi-logarithmic XY scatter chart presenting secretion of TNF-α on the y-axis and added concentrations of LPS (log) on the x-axis. Sandwich ELISA was used to measure the concentration of secreted TNF-α in the supernatant of THP-1 macrophages exposed to various concentrations of LPS and IFN-γ for 24 hours. In this graph, each line represents a constant concentration of IFN-γ with varying concentrations of LPS. Each point represents the average of duplicates, and the results are expressed as means $\pm$ standard deviation (n=3 independent biological replicates). The graph was used to estimate the concentration of LPS that would not result in overstimulated THP-1 macrophages.*

Based on the polarization study of THP-1 macrophages, a significantly increased secretion of TNF-α was detected following six hours of exposure to M1 polarizing agents. However, the standard deviation of the secretion decreased at 24 hours compared to six hours. Successively, THP-1 macrophages were exposed to M1 polarizing agents for 24

hours for the titration studies. PMA-differentiated THP-1 macrophages were exposed to various concentrations of LPS and IFN-γ, as described in Section 3.5.1. Figure 4.15 and 4.16 presents the resulting semi-logarithmic XY scatter charts that were used to decide the concentration of LPS and IFN-γ.

As seen in Figure 4.15, the concentration of secreted TNF-α increased upon exposure to higher concentrations of LPS. In this graph, each line represents a constant concentration of IFN-γ with varying concentrations of LPS. All the separate lines present a similar increasing tendency in the detected concentration of TNF-α upon exposure to higher amounts of LPS.

In Figure 4.16, each line represents a constant concentration of LPS with increasing concentrations of IFN-γ. In this graph, the various lines appear as horizontal rather than typical dose-response curves. Successively, the concentration of IFN-γ does not seem to have a decisive impact on the concentration of TNF-α that is secreted. Rather, each line that represents a higher value of LPS presents a higher amount of secreted TNF-α.

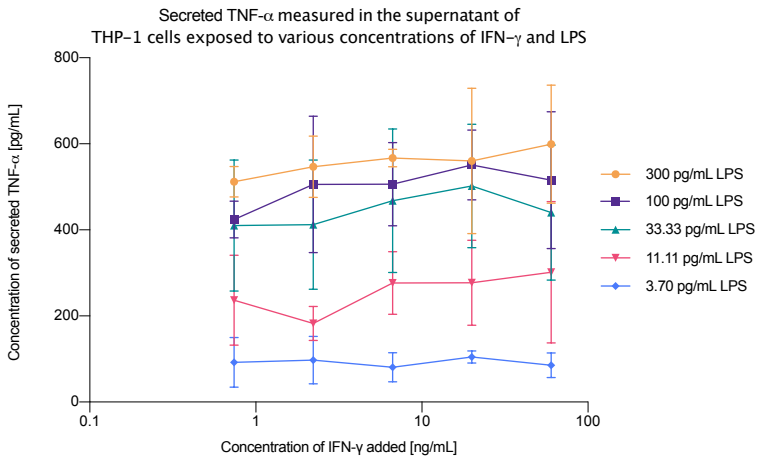

Figure 4.16: *Semi-logarithmic XY scatter chart presenting secretion of TNF-α on the y-axis and added concentrations of IFN-γ (log) on the x-axis. Sandwich ELISA was used to measure the concentration of secreted TNF-α in the supernatant of THP-1 macrophages exposed to various concentrations of LPS and IFN-γ for 24 hours. In this graph, each line represents a constant concentration of LPS with varying concentrations of IFN-γ. Each point represents the average of duplicates, and the results are expressed as means $\pm$ standard deviation (n=3 independent biological replicates). The graph was used to estimate the concentration of IFN-γ that would not result in overstimulated THP-1 macrophages.*

Based on the graphs presented in Figure 4.15 and 4.16, the concentration of LPS seemed to be the decisive stimuli for the secreted concentration of TNF-α. Using the graph in Figure 4.15, the concentration of LPS was calculated, as explained in Section 3.5.1, and approximated to 25 pg/mL in the following studies. The concentration of IFN-γ seemingly did not impact the amount of secreted TNF-α. Therefore, for simplicity, the concentration of IFN-γ was kept at 20 ng/mL, similar to the previous studies.

4.2.2 Effect of TH5487 on the secretion of TNF-α

The THP-1 macrophages were exposed to various concentrations of TH5487 together with LPS (25 pg/mL) and IFN-γ (20 ng/mL) to investigate the potential inhibitory effect on the NF-κB-dependent secretion of TNF-α. The bar charts in Figure 4.17 present the detected secretion of TNF-α (a) and metabolic activity (b) measured by Sandwich ELISA and CTG, respectively, in wells exposed to increasing concentrations of TH5487.

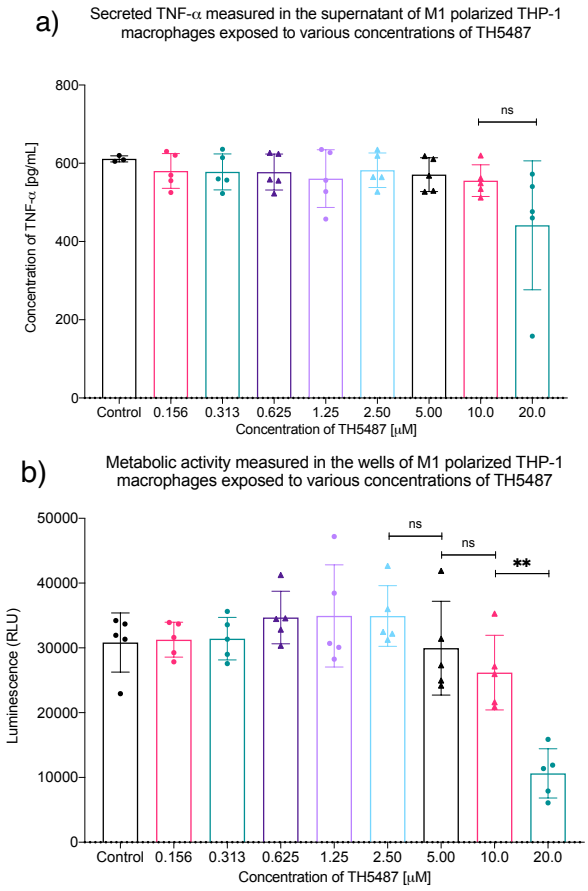

Figure 4.17: *Bar charts presenting the secretion of TNF-α (a) or the metabolic activity (b) on the y-axis versus added concentrations of TH5487 on the x-axis. The measurements were performed on THP-1 macrophages exposed to M1 polarizing stimuli and various concentrations of TH5487 for 24 hours. The control sample represents THP-1 macrophages exposed solely to M1 polarizing agents and DMSO. The concentration of TNF-α in the supernatant was measured by Sandwich ELISA, whereas CTG was performed directly in each well to investigate the metabolic activity. Each point represents the average of duplicates, and the results are expressed as means $\pm$ standard deviation (n=5 independent biological replicates). Statistical analysis was carried out using unpaired t-tests by GraphPad Prism version 8.4.2 for macOS. ns: not significantly different. $*$, $**$ or $***$: significantly different respectively with $p < 0.05$, 0.005 or 0.0005.*

As seen in Figure 4.17 a, the secretion of TNF-α from M1 polarized THP-1 macrophages did not significantly decrease upon exposure to increasing concentrations of TH5487. While a minor and non-significant decrease in the secretion of TNF-α can be observed at the highest investigated concentration of TH5487 (20 μM), a simultaneous and significant decrease is detected in the metabolic activity in similarly exposed wells, as seen in Figure 4.17 b. Collectively, these results indicate a reduced amount of viable cells with increasing concentrations of TH5487 and, therefore, fewer cells that can secrete the cytokine. Based on these graphs, TH5487 does not directly affect the secretion of TNF-α in M1 polarized THP-1 macrophages but exerts a cytotoxic effect against the THP-1 cells at increasing concentrations.

4.2.3 Effect of BMS-345541 on the secretion of TNF-α

The THP-1 macrophages were exposed to various concentrations of BMS-345541 together with LPS (25 pg/mL) and IFN-γ (20 ng/mL) to gain knowledge on the NF-κB-dependent secretion of TNF-α. BMS-345541, a highly selective and recognized inhibitor of signal-induced NF-κB activation, was investigated as a positive control to inhibit the NF-κB pathway [97]. The bar charts in Figure 4.18 present the detected secretion of TNF-α (a) and metabolic activity (b), measured by Sandwich ELISA and CTG, respectively, in wells exposed to increasing concentrations of BMS-345541.

As observed in figure 4.18 a, increasing concentrations of BMS-345541 did not significantly decrease the secretion of TNF-α. However, as seen in Figure 4.18 b, increasing concentrations of BMS-345541 did impact the cells' metabolic activity. Interestingly, the metabolic activity significantly increased upon exposure to the lowest investigated concentrations of BMS-345541, although no increase was detected in the secretion of TNF-α. On the other hand, a significant decrease in metabolic activity was measured upon exposure to the highest investigated concentrations of BMS-345541. Concurrently, although non-significant, there was detected a drop in the secretion of TNF-α. These results collectively indicate that BMS-345541 impacts the metabolic activity of the M1 polarized THP-1 macrophages. A similar effect on the metabolic activity upon exposure to BMS-345541 macrophages was noticed in unpolarized M0 cells, with the results presented in Appendix D, Figure 7. The secretion of TNF-α, however, did not significantly alter in M1 polarized THP-1 cells upon exposure to BMS-345541. Without further investigations, the results, therefore, suggest that BMS-345541 did not directly affect the secretion of TNF-α in M1 polarized THP-1 macrophages.

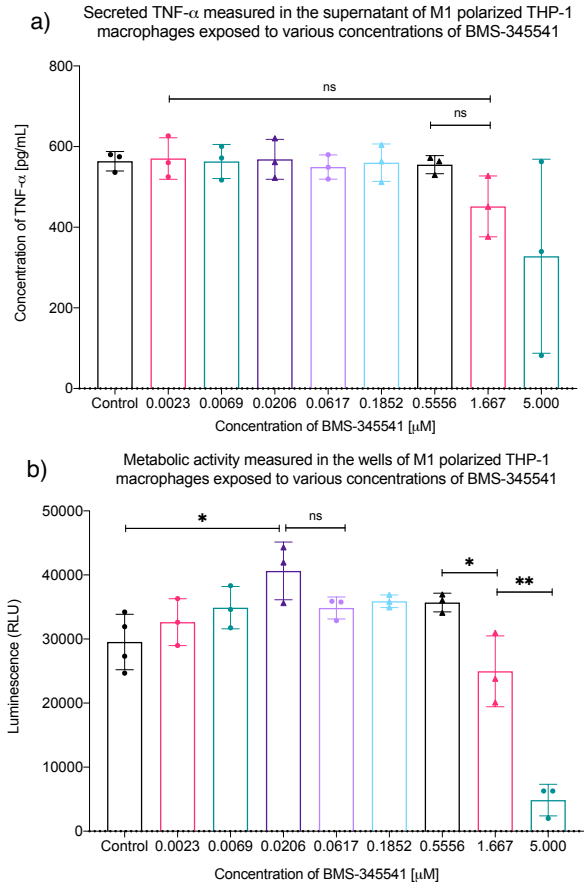

Figure 4.18: *Bar charts presenting the secretion of TNF-α (a) or the metabolic activity (b) on the y-axis versus added concentrations of BMS-345541 on the x-axis. The measurements were performed on THP-1 macrophages exposed to M1 polarizing stimuli and various concentrations of BMS-345541 for 24 hours. The control sample represents THP-1 macrophages exposed solely to M1 polarizing agents and DMSO. The concentration of TNF-α in the supernatant was measured by Sandwich ELISA, whereas CTG was performed directly in each well to investigate the metabolic activity. Each point represents the average of duplicates, and the results are expressed as means ± standard deviation (n=4 independent biological replicates). Statistical analysis was carried out using unpaired t-tests by GraphPad Prism version 8.4.2 for macOS. ns: not significantly different. ∗, ∗∗ or ∗ ∗ ∗: significantly different respectively with p <0.05, 0.005 or 0.0005.*

4.2.4 Effect of Rapamycin on the secretion of TNF-α

Given the multiple and contradictory roles of the mTOR pathway, we wanted to investigate the effect of Rapamycin on the THP-1 macrophage M1 polarization. Hence, we went on to investigate the LPS (25 pg/mL) and IFN-γ (20 ng/mL) stimulated secretion of TNF-α upon exposure to various concentrations of Rapamycin. The THP-1 macrophages were exposed

to various concentrations of Rapamycin in either free or PACA-encapsulated form. The bar charts in Figure 4.19 and 4.20 present the detected secretion of TNF-α (a) and metabolic activity (b), measured by Sandwich ELISA and CTG, respectively, in wells exposed to increasing concentrations of either free or PACA-encapsulated Rapamycin.

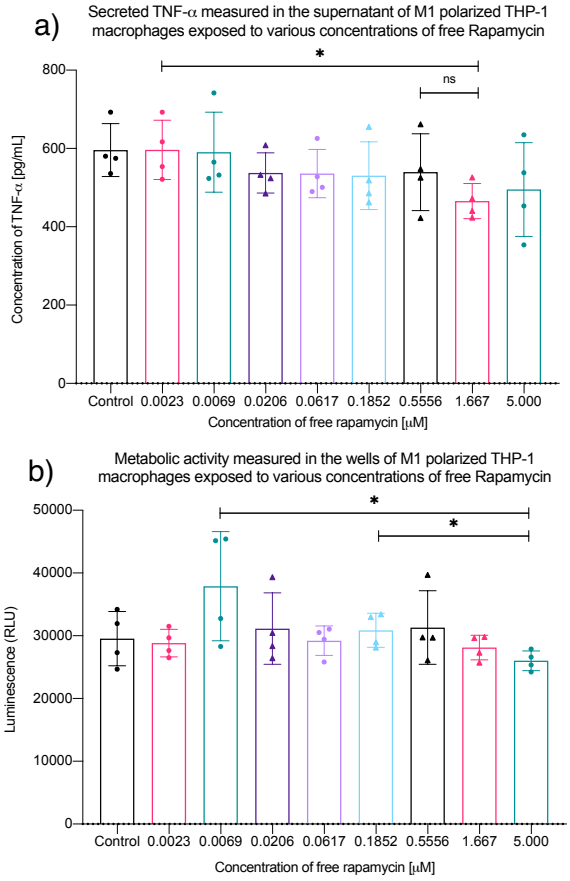

Figure 4.19: *Bar charts presenting the secretion of TNF-α (a) or the metabolic activity (b) on the y-axis versus added concentrations of free Rapamycin on the x-axis. The measurements were performed on THP-1 macrophages exposed to M1 polarizing stimuli and various concentrations of free Rapamycin for 24 hours. The control sample represents THP-1 macrophages exposed solely to M1 polarizing agents and DMSO. The concentration of TNF-α in the supernatant was measured by Sandwich ELISA, whereas CTG was performed directly in each well to investigate the metabolic activity. Each point represents the average of duplicates, and the results are expressed as means $\pm$ standard deviation (n=4 independent biological replicates). Statistical analysis was carried out using unpaired t-tests by GraphPad Prism version 8.4.2 for macOS. ns: not significantly different. $*$, $**$ or $***$: significantly different respectively with $p < 0.05$, 0.005 or 0.0005.*

The graph in Figure 4.19 presents the data obtained from THP-1 macrophage exposure to free Rapamycin. A significantly decreased secretion of TNF-α, seen in Figure 4.19

a, was detected between exposure to some of the lowest and highest concentrations of Rapamycin. However, metabolic activity was also significantly decreased upon exposure to the same concentration range, as seen in Figure 4.19 b. Consequently, the secretion of TNF-α likely decreases as a result of the reduced metabolic activity and is not directly affected by Rapamycin.

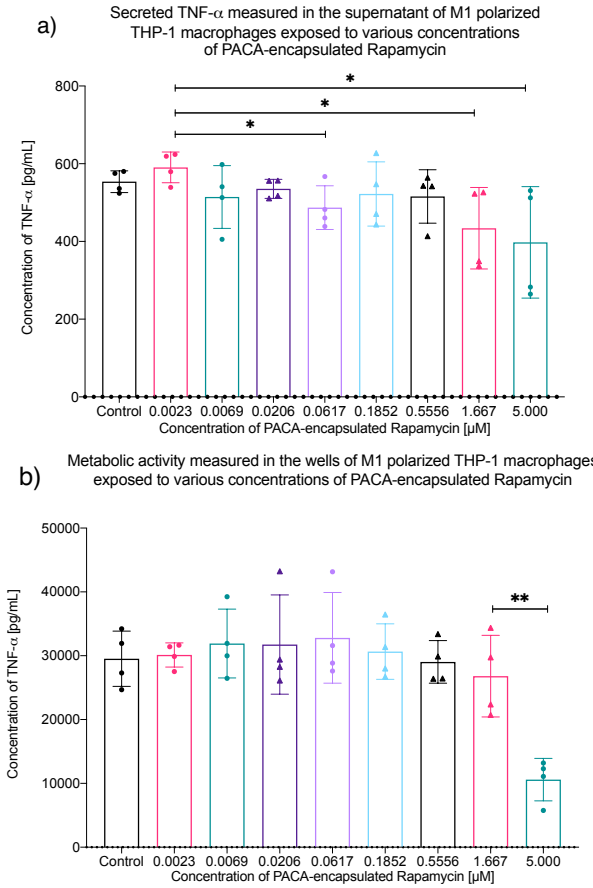

Figure 4.20: *Bar charts presenting the secretion of TNF-α (a) or the metabolic activity (b) on the y-axis versus added concentrations of PACA-encapsulated Rapamycin on the x-axis. The measurements were performed on THP-1 macrophages exposed to M1 polarizing stimuli and various concentrations of PACA-encapsulated Rapamycin for 24 hours. The control sample represents THP-1 macrophages exposed solely to M1 polarizing agents and DMSO. The concentration of TNF-α in the supernatant was measured by Sandwich ELISA, whereas CTG was performed directly in each well to investigate the metabolic activity. Each point represents the average of duplicates, and the results are expressed as means $\pm$ standard deviation (n=4 independent biological replicates). Statistical analysis was carried out using unpaired t-tests by GraphPad Prism version 8.4.2 for macOS. ns: not significantly different. $*$, $**$ or $***$: significantly different respectively with $p < 0.05$, 0.005 or 0.0005.*

The graph in Figure 4.20 presents the data obtained from THP-1 macrophage exposure to the PACA-encapsulated form of Rapamycin. As seen in Figure 4.20 b, the highest investigated concentration profoundly impacts the cells' metabolic activity. A significantly decreased secretion of TNF-α was detected across the range of increasing PACA-encapsulated Rapamycin concentrations, seen in Figure 4.20 a. Based on both Figures 4.19 and 4.20, the PACA-encapsulation, rather than the Rapamycin itself, seems to induce a more pronounced drop in the metabolic activity of the M1 polarized THP-1 cells. Furthermore, the metabolic activity rather than a direct effect of Rapamycin seems to be the decisive factor for the secretion of TNF-α.

4.2.5 Summarizing the measured effect of TH5487, Rapamycin and BMS-345541

Table 4.2: *The table presents the various chemical compounds tested and the observed effect on the M1 polarized THP-1 macrophage viability and the secretion of TNF-α.*

Marked observations		
Polarizing agents	**Effect on TNF-α**	**Metabolic activity**
TH5487	No significant decrease	Significant decrease above 10 μM
BMS-345541	No significant decrease	Significant increase between control to 0.206 μM Significant decrease above 0.5556 μM
Rapamycin, free	Significant but minor decrease between 0.0023 μM to 1.667 μM	Significant decrease between 0.0069 μM and 0.1852 μM to 5.000 μM
Rapamycin, PACA-enapsulated	Significant decrease between 0.0023 μM to 0.0167 μM, 1.667 μM, and 5.000 μM	Significant decrease above 1.667 μM

CHAPTER 5

Discussion

This study's major focus was to establish and investigate quantitative methods for the characterization of THP-1 macrophage polarization. The macrophage polarization model was based on a protocol of PMA-differentiated THP-1 macrophages, previously developed by the author [1]. Once differentiated, the THP-1 macrophages were incubated with IFN-γ and LPS, or IL-4 and IL-13 to induce an M1 or M2 macrophage phenotype, respectively. Polarized M1 and M2 THP-1 macrophages and unpolarized M0 THP-1 macrophages were harvested and investigated for expression of specific cell surface markers by flow cytometry. The supernatants were analyzed by Sandwich ELISA for the secretion of specific cytokines. The collected results of M1 polarized THP-1 macrophages presented both a significantly increased number of cells expressing the M1 cell surface markers and a significantly increased secretion of the M1 phenotypic cytokines. Thus, the results support the hypothesis that the THP-1 cell line can be controlled to induce M1-like macrophages characterized by classical M1 phenotype markers. The M2 polarized THP-1 macrophages, on the other hand, did neither present an increased amount of cells with M2 specific cell surface markers, nor did they significantly increase the secretion of the classical M2 phenotype cytokines. In this regard, the results do not support the hypothesis that the THP-1 cell line can be polarized towards an M2-like phenotype characterized by classical M2 phenotype markers. Although most TAM studies utilize IL-4 and IL-13 for M2 polarization, these stimuli might not be the optimal choice to induce an M2-like phenotype in THP-1 macrophages. Besides, other quantitative methods or markers should be evaluated to investigate successful M2 polarization.

Based on these results, the THP-1 macrophage model was further developed to investigate the potential effect of specific chemical substances targeting essential pathways of M1 polarization. As described in Theory Section 2.7.5, both TH5487 and BMS-345541 prevent inflammatory gene expression by perturbing NF-κB. BMS-345541 directly interferes with the NF-κB pathway by inhibiting IKKβ, whereas TH5487 is suggested to restrain

NF-κB-dependent transcription by preventing the recruitment of OGG1 to 8-oxoG at promoter regions in the DNA [27]. Thus, by exposing macrophages to TH5487 and BMS-345541, the aim was to investigate a potential inhibitory effect on the NF-κB-pathway be analyzing the LPS- and IFN-γ-stimulated secretion of TNF-α. Also, given the multiple and contradictory roles of the mTOR pathway, we wanted to investigate the effect of Rapamycin on the LPS- and IFN-γ stimulated secretion of TNF-α. The concentration of LPS and IFN-γ was optimized to avoid excessive secretion of TNF-α. Unexpectedly, upon THP-1 macrophage cultivation with M1 polarizing stimuli, neither of the investigated compounds affected the secretion of TNF-α. Thus, in these experimental conditions, an NF-κB-independent pathway of TNF-α upon stimulation by LPS and IFN-γ was suggested. Moreover, the induced secretion of TNF-α appeared unaltered after inhibiting the mTOR pathway.

5.1 Methodological considerations

5.1.1 The THP-1 cell line as a model system

Importantly, the THP-1 cells are derived from a human leukemia monocytic cell line and contain genetic and regulatory alterations [58, 61]. Thus, THP-1 macrophages' phenotypic and molecular characteristics might diverge from primary circulating monocytes. The reliability of utilizing THP-1 cell line-derived macrophages as an alternative model system of primary macrophages should be investigated for every experimental setting. Using THP-1 cells and primary monocytes side-by-side would allow informed considerations on the convenience of using THP-1 macrophages as a model for primary monocytes.

5.1.2 Cell surface marker analysis by flow cytometry

Detecting the upregulation of cell surface proteins is a widely used method to study macrophage polarization. Before the cells can be analyzed in the flow cytometer, they must be detached from the plate. The detachment procedure causes a certain obstacle when investigating PMA-differentiated THP-1 macrophages as these cells become strongly adherent to cell culture surfaces. Besides, cell viability and membrane properties, including surface molecules, might be sensitive to cell dissociation techniques. Accutase is the recommended replacement for Trypsin in FACS analysis of cell surface markers and phenotyping [80]. In their study, Chen et al. [80] compared phenotypic alterations resulting from different macrophage detachment methods. This research group reported on MDMs that enzymatic detachment techniques, using Trypsin and Accutase, resulted in advantageous cell yield and viability compared to non-enzymatic methods, using EDTA and temperature-induced cell detachment. However, the enzymatic methods also affected the phenotypic and functional properties of some surface proteins commonly used to characterize macrophage polarization. Accutase and Trypsin are enzymatic detachment reagents containing proteases that cleave proteins at specific amino acid sequences. Trypsin was found to significantly degrade the amount of CD14, CD163, and CD206 on the cell surface. In contrast, the level of CD80 and MHCII presented no significant difference in the surface protein level among the various detachment methods [80]. In their studies,

Chen et al. [80] found that Accutase did not affect surface protein levels of CD14, whereas CD163 and CD206 were degraded, but to a less extent as compared to the cells treated with Trypsin. In the project performed herein, the cells were detached using Accutase. Successively, exposure to Accutase might contribute to a reduced protein level of CD163 and CD206, as reported by Chen et al. [80]. Importantly, when evaluating the macrophage phenotype by flow cytometry, the impact of the cell detachment method should be considered. Other methods to confirm the detected level of surface markers should potentially be included to improve the reliability of the assay.

As previously reported by the author [1], the amount of M1 macrophages is reduced following increasing incubation times with LPS. Although the LPS concentration used herein was reduced to 0.1 ng/mL, as suggested based on results presented by Caras et al. [121] and Stadheim [1], a decreasing amount of M1 stimulated macrophages could be detected after three and five days of polarization. A sample that contains a reduced number of cells provides a less representative result compared to samples with a large number of cells, and the source of uncertainty increases.

During the development of the fluorescence compensation matrix in Section 3.4.1, it was found that the combination of PerCP-Cy5.5 Mouse Anti-Human HLA-DR and the other fluorochromes had to be avoided due to a high degree of emission overlap, especially against APC-H7 Mouse Anti-Human CD80. Successively, the expression of MHCII could not be included in the density plots and the percentual investigations of expressed surface markers on differently polarized macrophages, as presented in Section 4.1.1. In further studies, other fluorescent-conjugated antibodies detecting MHCII should be investigated to enable comparison. Furthermore, as M2 polarization did not induce an increased amount of THP-1 macrophages expressing CD163 and CD206, other markers of M2 polarization should be included to investigate this phenotype.

5.1.3 Cytokine secretion analysis by Sandwich ELISA

Sandwich ELISA was used to study the cytokine secretion profiles in the supernatant of variously polarized THP-1 macrophages. This method provides high sensitivity and specificity for the target antigen as two antibodies, one for capture and one for detection, are used [115]. However, insufficient binding of the detection antibody to the plate, target concentration below the detection range of the assay, or incorrect dilutions might contribute to weak or low signals. Conversely, high background or too much signal can result from insufficient plate washing, adding too much detection reagent, cross-reactivity of antibodies or samples, or contamination [115]. Herein, measurements were performed in duplicates, and the experiments were repeated at least three times to minimize such sources of error. To further validate the results, other antibodies for the specific antigen could be examined. Importantly, the polarizing medium was not changed following the various incubation times. Consequently, it complicates the detection of a potential decrease in cytokine secretion. For example, the concentration of secreted CXCL10 did not present a significant difference between 6 hours, one day, or three days of polarization. In further investigations, the medium could be changed following various incubation times.

While M1 polarized macrophages were characterized by significantly increased secretions of the hypothesized M1 cytokines, M2 polarized macrophages were challenging to identify based on the cytokines investigated herein. Probably, other M2 specific cytokines

should be included to examine these macrophages. Alternatively, other detection methods should be considered. Previous studies have reported that the grade of polarization varies if detected on the mRNA or protein level [129]. Similarly, in the work of Martinez et al. [130], few coincidences were detected between the mRNA and protein levels of M2 polarized macrophages. This research group suggested that the main alterations in mRNA upon macrophage exposure to IL-4 occurred in genes that cannot be detected by proteomics due to their medium to low expression levels. Furthermore, the results of Martinez et al. [130] indicated a particularly specific IL-4 generated gene profile when comparing the respective gene regulations to macrophages exposed to IFN-γ, M-CSF, or IL-10. Successively, gene detection rather than protein secretion might better work to investigate the M2 macrophage phenotype. However, it has to be kept in mind that Martinez et al. [130] investigated the gene profile of diverse human and mouse macrophage models and that the THP-1 monocyte cell line was not included in the study. In their work, Shiratori et al. [87] reported a generally higher gene expression in PBMC-derived macrophages compared to THP-1 macrophages. Similar observations were reported by Tedesco et al. [129], where MDMs overall led to a more pronounced response at the transcriptional level, whereas the secreted amount of proteins was significantly higher in THP-1 macrophages. Defining the THP-1 signature might reveal genes that are highly expressed in both THP-1 and PBMC-derived macrophages upon exposure to IL-4, potentially enabling the characterization THP-1 derived M2-like macrophages. Importantly, the methods used for detecting the various phenotypes have to be further examined to strengthen the comparison between research results on THP-1 and PBMC-derived macrophages.

5.1.4 CellTiter-Glo as a method to study the cell viability

The CellTiter-Glo Luminescent Cell Viability Assay was used to examine the level of toxicity upon macrophage exposure to increasing concentrations of various chemical substances. Importantly, CTG results do not directly indicate the number of viable cells, as this assay is based on ATP as a marker of viable cells. Practically all cell functions depend on the presence of intracellular ATP as an energy carrier. While a reduced CTG measurement can result from a cell death-dependent depletion of ATP, fluctuations in the intracellular ATP-level might also arise from variations in metabolic activity [131].

Importantly, the level of intracellular ATP is markedly affected during cell differentiation. It is not known whether incubation with the diverse investigated compounds affects the THP-1 macrophage differentiation. While little information exists regarding the intracellular ATP level in THP-1 cells during differentiation, the ATP level during differentiation in other cells has been reported both to increase or decrease, depending on the cell type [131]. One of the hallmarks of THP-1 cell differentiation includes an increase in the cytoplasmic volume [61, 122]. Alteration in the cytoplasmic volume is known to affect the ATP content and might contribute to a nonlinear relationship between the relative luminescence measured and the number of cells [128]. Besides, cell division can influence the intracellular level of ATP, also between genetically identical eukaryotic cells, as it might cause an unequal distribution of mitochondria. Hence, to achieve a more accurate measure of the TNF-α secretion relative to the cell number, other methods to detect the cell number could be investigated. Herein, an altered differentiation or cell division rate could obscure a potential change in the secretion of TNF-α.

The seeding of cells might result in uneven cell numbers in each well, and edge effects might result from increased condensation at the edges of the plate. Hence, samples were added in duplicates, and the cell number was counted three times in the *Countess II^{TM}Automated Cell Counter* (Invitrogen) before every seeding to minimize such potential sources of error. Also, cell seeding was avoided in the plates' outermost wells to reduce variations in the volume.

5.2 Polarization of THP-1 macrophages

The polarization study was performed to investigate quantitative methods to examine whether the THP-1 monocyte cell line could be controlled to induce the M1 and M2 macrophage phenotypes. While M1 macrophage phenotypes are known to be induced by IFN-γ and LPS, M2 macrophage phenotypes are commonly known to respond to IL-4 and IL-13 [17, 14, 48]. Flow cytometry was used to detect well-known M1 and M2 specific cell surface markers. MHCII and CD80 were used to identify M1 polarized macrophages, whereas CD163 and CD206 were used to identify M2 polarized macrophages. ELISA measurements were performed to study the secretion of putative M1 and M2 phenotypic cytokines and chemokines in the supernatant of polarized THP-1 macrophages. Here, secretion of TNF-α and CXCL10 were considered M1 specific, whereas secretion of IL-10 and IL-1Ra were considered M2 specific.

5.2.1 Polarization towards the M1 macrophage phenotype

Exposure of THP-1 macrophages to LPS (0.1 ng/mL) and IFN-γ (20 ng/mL) induced a significant increase in the expression and secretion of all investigated M1 phenotypic markers. The M1 polarization induced a significantly upregulated expression of both the investigated M1 phenotypic cell surface markers, MHCII and CD80, and a significantly increased and specific secretion of the M1 phenotypic cytokines, CXCL10 and TNF-α. An increased M1 phenotypic marker expression profile is in line with previous literature [63, 129, 87]. In the work of Genin et al. [63], THP-1 macrophage incubation with IFN-γ (20 ng/mL) and LPS (10 pg/mL) increased expression of M1 putative markers measured both at the mRNA and protein level. This research group reported an increased expression profile after combined exposure to IFN-γ and LPS, rather than to LPS alone [63]. Similarly, Shiratori et al. [87] reported an evident M1 phenotypic profile of both THP-1 and PBMC-derived macrophages in response to IFN-γ (20 mg/mL) and LPS (50 ng/mL) activating stimuli. In their work, Shiratori et al. [87] reported a significant increase in the expression of M1 genes following six and 24 hours of polarization, followed by a gradual decrease. Herein, the measurements were performed at the protein level, and an increase following 24 hours of polarization was detected for M1 cell surface markers. In contrast, a potential decrease in cytokine secretion was challenging to detect as the medium was not changed following increasing exposure time. However, the expression of both M1 specific cell surface markers increased between one to three days of polarization. The MHCII marker significantly increased the number of MHCII positive cells between these polarization times, while the number of MHCII molecules on the MHCII positive cells did not significantly change. On the other hand, increased incubation times did not significantly

increase the amount of CD80 positive cells between one and three days of polarization. However, the amount of CD80 molecules on the CD80 positive cells increased.

Under the specific conditions investigated herein, M1 polarization of THP-1 macrophages did not significantly upregulate the expression of the investigated M2 phenotypic cell surface markers, CD163 or CD206, or the secretion of the M2 phenotypic IL-10 cytokine. Only a significant increase of IL-1Ra was detected following three days of exposure to M1 polarizing agents as compared to M0 THP-1 macrophages. The absence of M2 markers in M1 polarized THP-1 cells is in line with the findings presented by Genin et al. [63], where no significant expression of CD206, CD163, or IL-10 was detected. Furthermore, in the study presented herein, unpolarized M0 macrophages did not express M1 phenotypic markers. These results indicate that the 15 nM PMA-concentration, and the resting period of three days used herein works to limit constitutive cytokine production, as suggested by Daigneault et al. [122] and Caras et al. [121].

Collectively, both the cell surface marker expression and the cytokine secretion profile of the M1 polarized THP-1 macrophages indicates a specifically induced expression of the M1 phenotype, which is in line with results presented in previous literature [63, 87, 129]. These results confirm the hypothesis that incubation of THP-1 macrophages with LPS (0.1 ng/mL) and IFN-γ (20 ng/mL) induces the expression of the investigated M1 macrophage markers. This finding enables the characterization and identification of M1 phenotype THP-1 macrophages.

5.2.2 Polarization towards the M2 macrophage phenotype

While M1 polarization induced the expected outcome, M2 polarization, by incubation with IL-4 (20 ng/mL) and IL-13 (20 ng/mL), apparently did not influence the THP-1 macrophage phenotype. Expression of the selected M2 phenotypic markers measured after incubation with M2 polarizing stimuli for the various exposure times did not match the expected hypothesis. Specifically, only a minimal significant increase was detected in the percentual surface expression of CD163 and the secretion of IL-1Ra, both measured after three days of polarization and compared to M0 macrophages.

Expression of the M2 specific cell surface marker CD206 was close to undetectable in all investigated THP-1 macrophage samples. Similar observations were reported by Genin et al. [63], where the cell surface expression of CD206 only slightly increased following one day of exposure. However, in their studies, Genin et al. [63] found a significantly higher expression of several M2 phenotype markers after three days of exposure to IL-4 (20 ng/mL) and IL-13 (20 ng/mL). Importantly, most of their analysis was conducted at the mRNA level. By Genin et al. [63], a significant increase at the protein level was only measured by FACS for CD206 and ELISA for IL-10. However, these findings are not confirmed herein, nor detected in the work of Tedesco et al. [129] in their THP-1 macrophage incubation with IL-4 (20 ng/mL) and IL-13 (5 ng/mL) in the presence of PMA (185 ng/mL). Tedesco et al. [129] detected a minimal increase in the expression of CD206 in less than 4% of the M2 polarized THP-1 macrophages, highly consistent with the percentage detected herein. However, no significant difference was detected between the M1 and M2 polarized THP-1 macrophages, either herein or by Tedesco et al. [129]. Shiratori et al. [87] also reported such a limited response to M2 polarization in their exposure of THP-1 macrophages to IL-4 (20 mg/mL). Although this research group used a

highly increased concentration of IL-4 compared to other studies, the exposed cells presented only a slightly upregulated expression of CD206 in THP-1 macrophages. Besides, the CD163 cell surface marker was undetectable in M2 polarized THP-1 macrophages but presented an increased expression in about 10% of M2 polarized MDMs in their work [129]. As reported by this research group, a consistent increase in the surface expression of M2a markers could only be detected on PBMC-derived macrophages and not on THP-1 macrophages.

Herein, the absent expression of M2 cell surface markers was further confirmed by the ELISA measurements of M2 specific cytokines. The secretion of IL-1Ra significantly increased only in comparison to M0 macrophages following three days of polarization. Furthermore, not only was there a non-significant difference in the secretion of IL-10 or IL-1Ra between M1 and M2 polarized cells, but the results indicated a trend toward increased secretion from the M1 polarized macrophages. Similarly, Tedesco et al. [129] measured no alteration in the secretion of IL-10 in either M2 polarized THP-1 macrophages or MDMs. Concerning the secretion of IL-1Ra measured by this group, only THP-1 macrophages presented increased secretion; however, both in M1 and M2 polarized cells Tedesco et al. [129].

Regarding the expression of M1 phenotypic markers in M2 polarized THP-1 cells, only the MHCII surface marker indicated a significant increase in the expression between one and three days of polarization. This MHCII-increase, however, was minor and significantly lower compared to the M1 polarized macrophages.

The flow cytometry and ELISA analysis collectively indicate that the investigated THP-1 macrophage polarization protocol for M2 polarization does not induce the expected expression of an M2-like phenotype. Although some mentioned research has detected certain M2 specific markers to be significantly upregulated on M2 polarized THP-1 macrophages, the total response appears to be highly inconsistent and limited compared to the response detected in PBMC-derived macrophages. The results either suggest that exposure to IL-4 and IL-13 does not induce the M2 macrophage phenotype in THP-1 macrophages under these conditions, or that the selected markers do not sufficiently represent the induced phenotype.

5.2.3 Implications of the polarization results

Importantly, care must be taken when comparing results generated in different experimental polarization protocols. Comparison to previous literature presents variability in the use of concentrations, incubation times, and detection methods. The work of Martinez et al. [130] further emphasizes that one must be cautious when comparing results attained from different experimental protocols [130]. This research group performed whole-genome microarray and proteomic analysis to compare alterations in gene and protein expression of various macrophage culture models previously investigated in the literature. Martinez et al. [130] focused on highly expressed genes, rather than the putative M2 specific markers. Their results indicated a more variable response in macrophages exposed to IL-4 than in unexposed macrophages of the various macrophage models. Importantly, M2 polarized macrophages appeared more sensitive and tuned by additional factors of the culture conditions, including cell type, differentiation stimulus, and culture surface [130].

Altogether, the results of the polarization studies indicate that THP-1 macrophages respond to the polarization protocol used for M1 polarization, whereas the protocol used for M2 polarization needs further development. Therefore, the data presented herein suggest that the THP-1 macrophage polarization model might be utilized when performing studies involving M1 polarization. Importantly, inflammation contributes in a complex manner in cancer, where it seems to exert both pro-tumorigenic and anti-tumorigenic functions. Understanding the immune cell signaling, cytokine production, and cross-talk in the TME is important to improve cancer therapeutics. Identifying the molecular mechanism underlying the pro- and anti-tumor immune responses is essential to enhance the cancer control [26, 62]. With a well-controlled and simplified macrophage model, essential pathways of macrophage polarization can potentially be identified and investigated. Therefore, we wanted to further investigate the M1 polarization of THP-1 macrophages under the exposure to various chemical substances that target pathways known to exert a regulatory role in inflammation.

5.2.4 TH5487 and BMS-345541

The NF-κB pathway has been extensively studied as a drug target as it contributes to regulating several essential effector genes, both in tumor cells and in healthy cells in the TME [26, 93]. We investigated the inhibitory effect of TH5487 on the NF-κB pathway by detecting the M1 polarization induced secretion of TNF-α. BMS-345541 is a well-known inhibitor of NF-κB activation and was investigated as a positive control to inhibit signal-induced activation and translocation of NF-κB [97].

In the experimental system used herein, the secretion of TNF-α was not affected by TH5487. Consequently, the results presented herein indicate an OGG1-independent secretion of TNF-α. This presented result is in contrast to the finding presented by Seifermann et al. [96], who suggested a direct gene regulatory function of OGG1 to activate the LPS-induced expression of TNF-α in macrophages [96].

Importantly, similarly to TH5487, exposure to BMS-345541 did not confirm the hypothesis of an inhibited LPS- and IFN-γ induced TNF-α secretion. The CTG measurements indicated a significantly increased metabolic activity in THP-1 cells after exposure to the lowest investigated concentrations of BMS-345541. At the same time, no significant decrease or increase in the secretion of TNF-α was detected. Accordingly, it can not be directly concluded that the TNF-α secretion was unaltered following exposure to BMS-345541 at the lowest concentrations. A significantly increased metabolic activity can potentially indicate increased cell numbers, obscuring a possible decrease in the cell-specific secretion of TNF-α. Further studies should be performed to more accurately investigate the secretion of TNF-α relative to the number of cells. However, a significant decrease in metabolic activity was detected upon exposure to the highest investigated concentrations of BMS-345541, with a simultaneous drop in the TNF-α secretion. These results indicate a decreased secretion of TNF-α due to increased cytotoxicity, which most certainly reduces the number of cells. Therefore, in total, BMS-345541 affects the metabolic activity in M1 polarized THP-1 macrophages but displays no evident direct influence on the TNF-α secretion. These results suggest that, under these experimental conditions, the LPS- and IFN-γ stimulated secretion of TNF-α in THP-1 macrophages is independent of the NF-κB pathway.

Collectively, the secretion of TNF-α in M1 polarized THP-1 macrophages appeared to be unaffected by both BMS-345541 and TH5487. Therefore, the absent response to TH5487 might be explained by an NF-κB-independent TNF-α secretion rather than disconfirming the hypothesis of an OGG1 regulatory function, suggested by Visnes et al. [27] and Seifermann et al. [96]. Together, these results suggest that the M1 stimulated secretion of TNF-α in the experimental conditions used herein is independent of the NF-κB-pathway.

Importantly, a great correlation between THP-1 cells and PBMC derived macrophages have previously been reported upon activation by LPS. Hence, THP-1 macrophages have been suggested as useful models to study several aspects of the LPS induced NF-κB response and alterations in gene expression [132]. Further research should be performed to investigate whether other NF-κB-related cytokines present similar independence of this pathway in this THP-1 macrophage model. However, it is not clear whether BMS-345541 and TH5487 truly affect the NF-κB pathway under the experimental conditions used herein. Hence, the expression of NF-κB should be investigated, for example, by using Western blot analysis. Besides, it would be interesting to include mRNA analysis of the TNF-α expression to investigate a potential inhibitory effect that can not be revealed at the protein level following 24 hours of exposure.

A suggestion of an NF-κB-independent TNF-α secretion is not in line with previous studies, which have presented the secretion of TNF-α to be dependent upon the NF-κB pathway [133, 97]. Interestingly, He et al. [133] and Burke et al. [97] both stimulated THP-1 macrophages solely by LPS without the addition of IFN-γ. Herein, IFN-γ and LPS were combined to provoke M1 polarization and stimulate TNF-α secretion. Although the secretion of TNF-α was found to primarily depended on the concentration of LPS, as presented in Figure 4.16 and 4.15, combinations of LPS and IFN-γ might contribute to a more complex activation. While the gene expression profiles of LPS and IFN-γ stimuli have been shown to express certain similarities, they are not homologous. There is a documented difference in the recorded gene expression profile if the stimuli consist of LPS and IFN-γ alone or in combination [21]. IFN-γ primes macrophages for augmented responses to TLR ligands by promoting the transcription of receptors, co-receptors, and signaling molecules. Maximal signaling of LPS requires the CD14 co-receptor, as well as the MyD88 signaling adaptors. IFN-γ is described to increase the TLR expression, and promote expression of the MyD88 adaptor and subsequent signaling molecules [64]. The synergistic effect of LPS and IFN-γ is highly relevant for THP-1 macrophages, as they have been described to not sufficiently respond to LPS alone, due to low expression of CD14. In THP-1 macrophages, the combination of LPS and IFN-γ induced a notably enhanced MyD88 mRNA expression compared to either agent alone [134].

Lu, Yeh, and Ohashi [67] describe several transcription factors downstream of MyD88 that might regulate the transcription of pro-inflammatory cytokines, including AP-1 and IRF5. As targeting NF-κB activation did not affect the secretion of TNF-α herein, it is possible that, in our THP-1 macrophage model, the LPS and IFN-γ induction of TNF-α mainly depends on other transcription factors not influenced by IκB kinases or OGG1. Presented in the study of [96], the MAPK-mediated activation pathway, in contrast to the NF-κB pathway, seems to be independent on the presence of OGG1. As mentioned by Shiratori et al. [87], the JAK-STAT pathway that is induced upon activation by IFN-γ,

induces IRF5, which activates genes encoding inflammatory cytokines. Moreover, mice deficient in IRF5 have been reported as partially defective in the induction of TNF-α upon *in vivo* challenge with LPS [67]. Hence, further studies should include inhibitors targeting other transcription factors that might initiate secretion of TNF-α.

5.2.5 Rapamycin

Regulations of the mTOR pathway have recently been reported to induce opposing effects on the survival and polarization of macrophages [28, 29, 101]. Apparently, inhibition of the mTOR pathway by Rapamycin can exert pro-inflammatory or anti-inflammatory effects depending on the cell type and environmental stimuli [98, 100]. Given the contradictory, complex, and incompletely understood roles of the mTOR pathway, we wanted to investigate the effect of Rapamycin in our THP-1 macrophage polarization model by detecting the M1 polarization induced secretion of TNF-α.

Exposure of free Rapamycin during M1 polarization of THP-1 macrophages by LPS (25 pg/mL) and IFN-γ (20 ng/mL) resulted in a corresponding significant decrease in the secretion of TNF-α and the metabolic activity. Besides, a significant decrease in the TNF-α secretion was detected upon exposure to increasing concentrations of PACA-encapsulated Rapamycin. However, although significant, the decreased secretion of TNF-α was minor in both cases. More profoundly, a decrease in the metabolic activity was detected upon exposure to the highest investigated PACA-encapsulated Rapamycin concentration, indicating a substantial effect of the compound on cellular viability. Due to this distinct drop in metabolic activity, the decreased secretion of TNF-α cannot directly be linked to an effect of the compound. Without further investigations, the PACA-encapsulated Rapamycin seems to influence the metabolic activity of the M1 polarized macrophages rather than the secretion of TNF-α. Furthermore, PACA-encapsulated Rapamycin more profoundly affects the metabolic activity than the free form of Rapamycin, indicating higher cytotoxicity against the THP-1 cells.

Absent alteration of the TNF-α expression in response to Rapamycin has previously been presented in the work of Ko et al. [30], on their study of how Rapamycin affects the transcription of LPS-induced pro-inflammatory genes in THP-1 macrophages. This research group found no alteration in the mRNA levels of IL-1β and TNF-α, whereas the levels of IL-6, IL-8, and IκBα transcripts were markedly reduced. Besides, exposure to Rapamycin did not influence the secretion of cytokines related to inflammation, including TNF-α, IL-4, IL-10, IL-12, and IL-13 [30]. On the contrary, Mercalli et al. [28] exposed PBMCs to Rapamycin during M1 polarization and reported a down-regulated secretion of M2 related cytokines, including IL-10 and CCL18, whereas secretion of IL-6, TNF-α and IL-1β were up-regulated. The presented findings are also different from a study on bone marrow-derived cells from rat femurs presenting a reduced LPS-induced TNF-α and IL-10 secretion in the presence of Rapamycin [135]. According to Ko et al. [30] and Weichhart, Hengstschläger, and Linke [101], inhibiting mTORC1 by Rapamycin can induce opposing effects due to the complex functions of mTORC1. Apparently, a pro-inflammatory or anti-inflammatory response to the inhibition of mTORC1 depends on the cell type and the cellular or environmental stress [30, 101].

Consequently, the inconsistency between the findings presented herein and by others could be explained by species-specific variabilities, and diverse differentiation protocols

and experimental conditions. Besides, the review of Weichhart, Hengstschläger, and Linke [101] suggests that researchers' observation of the different roles of mTOR inhibitors is affected by the investigated cytokines. A pro-inflammatory effect has often been suggested due to several findings of promoted IL-12 expression and blocked IL-10 expression. Contrary, an anti-inflammatory effect of mTOR inhibitors has also been suggested as the expression of TNF-α and IL-6 often is blocked [101].

Based on the study presented herein and the study by Ko et al. [30], Rapamycin does not seem to affect the expression of TNF-α in THP-1 macrophages. However, the potential effect on other inflammatory-related cytokines upon exposure to Rapamycin should be investigated in the macrophage model presented herein, both at the mRNA and protein levels.

5.2.6 Implications of the results

Our findings on the M1 polarized THP-1 macrophage model demonstrate an LPS- and IFN-γ-induce secretion of TNF-α that does not depend on the NF-κB pathway or the mTOR pathway under the investigated conditions. Future research should include the detection of an assortment of cytokines, in addition to TNF-α, both at the mRNA and protein level to gain increased knowledge of the compounds' effect. Besides, experiments should be performed to study whether the expression of NF-κB and mTOR actually is affected in our model.

5.2.7 Future research

A robust THP-1 macrophage model could be utilized as a tool to study the influence of specific pathways on the macrophage polarization. It could potentially be utilized to study the relationship between macrophages and cancer cells and investigate how specific pathways of macrophage polarization contribute to either protective or cytotoxic effects [63]. To be able to compare the effect on various macrophage phenotypes, other methods of M2 polarization and detection should be taken into consideration. Interestingly, according to Mercalli et al. [28], Rapamycin differently modulates macrophage survival in PBMCs polarized towards the M1 or M2 phenotype. This research group found that Rapamycin selectively killed macrophages exposed to M2 polarization, suggesting the mTOR pathway to be specifically essential in M2 phenotype macrophages [28]. With further development of the M2 polarization THP-1 macrophage protocol, this observation should be investigated in THP-1 cells.

Further studies investigating a potential M2 polarization of THP-1 macrophages should include incubation with other polarizing stimuli thought to provoke the M2 phenotype. For example, the upregulated expression of CD163 in macrophages is considered one of the major contributors to switching the macrophage activation towards an anti-inflammatory status [82]. However, according to Graversen, Madsen, and Moestrup [136] and RHoszer [51], the *in vitro* expression of CD163 is mainly upregulated in response to IL-6, IL-10, and glucocorticoids. Surprisingly, Etzerodt and Moestrup [82] and RHoszer [51] mention that the effect of IL-4 contribute to repress the expression of CD163. This suggestion is contradictory as most TAM studies utilize IL-4 and IL-13 to polarize macrophages towards the M2-like phenotype and use CD163 as a marker for successful polarization. Some

studies have already investigated the polarization of THP-1 macrophages after incubation with IL-10, also referred to as M2c polarization. Shiratori et al. [87] investigated M2c polarization by exposure to IL-10 (20 mg/ml), but it induced none of the hypothesized M2c specific markers, including CD163, in either THP-1 or PBMC-derived macrophages. Rather, the proposed M2c markers appeared to be more sensitive to LPS (50 ng/mL) and IFN-γ (20 mg/mL) [87].

A fascinating study performed by Alvarado-Vazquez et al. [137], investigated macrophage-specific nanotechnology driven overexpression of CD163. In this study, the CD163 gene was induced in THP-1 and PBMCs using polyethyleneimine nanoparticles coated with a mannose ligand (Man-PEI). Due to their expression of mannose receptors, Man-PEI nanoparticles target cells of the monocytic lineage. A single and double stimulation of CD163-overexpressing macrophages to LPS (5 μg/mL) presented reduced levels of TNF-α and increased levels of IL-10 and IL-1Ra, respectively. However, the concentration of 5 μg/mL LPS is high compared to the LPS-concentration utilized in other polarization studies mentioned herein [63, 87, 129]. In the work of Genin et al. [63], they suggested that an unspecific expression of M2 macrophage marker expression, including IL-10, could result from the cultivation of THP-1 macrophages to LPS concentrations exceeding 10 ng/mL. Also, the immune complex and TLR ligand activation of macrophages have been found to induce the M2b subset of activation [21]. Successively, further investigation of CD163-overexpressing THP-1 macrophages exposed to minimal concentrations of M1 polarizing agents could yield important information. However, such alternative methods to induce M2 polarization in THP-1 macrophages could be of great interest if future investigations of exposing the cells to M2 polarizing stimuli do not induce the desired effect.

In their studies, Genin et al. [63] developed a THP-1 macrophage model to demonstrate how M1 and M2 macrophages differently influenced the response of cancer cells to a chemotherapeutic drug. In their model, this research group demonstrated that M1 and M2 macrophages exerted opposite effects on the cancer cells [63]. Importantly, although previous research has reported that M2 and TAM macrophages have in common a considerable proportion of their transcriptome, TAMs do not fully resemble the M2-like macrophage phenotype [19, 17]. In future research, with the therapeutic aim of eradicating or re-educating TAMs towards the M1 phenotype, a macrophage polarization model should preferably identify the biological response of TAMs and their response to specific treatments. *In vitro* generated THP-1 and PBMC-derived macrophages stimulated towards the M1 or M2 phenotype will most certainly respond differently than TAMs. Besides, macrophages *in vivo* are not exposed to one stimulus alone. In a malignant context, the monocyte maturation is highly dependent on the tumor milieu [138]. To develop macrophages that better mimic TAMs, the *in vitro* differentiation phase should probably resemble the TME, as investigated in the study of Solinas et al. [138], where PBMCs were co-cultured with cancer cells or cancer-conditioned media. Their results presented a gene profile and phenotype that was more closely related to the findings of TAMs isolated from human tumors. In a follow-up study, Maeda et al. [17] reported that macrophages differentiated in the presence of supernatant from cultivated tumor cells versus macrophages stimulated by IL-4 responded differently upon drug exposure.

A well-controlled macrophage polarization model could potentially be exposed to various tumor cell supernatants to identify the TAM diversity in different tissues and cancer

types, potentially guiding patient selection. Identifying pathways in TAMs responsible for the tumor supporting functions could reveal novel drug targets, and assist the development of new treatment strategies. Besides, targeting the impact of TAMs on cancer cell response to current therapeutics will most likely be beneficial in the clinic [62].

CHAPTER 6

Conclusion

In conclusion, the data described in this study demonstrates the possibility of developing a simplified THP-1 model to study the polarization of macrophages, specifically towards the M1 phenotype. The expression of the selected M1 phenotype macrophage markers did indeed match the expected hypothesis upon exposure to LPS and IFN-γ. In contrast, no specific expression of the M2 phenotypic markers was observed following exposure to IL-4 and IL-13. Future work should investigate alternative approaches to induce the M2 macrophage phenotype.

This study demonstrates a potentially NF-κB independent mechanism in the LPS- and IFN-γ-stimulated secretion of TNF-α in THP-1 macrophages. Moreover, inhibiting the mTOR pathway in these macrophages do not alter the secretion of TNF-α. The effect of the investigated compounds and their target pathways should be further investigated by studying an assortment of cytokines, both at the mRNA and protein levels.

Bibliography

[1] Maria Stadheim. *Development of protocols for macrophage polarization and characterization of resulting phenotypic morphological signatures*. Spezialization project, NTNU, 2019.

[2] World Health Organization. *Cancer*. URL: https://www.who.int/health-topics/cancer#tab=tab_1 (visited on 11/18/2019).

[3] Douglas Hanahan and Robert A Weinberg. "The hallmarks of cancer". In: *cell* 100.1 (2000), pp. 57–70.

[4] Don S Dizon et al. "Clinical cancer advances 2016: annual report on progress against cancer from the American Society of Clinical Oncology". In: *Journal of clinical oncology: official journal of the American Society of Clinical Oncology* 34.9 (2016), p. 987.

[5] Abul K Abbas, Andrew HH Lichtman, and Shiv Pillai. *Basic Immunology E-Book: Functions and Disorders of the Immune System*. Elsevier Health Sciences, 2015. Chap. 10.

[6] Alberto Mantovani et al. "Cancer-related inflammation". In: *Nature* 454.7203 (2008), p. 436.

[7] Sergei I Grivennikov, Florian R Greten, and Michael Karin. "Immunity, inflammation, and cancer". In: *Cell* 140.6 (2010), pp. 883–899.

[8] Hongming Zhang and Jibei Chen. "Current status and future directions of cancer immunotherapy". In: *Journal of Cancer* 9.10 (2018), p. 1773.

[9] Hossein Borghaei, Mitchell R Smith, and Kerry S Campbell. "Immunotherapy of cancer". In: *European journal of pharmacology* 625.1-3 (2009), pp. 41–54.

[10] Sofia Farkona, Eleftherios P Diamandis, and Ivan M Blasutig. "Cancer immunotherapy: the beginning of the end of cancer?" In: *BMC medicine* 14.1 (2016), p. 73.

[11] Axel Hoos et al. "Improved endpoints for cancer immunotherapy trials". In: *Journal of the National Cancer Institute* 102.18 (2010), pp. 1388–1397.

[12] Axel Hoos et al. “A methodological framework to enhance the clinical success of cancer immunotherapy”. In: *Nature biotechnology* 29.10 (2011), p. 867.

[13] Florent Ginhoux and Steffen Jung. “Monocytes and macrophages: developmental pathways and tissue homeostasis”. In: *Nature Reviews Immunology* 14.6 (2014), pp. 392–404.

[14] Alberto Mantovani et al. “Tumour-associated macrophages as treatment targets in oncology”. In: *Nature reviews Clinical oncology* 14.7 (2017), p. 399.

[15] Sebastian R Nielsen and Michael C Schmid. “Macrophages as key drivers of cancer progression and metastasis”. In: *Mediators of inflammation* 2017 (2017).

[16] Alberto Mantovani et al. “Macrophage plasticity and polarization in tissue repair and remodelling”. In: *The Journal of pathology* 229.2 (2013), pp. 176–185.

[17] Akihiro Maeda et al. “Poly (I: C) stimulation is superior than Imiquimod to induce the antitumoral functional profile of tumor-conditioned macrophages”. In: *European journal of immunology* 49.5 (2019), pp. 801–811.

[18] Arsen Osipov et al. “Small molecule immunomodulation: the tumor microenvironment and overcoming immune escape”. In: *Journal for immunotherapy of cancer* 7.1 (2019), p. 224.

[19] Inc. Bio-Rad Laboratories. *Mini-review: Macrophage Polarization*. URL: `https://www.bio-rad-antibodies.com/macrophage-polarization-minireview.html`.

[20] Mirco Ponzoni et al. “Targeting macrophages as a potential therapeutic intervention: impact on inflammatory diseases and cancer”. In: *International journal of molecular sciences* 19.7 (2018), p. 1953.

[21] Fernando O Martinez and Siamon Gordon. “The M1 and M2 paradigm of macrophage activation: time for reassessment”. In: *F1000prime reports* 6 (2014).

[22] Fernando Oneissi Martinez et al. “Macrophage activation and polarization”. In: *Front Biosci* 13.1 (2008), pp. 453–461.

[23] Le-xun Wang et al. “M2b macrophage polarization and its roles in diseases”. In: *Journal of leukocyte biology* 106.2 (2019), pp. 345–358.

[24] Arjun Saradna et al. “Macrophage polarization and allergic asthma”. In: *Translational Research* 191 (2018), pp. 1–14.

[25] David G DeNardo, Pauline Andreu, and Lisa M Coussens. “Interactions between lymphocytes and myeloid cells regulate pro-versus anti-tumor immunity”. In: *Cancer and Metastasis Reviews* 29.2 (2010), pp. 309–316.

[26] Omer M Ozpiskin, Lu Zhang, and Jian Jian Li. “Immune targets in the tumor microenvironment treated by radiotherapy”. In: *Theranostics* 9.5 (2019), p. 1215.

[27] Torkild Visnes et al. “Small-molecule inhibitor of OGG1 suppresses proinflammatory gene expression and inflammation”. In: *Science* 362.6416 (2018), pp. 834–839.

[28] Alessia Mercalli et al. “Rapamycin unbalances the polarization of human macrophages to M1”. In: *Immunology* 140.2 (2013), pp. 179–190.

[29] Vanessa Byles et al. “The TSC-mTOR pathway regulates macrophage polarization”. In: *Nature communications* 4.1 (2013), pp. 1–11.

[30] Jung Hwa Ko et al. “Rapamycin regulates macrophage activation by inhibiting NLRP3 inflammasome-p38 MAPK-NFκB pathways in autophagy-and p62-dependent manners”. In: *Oncotarget* 8.25 (2017), p. 40817.

[31] Fiona Macdonald, Christopher Ford, and Alan Casson. *Molecular biology of cancer*. Taylor & Francis, 2004.

[32] Douglas Hanahan and Robert A Weinberg. “Hallmarks of cancer: the next generation”. In: *cell* 144.5 (2011), pp. 646–674.

[33] Abul K Abbas, Andrew HH Lichtman, and Shiv Pillai. *Basic Immunology E-Book: Functions and Disorders of the Immune System*. Elsevier Health Sciences, 2015. Chap. 1.

[34] Abul K Abbas, Andrew HH Lichtman, and Shiv Pillai. *Basic Immunology E-Book: Functions and Disorders of the Immune System*. Elsevier Health Sciences, 2015. Chap. 2.

[35] Ruslan Medzhitov. “Origin and physiological roles of inflammation”. In: *Nature* 454.7203 (2008), p. 428.

[36] Glauben Landskron et al. “Chronic inflammation and cytokines in the tumor microenvironment”. In: *Journal of immunology research* 2014 (2014).

[37] TL Whiteside. “The tumor microenvironment and its role in promoting tumor growth”. In: *Oncogene* 27.45 (2008), pp. 5904–5912.

[38] Vasilena Gocheva et al. “IL-4 induces cathepsin protease activity in tumor-associated macrophages to promote cancer growth and invasion”. In: *Genes & development* 24.3 (2010), pp. 241–255.

[39] Christian Frantz, Kathleen M Stewart, and Valerie M Weaver. “The extracellular matrix at a glance”. In: *J Cell Sci* 123.24 (2010), pp. 4195–4200.

[40] Beatrice Yue. “Biology of the extracellular matrix: an overview”. In: *Journal of glaucoma* (2014), S20.

[41] Padmanee Sharma et al. “Novel cancer immunotherapy agents with survival benefit: recent successes and next steps”. In: *Nature Reviews Cancer* 11.11 (2011), p. 805.

[42] Jeremy B Swann and Mark J Smyth. “Immune surveillance of tumors”. In: *The Journal of clinical investigation* 117.5 (2007), pp. 1137–1146.

[43] Gavin P Dunn et al. “Cancer immunoediting: from immunosurveillance to tumor escape”. In: *Nature immunology* 3.11 (2002), p. 991.

[44] Ruth A Franklin et al. “The cellular and molecular origin of tumor-associated macrophages”. In: *Science* 344.6186 (2014), pp. 921–925.

[45] Florent Ginhoux and Martin Guilliams. “Tissue-resident macrophage ontogeny and homeostasis”. In: *Immunity* 44.3 (2016), pp. 439–449.

[46] Paola Italiani and Diana Boraschi. “From monocytes to M1/M2 macrophages: phenotypical vs. functional differentiation”. In: *Frontiers in immunology* 5 (2014), p. 514.

[47] Jeffrey W Pollard. “Tumour-educated macrophages promote tumour progression and metastasis”. In: *Nature Reviews Cancer* 4.1 (2004), p. 71.

[48] Francesca R Bertani et al. “Classification of M1/M2-polarized human macrophages by label-free hyperspectral reflectance confocal microscopy and multivariate analysis”. In: *Scientific reports* 7.1 (2017), p. 8965.

[49] David M Mosser and Justin P Edwards. “Exploring the full spectrum of macrophage activation”. In: *Nature reviews immunology* 8.12 (2008), p. 958.

[50] Peter J Murray et al. “Macrophage activation and polarization: nomenclature and experimental guidelines”. In: *Immunity* 41.1 (2014), pp. 14–20.

[51] Tamas RHoszer. “Understanding the mysterious M2 macrophage through activation markers and effector mechanisms”. In: *Mediators of inflammation* 2015 (2015).

[52] Huiyan Cheng et al. “Macrophage polarization in the development and progression of ovarian cancers: an overview”. In: *Frontiers in oncology* 9 (2019), p. 421.

[53] Alberto Mantovani et al. “The chemokine system in diverse forms of macrophage activation and polarization”. In: *Trends in immunology* 25.12 (2004), pp. 677–686.

[54] Li Yang and Yi Zhang. “Tumor-associated macrophages: from basic research to clinical application”. In: *Journal of hematology & oncology* 10.1 (2017), p. 58.

[55] Yoshihiro Komohara, Masahisa Jinushi, and Motohiro Takeya. “Clinical significance of macrophage heterogeneity in human malignant tumors”. In: *Cancer science* 105.1 (2014), pp. 1–8.

[56] Yoshihiro Komohara et al. “Tumor-associated macrophages: Potential therapeutic targets for anti-cancer therapy”. In: *Advanced drug delivery reviews* 99 (2016), pp. 180–185.

[57] Inmoo Rhee. “Diverse macrophages polarization in tumor microenvironment”. In: *Archives of pharmacal research* 39.11 (2016), pp. 1588–1596.

[58] Wasaporn Chanput, Jurriaan J Mes, and Harry J Wichers. “THP-1 cell line: an in vitro cell model for immune modulation approach”. In: *International immunopharmacology* 23.1 (2014), pp. 37–45.

[59] Zhenyu Qin. “The use of THP-1 cells as a model for mimicking the function and regulation of monocytes and macrophages in the vasculature”. In: *Atherosclerosis* 221.1 (2012), pp. 2–11.

[60] Catheryne Chen et al. “Human THP-1 monocytic leukemic cells induced to undergo monocytic differentiation by bryostatin 1 are refractory to proteasome inhibitor-induced apoptosis”. In: *Cancer research* 60.16 (2000), pp. 4377–4385.

[61] Maria E Lund et al. “The choice of phorbol 12-myristate 13-acetate differentiation protocol influences the response of THP-1 macrophages to a pro-inflammatory stimulus”. In: *Journal of immunological methods* 430 (2016), pp. 64–70.

[62] Alberto Mantovani and Paola Allavena. “The interaction of anticancer therapies with tumor-associated macrophages”. In: *Journal of Experimental Medicine* 212.4 (2015), pp. 435–445.

[63] Marie Genin et al. “M1 and M2 macrophages derived from THP-1 cells differentially modulate the response of cancer cells to etoposide”. In: *BMC cancer* 15.1 (2015), p. 577.

[64] Kate Schroder et al. “Interferon-γ: an overview of signals, mechanisms and functions”. In: *Journal of leukocyte biology* 75.2 (2004), pp. 163–189.

[65] Daniel J Gough et al. “IFNγ signaling—Does it mean JAK–STAT?” In: *Cytokine & growth factor reviews* 19.5-6 (2008), pp. 383–394.

[66] Xiaoyu Hu and Lionel B Ivashkiv. “Cross-regulation of signaling pathways by interferon-γ: implications for immune responses and autoimmune diseases”. In: *Immunity* 31.4 (2009), pp. 539–550.

[67] Yong-Chen Lu, Wen-Chen Yeh, and Pamela S Ohashi. “LPS/TLR4 signal transduction pathway”. In: *Cytokine* 42.2 (2008), pp. 145–151.

[68] Abul K Abbas, Andrew HH Lichtman, and Shiv Pillai. *Basic Immunology E-Book: Functions and Disorders of the Immune System*. Elsevier Health Sciences, 2015. Chap. 3.

[69] Taku Kambayashi and Terri M Laufer. “Atypical MHC class II-expressing antigen-presenting cells: can anything replace a dendritic cell?” In: *Nature Reviews Immunology* 14.11 (2014), pp. 719–730.

[70] Mary Collins, Vincent Ling, and Beatriz M Carreno. “The B7 family of immune-regulatory ligands”. In: *Genome biology* 6.6 (2005), p. 223.

[71] Weiping Zou and Lieping Chen. “Inhibitory B7-family molecules in the tumour microenvironment”. In: *Nature Reviews Immunology* 8.6 (2008), pp. 467–477.

[72] Lieping Chen. “Co-inhibitory molecules of the B7–CD28 family in the control of T-cell immunity”. In: *Nature Reviews Immunology* 4.5 (2004), pp. 336–347.

[73] Mingli Liu, Shanchun Guo, and Jonathan K Stiles. “The emerging role of CXCL10 in cancer”. In: *Oncology letters* 2.4 (2011), pp. 583–589.

[74] H Wajant, K Pfizenmaier, and P Scheurich. “Tumor necrosis factor signaling”. In: *Cell Death & Differentiation* 10.1 (2003), pp. 45–65.

[75] Narayanan Parameswaran and Sonika Patial. “Tumor necrosis factor-α signaling in macrophages”. In: *Critical Reviews^{TM} in Eukaryotic Gene Expression* 20.2 (2010).

[76] Frances Balkwill. “Tumour necrosis factor and cancer”. In: *Nature reviews cancer* 9.5 (2009), pp. 361–371.

[77] Anne Montfort et al. “The TNF paradox in cancer progression and immunotherapy.” In: *Frontiers in immunology* 10 (2019), p. 1818.

[78] Ilkka S Junttila. “Tuning the cytokine responses: an update on interleukin (IL)-4 and IL-13 receptor complexes”. In: *Frontiers in immunology* 9 (2018), p. 888.

[79] Ivan Shabo et al. “Macrophage infiltration in tumor stroma is related to tumor cell expression of CD163 in colorectal cancer”. In: *Cancer microenvironment* 7.1-2 (2014), pp. 61–69.

[80] Shaodong Chen et al. “Impact of detachment methods on M2 macrophage phenotype and function”. In: *Journal of immunological methods* 426 (2015), pp. 56–61.

[81] Holger J Møller. “Soluble CD163”. In: *Scandinavian journal of clinical and laboratory investigation* 72.1 (2012), pp. 1–13.

[82] Anders Etzerodt and Søren K Moestrup. “CD163 and inflammation: biological, diagnostic, and therapeutic aspects”. In: *Antioxidants & redox signaling* 18.17 (2013), pp. 2352–2363.

[83] Abul K Azad, Murugesan VS Rajaram, and Larry S Schlesinger. “Exploitation of the macrophage mannose receptor (CD206) in infectious disease diagnostics and therapeutics”. In: *Journal of cytology & molecular biology* 1.1 (2014).

[84] Paola Allavena et al. “Engagement of the mannose receptor by tumoral mucins activates an immune suppressive phenotype in human tumor-associated macrophages”. In: *Clinical and Developmental Immunology* 2010 (2011).

[85] Umut Gazi and Luisa Martinez-Pomares. “Influence of the mannose receptor in host immune responses”. In: *Immunobiology* 214.7 (2009), pp. 554–561.

[86] Margarida Saraiva and Anne O’garra. “The regulation of IL-10 production by immune cells”. In: *Nature reviews immunology* 10.3 (2010), pp. 170–181.

[87] Hiromi Shiratori et al. “THP-1 and human peripheral blood mononuclear cell-derived macrophages differ in their capacity to polarize in vitro”. In: *Molecular immunology* 88 (2017), pp. 58–68.

[88] Shankar Subramanian Iyer and Gehong Cheng. “Role of interleukin 10 transcriptional regulation in inflammation and autoimmune disease”. In: *Critical Reviews™ in Immunology* 32.1 (2012).

[89] Iona Evans et al. “Action of intracellular IL-1Ra (Type 1) is independent of the IL-1 intracellular signalling pathway”. In: *Cytokine* 33.5 (2006), pp. 274–280.

[90] William P Arend and Carla J Guthridge. “Biological role of interleukin 1 receptor antagonist isoforms”. In: *Annals of the rheumatic diseases* 59.suppl 1 (2000), pp. i60–i64.

[91] Bastian Hoesel and Johannes A Schmid. “The complexity of NF-κB signaling in inflammation and cancer”. In: *Molecular cancer* 12.1 (2013), p. 86.

[92] Michael Karin. “How NF-κB is activated: the role of the IκB kinase (IKK) complex”. In: *Oncogene* 18.49 (1999), pp. 6867–6874.

[93] Rinat Zaynagetdinov et al. “Chronic NF-κB activation links COPD and lung cancer through generation of an immunosuppressive microenvironment in the lungs”. In: *Oncotarget* 7.5 (2016), p. 5470.

[94] Spiros Vlahopoulos et al. “Roles of DNA repair enzyme OGG1 in innate immunity and its significance for lung cancer”. In: *Pharmacology & therapeutics* 194 (2019), pp. 59–72.

[95] Xueqing Ba and Istvan Boldogh. "8-Oxoguanine DNA glycosylase 1: beyond repair of the oxidatively modified base lesions". In: *Redox biology* 14 (2018), pp. 669–678.

[96] Marco Seifermann et al. "Role of the DNA repair glycosylase OGG1 in the activation of murine splenocytes". In: *DNA repair* 58 (2017), pp. 13–20.

[97] James R Burke et al. "BMS-345541 is a highly selective inhibitor of IκB kinase that binds at an allosteric site of the enzyme and blocks NF-κB-dependent transcription in mice". In: *Journal of Biological Chemistry* 278.3 (2003), pp. 1450–1456.

[98] Jing Li, Sang Gyun Kim, and John Blenis. "Rapamycin: one drug, many effects". In: *Cell metabolism* 19.3 (2014), pp. 373–379.

[99] Mathieu Laplante and David M Sabatini. "mTOR signaling at a glance". In: *Journal of cell science* 122.20 (2009), pp. 3589–3594.

[100] Sebastian I Arriola Apelo and Dudley W Lamming. "Rapamycin: an InhibiTOR of aging emerges from the soil of Easter Island". In: *Journals of Gerontology Series A: Biomedical Sciences and Medical Sciences* 71.7 (2016), pp. 841–849.

[101] Thomas Weichhart, Markus Hengstschläger, and Monika Linke. "Regulation of innate immune cell function by mTOR". In: *Nature Reviews Immunology* 15.10 (2015), pp. 599–614.

[102] ThermoFisher Scientific. *Fluorescence Fundamentals*. URL: https://www.thermofisher.com/no/en/home/references/molecular-probes-the-handbook/introduction-to-fluorescence-techniques.html (visited on 11/17/2019).

[103] ThermoFisher Scientific. *Fluorescent Probes*. URL: https://www.thermofisher.com/no/en/home/life-science/protein-biology/protein-biology-learning-center/protein-biology-resource-library/pierce-protein-methods/fluorescent-probes.html (visited on 03/30/2020).

[104] Inc. Bio-Rad Laboratories. *Fluorescence*. URL: https://www.bio-rad-antibodies.com/flow-cytometry-fluorescence.html (visited on 04/03/2020).

[105] Edinburgh Instruments. *What is a Jablonski Diagram (Perrin-Jablonski Diagram)?* URL: https://www.edinst.com/blog/jablonski-diagram/ (visited on 04/03/2020).

[106] Aysun Adan et al. "Flow cytometry: basic principles and applications". In: *Critical reviews in biotechnology* 37.2 (2017), pp. 163–176.

[107] ThermoFisher Scientific. *How a Flow Cytometer Works*. URL: https://www.thermofisher.com/no/en/home/life-science/cell-analysis/cell-analysis-learning-center/molecular-probes-school-of-fluorescence/flow-cytometry-basics/flow-cytometry-fundamentals/how-flow-cytometer-works.html (visited on 09/30/2019).

[108] Sino Biological. *Flow Cytometry (FCM)/FACS — Fluorescence-activated cell sorting (FACS)*. URL: https://www.sinobiological.com/flow-cytometry-fcm-facs-fluorescence-activated-cell-sorting-facs.html (visited on 01/23/2020).

[109] Bio-Rad Laboratories. *Fluorescence-Activated Cell Sorting*. URL: https://www.bio-rad.com/featured/en/fluorescence-activated-cell-sorting.html (visited on 01/23/2020).

[110] Abcam. *Compensation in flow cytometry*. URL: https://www.abcam.com/protocols/fluorescence-compensation-in-flow-cytometry (visited on 12/02/2020).

[111] Richard R Jahan-Tigh et al. "Flow cytometry". In: *The Journal of investigative dermatology* 132.10 (2012), e1.

[112] Inc. Bio-Rad Laboratories. *Fluorescence Compensation*. URL: https://www.bio-rad-antibodies.com/flow-cytometry-fluorescence-compensation.html (visited on 04/03/2020).

[113] Aroonima Misra et al. "Real-Time Compensation in Flow Cytometry: A Real Need of Time". In: *Indian Journal of Hematology and Blood Transfusion* 34.3 (2018), pp. 585–588.

[114] Inc. Bio-Rad Laboratories. *Controls in Flow Cytometry*. URL: https://www.bio-rad-antibodies.com/flow-cytometry-controls.html (visited on 04/03/2020).

[115] ThermoFisher Scientific. *What is ELISA (enzyme-linked immunosorbent assay)?* URL: https://www.thermofisher.com/no/en/home/life-science/protein-biology/protein-biology-learning-center/protein-biology-resource-library/pierce-protein-methods/overview-elisa.html (visited on 01/23/2020).

[116] CellSignaling Technology. *ELISA (Enzyme-linked Immunosorbent Assay) Owerview*. URL: https://www.cellsignal.com/contents/_/elisa-(enzyme-linked-immunosorbent-assay)-overview/elisa-solutions (visited on 01/23/2020).

[117] Bio-Rad Laboratories. *ELISA: Types of ELISA*. URL: https://www.bio-rad-antibodies.com/elisa-types-direct-indirect-sandwich-competition-elisa-formats.html#4 (visited on 01/24/2020).

[118] Terry L Riss et al. "Cell viability assays". In: *Assay Guidance Manual [Internet]*. Eli Lilly & Company and the National Center for Advancing Translational Sciences, 2016.

[119] Rita Hannah et al. "CellTiter-Glo Luminescent cell viability assay: a sensitive and rapid method for determining cell viability". In: *Promega Cell Notes* 2 (2001), pp. 11–13.

[120] EK Park et al. "Optimized THP-1 differentiation is required for the detection of responses to weak stimuli". In: *Inflammation research* 56.1 (2007), pp. 45–50.

[121] Iuliana Caras et al. “Influence of tumor cell culture supernatants on macrophage functional polarization: in vitro models of macrophage-tumor environment interaction”. In: *Tumori Journal* 97.5 (2011), pp. 647–654.

[122] Marc Daigneault et al. “The identification of markers of macrophage differentiation in PMA-stimulated THP-1 cells and monocyte-derived macrophages”. In: *PloS one* 5.1 (2010), e8668.

[123] F Porcheray et al. “Macrophage activation switching: an asset for the resolution of inflammation”. In: *Clinical & Experimental Immunology* 142.3 (2005), pp. 481–489.

[124] Daphne YS Vogel et al. “Human macrophage polarization in vitro: maturation and activation methods compared”. In: *Immunobiology* 219.9 (2014), pp. 695–703.

[125] Frances Y McWhorter et al. “Modulation of macrophage phenotype by cell shape”. In: *Proceedings of the National Academy of Sciences* 110.43 (2013), pp. 17253–17258.

[126] ThermoFisher Scientific. *Propidium Iodide*. URL: `https://www.thermofisher.com/no/en/home/life-science/cell-analysis/fluorophores/propidium-iodide.html` (visited on 04/17/2020).

[127] Xiaoqi Jiang and Annette Kopp-Schneider. “Summarizing EC50 estimates from multiple dose-response experiments: A comparison of a meta-analysis strategy to a mixed-effects model approach”. In: *Biometrical Journal* 56.3 (2014), pp. 493–512.

[128] Promega Corporation. *CellTiter-Glo Luminescent Cell Viability Assay*. URL: `www.promega.com/protocols/` (visited on 12/10/2019).

[129] Serena Tedesco et al. “Convenience versus biological significance: are PMA-differentiated THP-1 cells a reliable substitute for blood-derived macrophages when studying in vitro polarization?” In: *Frontiers in pharmacology* 9 (2018), p. 71.

[130] Fernando O Martinez et al. “Genetic programs expressed in resting and IL-4 alternatively activated mouse and human macrophages: similarities and differences”. In: *Blood* 121.9 (2013), e57–e69.

[131] Fazoil I Ataullakhanov and Victor M Vitvitsky. “What determines the intracellular ATP concentration”. In: *Bioscience reports* 22.5-6 (2002), pp. 501–511.

[132] Omar Sharif et al. “Transcriptional profiling of the LPS induced NF-κB response in macrophages”. In: *BMC immunology* 8.1 (2007), p. 1.

[133] Xiaojuan He et al. “Inhibitory effect of Astragalus polysaccharides on lipopolysaccharide-induced TNF-a and IL-1β production in THP-1 cells”. In: *Molecules* 17.3 (2012), pp. 3155–3164.

[134] Riyoko Tamai et al. “Synergistic effects of lipopolysaccharide and interferon-γ in inducing interleukin-8 production in human monocytic THP-1 cells is accompanied by up-regulation of CD14, Toll-like receptor 4, MD-2 and MyD88 expression”. In: *Journal of endotoxin research* 9.3 (2003), pp. 145–153.

[135] Guo-Ying Wang et al. “Rapamycin-treated mature dendritic cells have a unique cytokine secretion profile and impaired allostimulatory capacity”. In: *Transplant International* 22.10 (2009), pp. 1005–1016.

[136] Jonas Heilskov Graversen, Mette Madsen, and Søren K Moestrup. “CD163: a signal receptor scavenging haptoglobin–hemoglobin complexes from plasma”. In: *The international journal of biochemistry & cell biology* 34.4 (2002), pp. 309–314.

[137] Perla Abigail Alvarado-Vazquez et al. “Macrophage-specific nanotechnology-driven CD163 overexpression in human macrophages results in an M2 phenotype under inflammatory conditions”. In: *Immunobiology* 222.8-9 (2017), pp. 900–912.

[138] Graziella Solinas et al. “Tumor-conditioned macrophages secrete migration-stimulating factor: a new marker for M2-polarization, influencing tumor cell motility”. In: *The Journal of Immunology* 185.1 (2010), pp. 642–652.

Appendix A

The compensation matrix that was developed and used in the flow cytometry measurements is presented in Table 1.

Table 1: *The compensation matrix used to compensate for fluorescence spillover between the various detectors. This compensation file was used in all flow cytometry measurements.*

Spillover (%)										
	FL1	FL2	FL3	FL4	FL5	FL6	FL7	FL8	FL9	FL10
FL1		0,00	0,90	0,00	0,00	0,00	0,00	4,00	10,00	0,00
FL2	0,00		0,00	0,00	0,00	0,00	0,00	0,00	0,00	0,00
FL3	17,00	0,00		0,00	0,00	0,00	0,00	1,30	5,00	0,00
FL4	30,00	0,00	100,00		0,00	0,00	0,00	2,00	7,00	0,00
FL5	0,00	0,00	0,00	0,00		0,00	0,00	0,00	0,00	0,00
FL6	0,00	0,00	0,00	0,00	0,00		0,00	0,00	0,00	0,00
FL7	0,00	0,00	0,00	0,00	0,00	0,00		0,00	0,00	0,00
FL8	20,00	0,00	0,50	50,00	0,00	0,00	0,00		0,00	0,00
FL9	8,00	0,00	0,00	0,00	0,00	0,00	0,00	1,00		0,00
FL10	0,00	0,00	0,00	0,00	0,00	0,00	0,00	0,00	0,00	

The utilized detectors and their target fluorescent-conjugated antibodies:

- FL1: FITC Mouse Anti-Human CD206
- FL3: Propidium Iodide
- FL4: PerCP-Cy 5.5 Mouse Anti-Human HLA-DR
- FL8: APC-H7 Mouse Anti-Human CD80
- FL9: BV421 Mouse Anti-Human CD163

Appendix B

The overlay plots of histograms presented in Figure 1 a) and b) indicate that five days of polarization to IL-4 and IL-13 did not result further increase the amount of M2 polarized cells expressing the CD206 and CD163 surface markers.

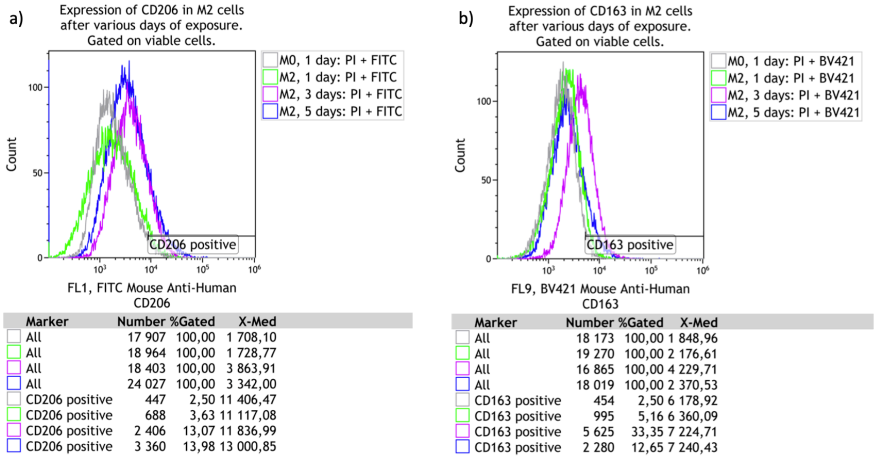

Marker	Number	%Gated	X-Med
All	17 907	100,00	1 708,10
All	18 964	100,00	1 728,77
All	18 403	100,00	3 863,91
All	24 027	100,00	3 342,00
CD206 positive	447	2,50	11 406,47
CD206 positive	688	3,63	11 117,08
CD206 positive	2 406	13,07	11 836,99
CD206 positive	3 360	13,98	13 000,85

Marker	Number	%Gated	X-Med
All	18 173	100,00	1 848,96
All	19 270	100,00	2 176,61
All	16 865	100,00	4 229,71
All	18 019	100,00	2 370,53
CD163 positive	454	2,50	6 178,92
CD163 positive	995	5,16	6 360,09
CD163 positive	5 625	33,35	7 224,71
CD163 positive	2 280	12,65	7 240,43

Figure 1: *Overlay plots of histograms presenting cell surface CD206 and CD163 expression by M2 macrophages. Overlay plot a) and b) presents the fluorescence intensity (log) of FITC Mouse Anti-Human CD206 or BV421 Mouse Anti-Human CD163, respectively, against the number of cells. THP-1 macrophages were incubated during one, three or five days with medium containing IL-4 and IL-13 to achieve polarization towards the M2 phenotype. THP-1 macrophages unexposed to polarizing stimuli, M0, was included as biological controls for each exposure time performed. The overlay plot includes the resulting histogram of the M0 control group following one day of incubation. The overlay marker in each of the overlay plots is included to evaluate the percentage of cells that express the antibody of interest. 2.5% of the control group (M0) are included in the gate. The number of cells and X-median for the fluorescence intensity signal from the different samples are presented in both of the overlay plots.*

The overlay plot of histograms presented in Figure 2 indicates that five days of polarization to LPS and IFN-γ resulted in an unacceptably low amount of viable cells that could be detected by flow cytometry.

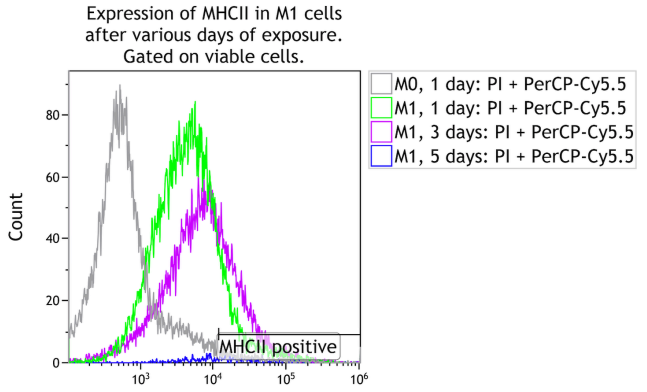

Marker	Number	%Gated	X-Med
All	19 448	100,00	456,75
All	19 416	100,00	4 371,34
All	14 964	100,00	6 768,20
All	506	100,00	14 408,56
MHCII positive	487	2,50	30 238,54
MHCII positive	2 660	13,70	18 440,11
MHCII positive	4 383	29,29	20 429,57
MHCII positive	283	55,93	35 393,23

Figure 2: *Overlay plot of histograms presenting cell surface MHCII expression by M1 macrophages. The overlay plot presents the fluorescence intensity (log) of PerCP-Cy5.5 Mouse Anti-Human HLA-DR (MHCII), against the number of cells. THP-1 macrophages were incubated during one, three or five days with medium containing LPS and IFN-γ to achieve polarization towards the M1 phenotype. THP-1 macrophages unexposed to polarizing stimuli, M0, was included as biological controls for each exposure time performed. The overlay plot includes the resulting histogram of the M0 control group following one day of incubation. The overlay marker in each of the overlay plots is included to evaluate the percentage of cells that express the antibody of interest. 2.5% of the control group (M0) are included in the gate. The number of cells and X-median for the fluorescence intensity signal from the different samples are presented in the overlay plots.*

Appendix C

Representative density plots indicating the expression of CD80, CD163 and CD206 on THP-1 macrophages exposed to M2 polarizing agents are presented in Figures 3 and 4. Investigating these figures, the relative proportion of M1, M2, and M0 macrophages, as defined by their expression of surface markers, can be visualized.

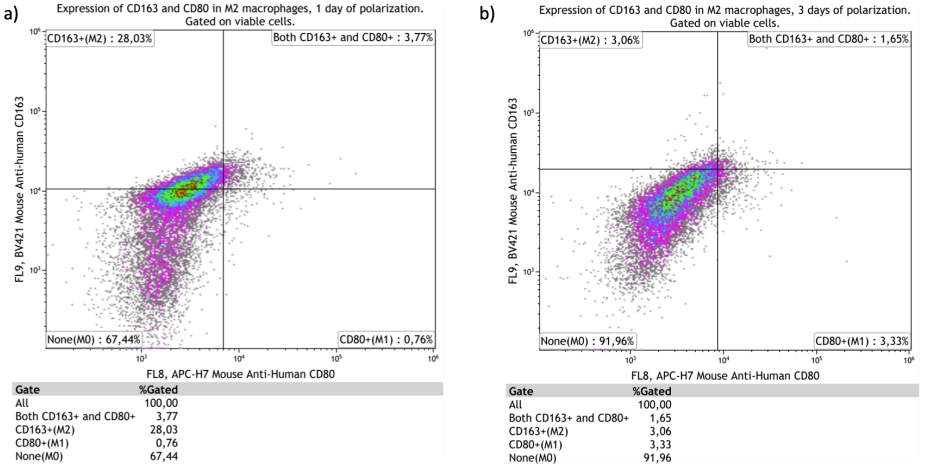

Figure 3: *Density plots presenting the APC-H7 Mouse Anti-Human CD80 fluorescence intensity (log) versus the BV421 Mouse Anti-Human CD163 fluorescence intensity (log) by M2 polarized THP-1 macrophages following exposure to IL-4 and IL-13 for one (a) or three (b) days. The density plots are generated from overlay histograms, based on the same sample of cells, expressing fluorescence intensities of each of these antibodies versus cell count, and their associated overlay markers evaluating the percentage of cells that express the antibody of interest. 2.5% of the control groups (M0) were included in the gates. The percentage of cells in the four different quadrants in the density plot indicate the amount of THP-1 macrophages exposed to M2 polarizing stimuli that, as defined by the expression or absence of CD163 and CD80 surface markers, either remain unpolarized as M0 macrophages, or develop into the M2 or the M1 macrophage phenotype. Representative density plots from three independent biological replicates.*

In Figure 3, it seems like most of the M2 polarized THP-1 macrophages maintain an unpolarized M0 phenotype, although a considerable portion of cells express the CD163 marker following one day of polarization. A substantial percentage of the M2 polarized macrophages does neither express CD163 nor CD80 following one (Figure 3a) day of polarization. Following three days of polarization 3a), there is a minimal percentage of cells expressing either of the cell surface markers (Figure 3a).

Correspondingly, as seen in Figure 4, a noteworthy percentage of M2 polarized macrophages does not develop to express the CD206 surface marker following one (Figure 4a) or three (Figure 4b) days of polarization. The percentage of M2 polarized THP-1 macrophages that are single positive for CD206, CD80 or double positive for CD206 and CD80 are minimal.

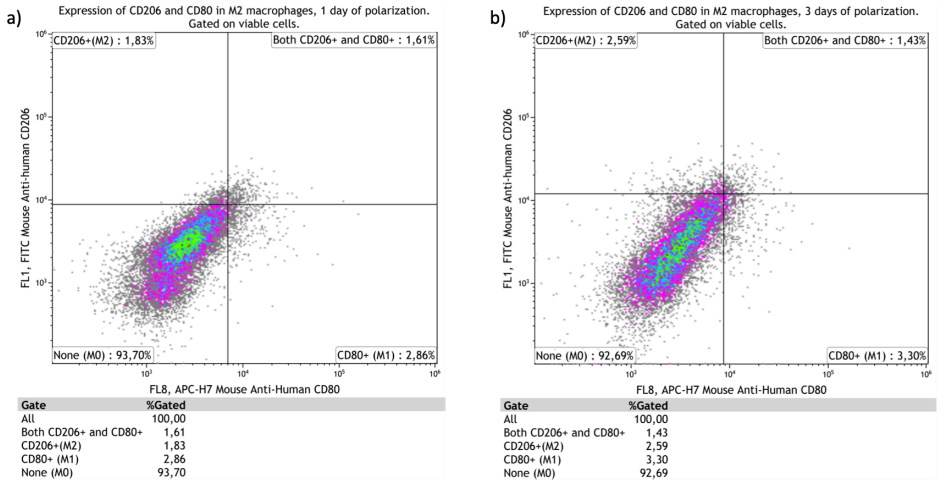

Figure 4: *Density plots presenting the APC-H7 Mouse Anti-Human CD80 fluorescence intensity (log) versus the FITC Mouse Anti-Human CD206 fluorescence intensity (log) by M2 polarized THP-1 macrophages following exposure to IL-4 and IL-13 for one (a) or three (b) days. The density plots are generated from overlay histograms, based on the same sample of cells, expressing fluorescence intensities of each of these antibodies versus cell count, and their associated overlay markers evaluating the percentage of cells that express the antibody of interest. 2.5% of the control groups (M0) were included in the gates. The percentage of cells in the four different quadrants in the density plot indicate the amount of THP-1 macrophages exposed to M2 polarizing stimuli that, as defined by the expression or absence of CD206 and CD80 surface markers, either remain unpolarized as M0 macrophages, or develop into the M2 or the M1 macrophage phenotype. Representative density plots from three independent biological replicates.*

Representative density plots indicating the expression of CD163 and CD206 on THP-1 macrophages exposed to M2 polarizing agents are presented in Figure 5. When investigating these figures, it can be seen that the highest percentage of M2 polarized macrophages does not develop to express the CD163 or the CD206 surface marker following one (Figure 5a) or three (Figure 5b) days of polarization. However, there is a certain percentage of M2 polarized cells that express the CD163 cell surface marker following one day of polarization, seen in Figure 5a.

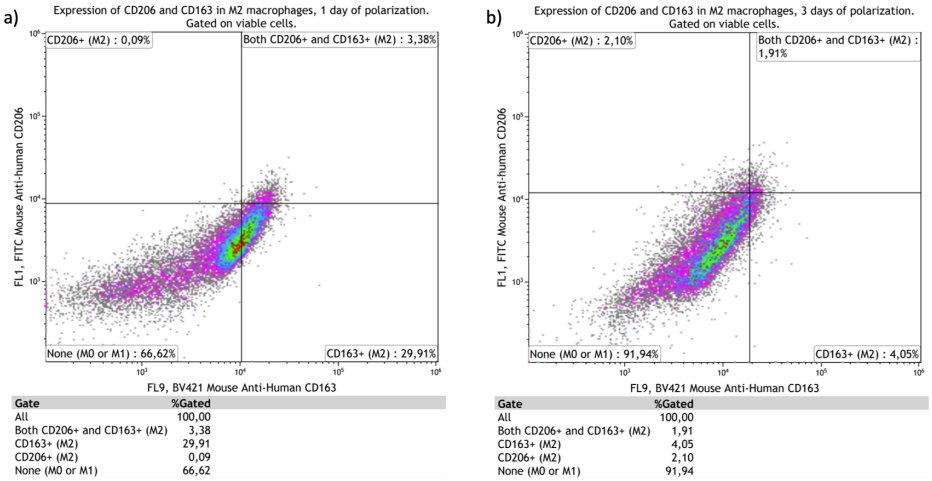

Figure 5: *Density plots presenting the BV421 Mouse Anti-Human CD163 fluorescence intensity (log) versus the FITC Mouse Anti-Human CD206 fluorescence intensity (log) by M2 polarized THP-1 macrophages following exposure to IL-4 and IL-13 for one (a) or three (b) days. The density plots are generated from overlay histograms, based on the same sample of cells, expressing fluorescence intensities of each of these antibodies versus cell count, and their associated overlay markers evaluating the percentage of cells that express the antibody of interest. 2.5% of the control groups (M0) were included in the gates. The percentage of cells in the four different quadrants in the density plot indicate the amount of THP-1 macrophages exposed to M2 polarizing stimuli that, as defined by the expression or absence of CD206 and CD163 surface markers, either remain unpolarized as M0 macrophages, or develop into the M2 macrophage phenotype expressing one or both of these classical M2 macrophage surface markers. Representative density plots from three independent biological replicates.*

The percentages of negative, single positive, or double-positive macrophages of CD163 and CD206 were collected for three independent biological replicates. The summarized expression of these markers on M0, M1, and M2 polarized THP-1 macrophages are presented in Figure 6. As can be seen, the summarized mean ± standard deviation (n=2) in the bar chart further presents the lack of M2 surface marker expression. In this graph, no significant increase in the percentual expression of either CD163 or CD206 was detected.

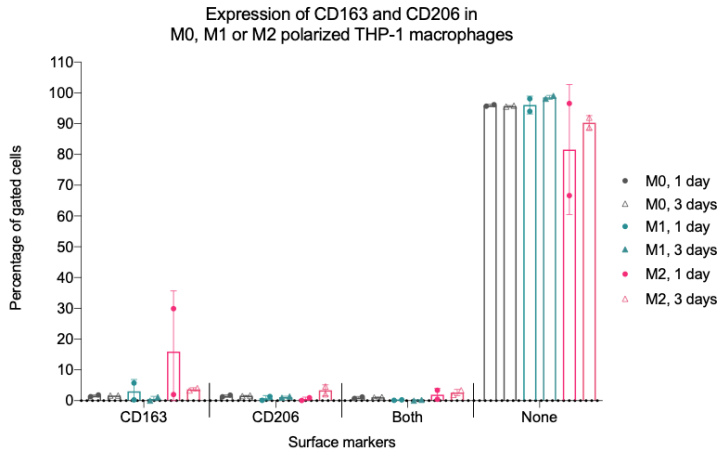

Figure 6: *Graph presenting the mean percentage of M0, M1, or M2 polarized THP-1 macrophages expressing either CD163, CD206, both CD163 and CD206, or neither of these markers, as measured by flow cytometry and collected from all generated density plots. The graph includes macrophages exposed to polarizing stimuli for one and three days. Results are expressed as means ± standard deviation (n=2). Statistical analysis was carried out using unpaired t-tests by GraphPad Prism version 8.4.2 for macOS. ns: not significantly different. ∗, ∗∗ or ∗ ∗ ∗: significantly different respectively with p <0.05, 0.01 or 0.001.*

Appendix D

As seen in Figure 7 b) increasing concentrations of BMS-345541 has an impact on the cells' metabolic activity. Similar observations were found on M1 polarized cells upon exposure to equal concentrations of BMS-345541, presented in Figure 4.18 b) in Section 4.2.3. Both for M1 polarized cells and M0 unpolarized cells, the metabolic activity significantly increased upon exposure to the lowest investigated concentrations of BMS-345541. On the other hand, a significant decrease in metabolic activity was measured upon exposure to the highest investigated concentrations of BMS-345541. However, as seen in Figure 7, the secretion of TNF-α is minimal or below the detection limit on THP-1 macrophages incubated with BMS-345541 without exposure to LPS and IFN-γ.

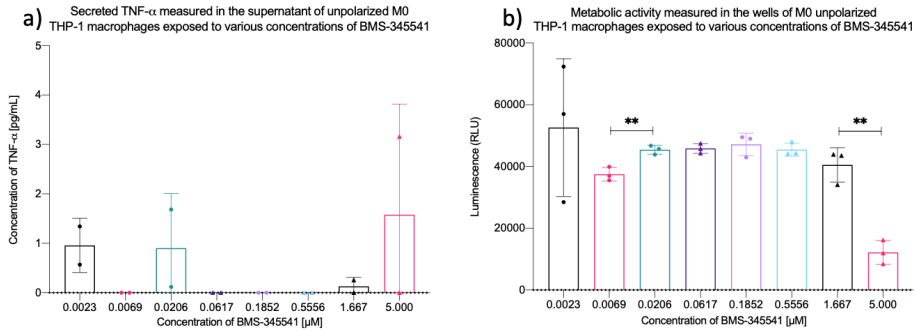

Figure 7: *Bar charts presenting the secretion of TNF-α (a) or the metabolic activity (b) on the y-axis versus added concentrations of BMS-345541 on the x-axis. The measurements were performed on M0 unpolarized THP-1 macrophages exposed to various concentrations of BMS-345541 for 24 hours. The concentration of TNF-α was measured by Sandwich ELISA on the supernatant, whereas the metabolic activity was measured by CTG directly in each well. Each point represents the average of duplicates, and the results are expressed as means $\pm$ standard deviation (n=2 for the ELISA-measurements; n=3 for the CTG-measurements). Statistical analysis was carried out using unpaired t-tests by GraphPad Prism version 8.4.2 for macOS. ns: not significantly different. $*$, $**$ or $***$: significantly different respectively with $p < 0.05$, 0.005 or 0.0005.*

Maria Stadheim

Development of macrophage characterization assays

NTNU
Norwegian University of
Science and Technology

SINTEF